POLITECNICO DI TORINO

Department of Electronics and Telecommunications
Master's Degree in Electronic Engineering

Master's Thesis

Definition of a numerical methodology for the evaluation of Lightning Indirect Effects (LIE) on Aircraft during the design and certification phases

Supervisor
Prof. Flavio Canavero

Candidate
Serena Gatti

Tutor Leonardo Aircraft Division
Ing. Luigi Pisu

Academic year
2018/2019

POLITECNICO
DI TORINO

LEONARDO

Department of Electronics and Telecommunications
Master's Degree in Electronic Engineering

Master's Thesis

Definition of a numerical methodology for the evaluation of Lightning Indirect Effects (LIE) on Aircraft during the design and certification phases

Supervisor
Prof. Flavio Canavero

Candidate
Serena Gatti

Tutor Leonardo Aircraft Division
Ing. Luigi Pisu

Academic year
2018/2019

Acknowledgements

Ho sempre associato metaforicamente il percorso universitario, ad una montagna. Una montagna insormontabile, della quale non riuscivo a vedere mai la vetta. Finalmente dopo un passo dietro l'altro, riesco a vedere quel tanto atteso traguardo.
E' stato lungo il percorso che mi ha portata fin in vetta, ma ricco di una miriade di emozioni, sacrifici, crescita professionale e personale.
Oggi posso ritenermi soddisfatta ed orgogliosa.
Desidero ringraziare il relatore: Prof. Flavio Canavero, per avermi indirizzato e permesso di entrare in una realtà aziendale come quella di Leonardo S.p.A.
Un ringraziamento speciale lo rivolgo al mio tutor aziendale della divisione velivoli: Ing. Luigi Pisu, con il quale ho collaborato nel lavoro di tesi, per arrivare all'acquisizione del metodo e di interpretazione dei dati.
Ad Enrico, mio compagno di viaggio, amico e infine collega, con il quale siamo riusciti a portare a termine questo importante traguardo.
Dedico e ringrazio infinitamente la mia famiglia, per avermi supportata/sopportata e permesso di ottenere questo desiderato e tanto atteso Titolo.

Abstract

Lightning is an high current and high voltage phenomenon that can statistically strike an aircraft once a year during the flight phases of takeoff and landing. Certification bodies have categorized the overall lightning effects on the aircraft into three main categories: **Lightning Direct Effects (LDE)**, **Lightning Indirect Effects (LIE)** and **Effects** on the **Fuel System**. In particular, the Indirect Effects are the result of interactions of the high electromagnetic fields correlated to the lightning flash with the aircraft internal cables architecture. If not properly addressed, the lightning phenomenon may consequentially cause dysfunctions or damages to the internal safety-critical equipment connected to the wiring system. This thesis focuses on the evaluation of the **Lightning Indirect Effects (LIE)** on a simplified **3D Digital Mock-up Model of a Transport-Aircraft**; in detail, the main purpose of the thesis is to set-up a numerical methodology suitable for the calculation of the Actual Transient Levels (ATL), in correspondence of the terminals of a simplified wiring network displaced into the aircraft. The simulation campaign was based on the use of **CST Studio Suite** exploiting the capabilities of two interacting packages: **CST MICROWAVE STUDIO**, dedicated to the EM modeling of the **3D Digital Mock-up Model of a Transport-Aircraft** and **CST CABLE STUDIO**, utilized to model the internal cables architecture in terms of both 3D routing and electrical characteristics of the wires.
The simulation approach for the analysis of the indirect effects of lightning strike on aircraft was consequentially based on:

- **Full-Wave Time-domain method TLM (Transmission Line Matrix)**, to analyze the return stroke current on the surface of the aircraft and to predict the EM fields penetration both through the apertures (windows, Radomes, etc.) and through CFC (Carbon Fiber Composite) materials with a defined electrical conductivity .

- **2D TL (Transmission Line) Solver** which, taking inputs from the 3D simulation, is able to evaluate the coupled currents on each wire composing a specific cable harness.

Being the simulation campaign certification-oriented, several and different entry/exit points configurations were tested, according to the zones of major probability of lightning attachment. Finally, a worst-case (amongst all 9 configurations) of the coupled current evaluated at each terminal of wiring network is presented. The main purpose of Thesis was (using the worst-case of the screen/core of the cable for each configurations), to estimate the ATLs for the three different configurations of materials (PEC-Perfect Electric Conductor, Carbon Fiber Composite and the advanced Carbon Fiber Composite with Copper Mesh). An important result achieved by the present Thesis Work is the evaluation of the impact of composite materials on the ATLs worst cases. An interesting outcome is highlighted by the comparison between the configurations of standard CFC and advanced CFC. The present methodology described in this Thesis can be applied during both the aircraft preliminary design phase, in order to tailor the equipment hardening against lightning

induced currents and during the certification phase in order to support the testing campaign, cutting down testing time and time-to-market.

Contents

List of Figures

List of Tables

Introduction

The present Thesis has the purpose, starting from the study of natural phenomenon of lightning, to obtain a *Definition of a numerical methodology for the evaluation of Lightning Indirect Effects (LIE) on a simplified 3D Digital Mock-up Model of a Transport-Aircraft* .
The Thesis work was carried out at the headquarters of **Leonardo S.p.A**, located in Turin.
Leonardo S.p.A is a **global high-tech Aerospace, Defence and Security company**, it works in related field of Air, land, sea, space and cybersecurity; whenever defence and security are needed, providing solutions for their requirements in each of these aereas through a complete and integrated offer in strategic sectors as helicopter, aeronautics, unmanned systems, defence and security electronics, defence systems, satellite systems and services. [27] Joining the world of Leonardo S.p.A, for a period of about ten months in the **aircraft division**, meant the access to a dynamic and challenging context that demands utmost diligence in developing skills.
The Thesis is organized in chapters and for each one following is presented a briefly summary.
Chapter 1 - *Introduction to High Voltage Phenomena*: presents several phenomena associated with the electric discharge in gases, among them sparks, streamers, corona and leader. That corresponds to the starting point to understand the natural phenomenon of lightning.
Chapter 2 - *The Lightning Environment*: presents the natural phenomena of lightning starting from the formation of an electrical charge centers in the air, in particular in the Cumulonimbus thunderclouds. The different types of Lightning flashes: **cloud to ground** and **ground to cloud** lightnings of either polarity, **cloud to cloud lightnings**, **intracloud lightnings**.
Chapter 3 - *Aircraft Lightning interaction*: presents the different kind of approaches with which aircraft is struck by lightning and zone definition and methods of locating them on particular aircraft are given in the documents: **ARP-5414 Aircraft Lightning Zoning** and **ARP-5412 Aircraft Lightning Environment and Related Test Waveform**.
Chapter 4 - *The Certification process*: its purpose is to describes the waveforms represented in idealized environments which are to be applied to the aircraft with the aim of analysis and testing. It must be taken in considerations that the waveforms does not have the task to replicate a specifics lightning event, but should be reproduce the same effects on the aircraft as those from natural lightning. In particular standard lightning environment includes voltage waveforms and current waveforms components which represent the important characteristics of natural lightning flashes.
Chapter 5 - *Lightning Effects on Aircraft*: is focused mainly on the *Light-*

ning Direct Effects (LDE) and *Lightning Indirect Effects (LIE)* and what types of consequences the aircraft suffered. For the purpose of the thesis, more attention was given at the **Lightning Indirect Effects (LIE)**, that occurs when in the electrical equipment of the aircraft there is a dysfunction or some damages due to the strike of lightning flashes.

Chapter 6 - *Simulation Methodology for the evaluation of the Lightning Indirect Effects (LIE)*: presents in order to investigated and simulated virtually the Lightning Indirect effect, it is presented and analyzed a simplified structure of a Cylinder, so that it aims to represents the fuselage. A first trial of realization of a cable network is also implemented and discussed.

Chapter 7- *The effects of Lightning on a simplified 3D Digital Mock-up Model of a Transport-Aircraft*: presents a path characterized by the design of the single sub-parts that make up the aircraft. After having conducted all the simulations for the individual parts of the plane, the subsequent step was to assemble them. According to the most updated in force guidelines, nine simulation configurations, with differing for entry/exit points of the lightning current were setup. The simulation campaign had as a final purpose to obtain the **ATLs- Actual Transient Levels** associated at each maximum current-voltage peak occurred, among all the entry/exit points configurations, at each LRU connection.

Chapter 8- *Further results*: presents 2D/3D graphics results related to the H-field, Surface current and frequency spectrum.

Chapter 9- *Conclusion and future work*: the main results got in the Thesis are summarized and an outlook towards possible future activities and applications on real platforms is given.

Chapter 1

Introduction to High Voltage Phenomena

1.1 Introduction

The analysis of high voltage phenomena is important when dealing with an aircraft that is struck by lightning. Indeed lightning is a high current and high voltage phenomenon. The aim of this chapter is to briefly provide an overview of the general physics involved.

1.2 Physic review

Several phenomena are associated with the electric discharge in gases, among them this chapter will focus on sparks, streamers, corona and leader.
Townsend and Sparks [1][9] presented two types of theories which elucidate **the Mechanism of Breakdown**. In order to conduct electricity are required two electrodes immersed in a gas and an electric field to produce the directional motion of the charges as illustrated in Figure 1.1

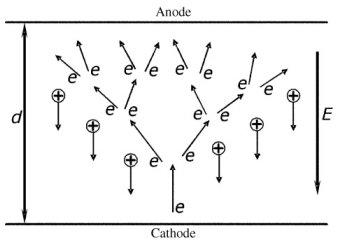

Figure 1.1: Electrode configuration [11]

In order to understand the complete breakdown of a gas or the formation of a spark between two electrodes, the electrical properties of gases should be studied.

The electrical discharges in gases are of two types :

- non-self sustaining discharge,
- self sustaining discharge.

The breakdown in a gas is the transition from one non-self sustaining discharge to one of several types of self sustaining discharge as in Figure 1.2

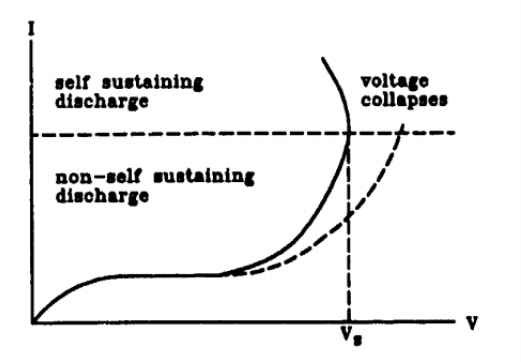

Figure 1.2: V-I characteristic [12]

In the region of breakdown, there is an increase of current due to the ionization of electrons and ions, which are obtained from neutral atoms and from their migration from negative electrode to the positive one. The result is an avalanche of electrons and the total numbers of electrons produced by the acceleration of a group of electrons are:

$$N^- = n_0^- e^{\alpha d} \tag{1.1}$$

assuming N^- the final number of electrons, n_0 the number of initial electrons and d the distance between the two electrodes. The quantity α is called **Townsend's first ionization coefficient** and indicates the average number of ionizing collisions made by an electron per centimeter. [20]
The electric field determines of how much the electrons are accelerated and how new electrons being liberated by other mechanisms and allows further avalanches that represents the second ionization process. The other mechanisms are:

- **Electron emission due to positive ions impact**: the positive ions are obtained due to the ionization and if they have sufficient energy can cause the emission of electrons from the cathode.
- **Electron emission due to photons**: the excited atoms may emit photons and this carry on to the emission of electrons due photo-emission.
- **Electron emission due to metastable and neutral atoms**: rare gases or mercury that are metastable particles may diffuse back causing electrons emission.

Townsend attributed that the total current is characterized by two components, one already obtained in the Equation 1.1 and one due to the motion of the positive charge particles:

$$N^+ = n_0^+ e^{\gamma d} \tag{1.2}$$

assuming N^+ the final number of positive charge particles, n_0 the initial number and d the distance traversed. γ is **Townsend's second ionization coefficient** and is defined in the same way as α.

$$N = (N^+ + N^-) \tag{1.3}$$

Considering the total number of electrons reaching the anode is:

$$N = \frac{n_0 e^{\alpha d}}{1 - \gamma(e^{\alpha d} - 1)} \tag{1.4}$$

The Equation 1.4 provides the total average current in a gap before the breakdown. The denominator is possible to write like:

$$\gamma(e^{\alpha d} - 1) = 1 \tag{1.5}$$

that is called **Townsend's Breakdown criterion**.

So, taking into account that

$$e^{\alpha d} >> 1 \tag{1.6}$$

the Equation 1.5 is reduced to

$$\gamma(e^{\alpha d}) = 1 \tag{1.7}$$

Finally, at the **sparking voltage** V_s the gap will breaks down and the voltage will collapse. [20][9][28]

1.3 Streamer

Townsend's breakdown criterion is seldom used since the process is very complicated and as a result **Sparks theory** was proposed. [9]
This theory is based on the mechanism of sparks breakdown, in which there is a much faster development of over-voltage respect to the time necessary for ions to cross the gap and produce the second emission. The spark channel has an high conductivity which can be formed even faster than electron drift time from cathode to anode, highlighting that this is the big difference between the Townsend and Sparks mechanisms of breakdown. The theory describes that the breakdown is attributed to growth of a **streamer** that drives in to ionization of the gas and is independent from other processes that can take place at the electrodes. It is important to consider if the streamer extends towards the total breakdown between the two electrodes or if it is confined to the localized discharge called **corona** and that depends on how the electric field is distributed across the gap. [11]

1.4 Corona

The term **Corona** corresponds to the visible blue glow that takes place around a point of conductor held to a high electrical potential. [15]
The electric field strength around that point can be precursor to complete breakdown and can be a source of power loss and also interference in radio receivers. The Corona can be formed on the extremities of aircraft when they are charged by flying though clouds and also on grounded object exposed to high electric field. The phenomenon is called **St.Elmo's fire** that is a corona discharge and the mechanism is the same as observed for the high voltage conductors. The characteristics of Corona discharge are influenced by the electrode configurations. The typical configurations are illustrated in Figure 1.3 and consist of an energized sphere or rod placed above a grounded plane, a sphere plane or rod plane configuration. Another one consists of two rods, one energized and one grounded. [11]

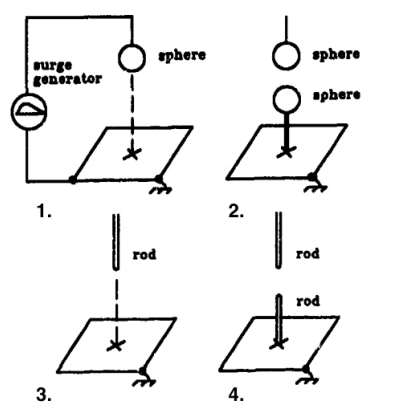

Figure 1.3: Electrode configurations [11]
1.Sphere to plane **2.**Sphere to sphere
3.Rod to plane **4.**Rod to rod

When high voltage tests are made, the most convenient electrode configuration which can help to determine the points at which lightning might attach to an aircraft is rod to plane.

1.4.1 Corona discharges

If the electric field is uniform and it is starting to increase the voltage across the gap, this will involves into a breakdown of the gap in the form of a stream, instead if the electric field is nonuniform and it is starting to increase in voltage will cause a discharge in the gas manifesting at points with a high electric field intensity. This kind of discharge is the **corona discharge**. In non-uniform fields various manifestations of luminous and audible discharges were observed long before the complete breakdown occurs. There is a difference in visual appearance of corona at wires under different polarities of the applied voltage and it is convenient to distinguish between positive and negative coronas. [28]

1.4.2 Generation of pulse type corona

It is very difficult monitor in a precise way what happen when an impulse voltages is applied, precisely at a level above the ionization threshold and this is because of the growth of discharges. It has been possible to understand the different discharges steps before breakdown under the impulses voltages. When a positive voltage is applied to a rod electrode, the first ionization consist in a filament branch as in Figure 1.4 and this kind of discharge is nothing more than a streamer like in the case of uniform field.

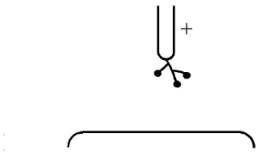

Figure 1.4: 1 step [9]

Increasing the impulse voltage level, streamers grow both in length and in number of branches as in Figure 1.5.

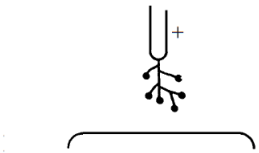

Figure 1.5: 2 step [9]

It is possible to observe an interesting thing that is despite the large amount of number of branches they never cross each other as in Figure 1.6.

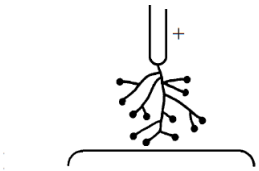

Figure 1.6: 3 step [9]

Positive Polarity Voltage

To study the various discharge modes and breakdown characteristics it is taken into consideration the Figure 1.7, where it is for example applied a **positive polarity voltage** to a rod-plane configuration with a rod tip of radius of 1 cm.
If the voltage is increased gradually and the gap length is small ($< 5cm$) there isn't an appreciable ionization to causes a breakdown, visible from the *Curve 1.* As the voltage and the gap increased above 10 cm, the field becomes non uniform and the first branches filaments discharge appears (*Curve 2*). The *Curve 3* corresponds to the transition from streamers to steady glow corona without sparking but when the gap became larger, there is a considerable rise of voltage and more streamers appear which ultimately led to a complete breakdown of the gap. The region with dashed lines corresponds to an uncertain transition, where the first part corresponds at the

beginning of the streamers followed by a sparks and the second part corresponds at the increasing of the gap until the point in which glow is established and then reduced taking the voltage constant. The glow discharge will have stabilized gap against breakdown at a voltage that otherwise it would be broken. At the end the voltage is then raised, a spark is induced by glow corona as in *Curve 4*, but if it is lowered a streamer breakdown is induced. [9][28]

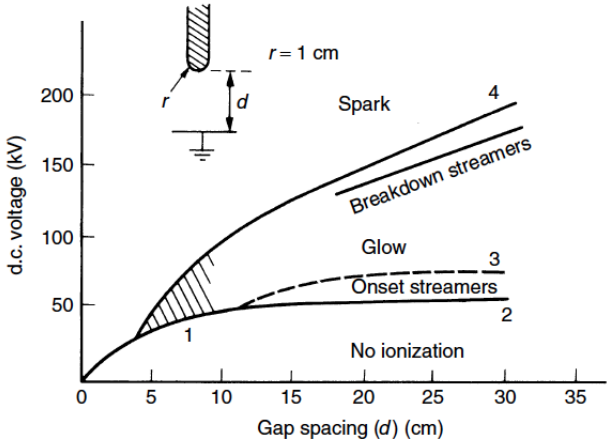

Figure 1.7: Curves of different modes of anode corona [16] [17]

Negative Polarity Voltage

Taking as reference the electrode configuration of rod to plane, when **negative polarity voltage** is applied to the rod, there is the formation of current that flows in vary regular pulses called **Trichel pulses**. The starting voltage is equal to the starting streamer under positive voltage but completely independent of the gap length.
A common example is the one that shows the onset voltage of various negative coronas as function of electrode separation with 0.75 mm radius's cathode. Starting from the lowest curve it is possible to observe that the onset voltage for Trichel pulses are not disturbed by the gap length. Increasing the voltage, as a first point will cause a glow discharge than if you further increase will occur in a completely breakdown. It is important of must be conscious of the fact that the breakdown voltage with negative polarity is higher than with positive polarity except at low pressure. [9]

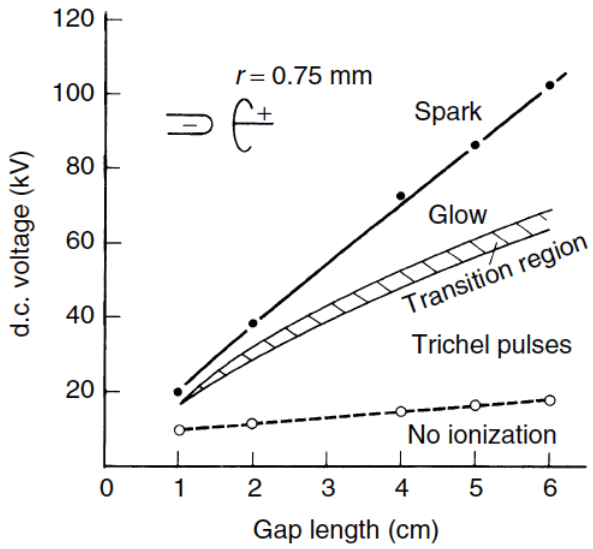

Figure 1.8: Curves of different modes of cathode corona [16] [17]

1.5 Leader

Considering a long air gap that is stressed with a **positive** or **negative** voltage impulse, it is observed, thanks to the use of particular camera, that there are several stages until the breakdown occurs. [9]
Starting from the initial burst of corona that take place near the electrode with the highest electrical stress and with a further increase of the electrical field, the corona will be formed in a small fraction of microsecond. If the voltage is maintained a more intense, localized streamer develops out of the initial corona. Streamers attract several electron avalanches into a single channel called **leader**, which is a sufficiently conductive channel that acts as an extension of the rod and it can have an electrical conductivity approaching that of an electric arc. - An electrical arc is a self-sustaining discharge having a low voltage drop and capable to support large current. Indeed, in the context of aircraft lightning protection, arcs forms most commonly in response to an initial breakdown brought due to the excessive voltage applied.- The result is that under sufficiently high voltages, the leader progresses faster and carries more current and extending itself further into the gap, doing a series of jump until the entire gap has been bridged. [11]

Chapter 2

The Lightning Environment

2.1 Introduction

The lightning is one of the most spectacular of natural phenomena and behind of this there are numerous theories, as it has always been a matter of disputes. The lightning flashes originate from the formation of an electrical charge centers in the air, in particular in the *Cumulonimbus thunderclouds*. Lightning can occur in the clouds over erupting volcanoes or during sandstorms and this is not so dangerous for the aircraft, but during the snowstorms could be a problem because it could happen when it is not expected. [12]
Numerous pilot's reports problem on aircraft are due to the fact that they were struck by lightning under conditions where them were not expected. The events for which the aircraft were struck are not always known, in fact there is still more to learn about the mechanism of lightning flash. This chapter will give the information about the natural lightning phenomena, the different type of lightning and it is mostly concerned on cloud-to-ground ones.

2.2 Natural lightning description

Many theories have been proposed for the electrification of the cloud but according to one it is possible to understand the mechanism by which electrical charge develops in the clouds. The ice crystals became hailstones due to the process of freezing, these falls through the cloud and mixing with additional supercooled water droplets. From the hailstones some small splinters chip off and positive electrical charges are taken away. At the end the hailstones remained with a negative electrical charges. [25]
Typically, on the top of the ***Cumulonimbus Clouds*** most positive charges accumulate, leaving the lower region negative, although there may be a small positive region near the base as presented in Figure 2.1.

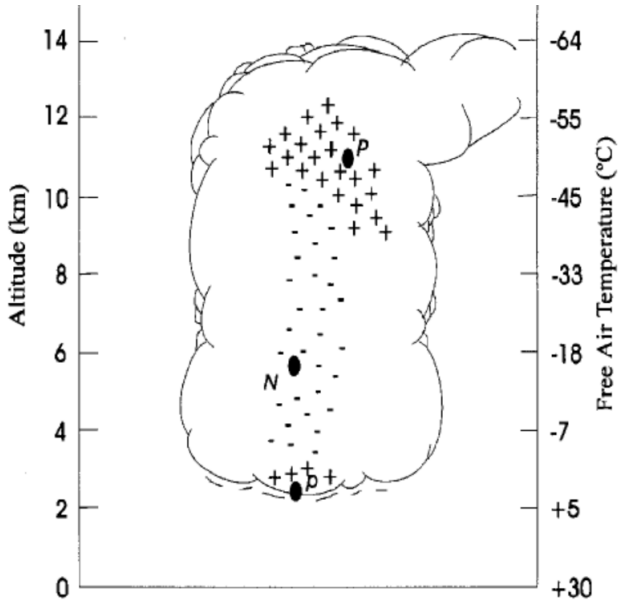

Figure 2.1: Distribution of electric charge in a typical *Cumulonibus Cloud* [25]

2.2.1 Development of the all process: from the stepped leader to return stroke

At the apex of the process of lightning flash there is the electrification of the clouds, after a discharge towards the earth moves likely from 30 to 50 m, this column of ionized air is called ***pilot streamer*** and at the end takes place a more intense charge called ***stepped leader***. This kind of ***streamer discharge*** moves an extra negative charge allowing to give the possibility at the streamer to extend for another 30 to 50 m. The diameter of the stepped leader is between 1-10 cm although the current, which is about 100 A, it is concentrated in a small highly ionized core of about 1 cm diameter.
Photographs of lightning leaders may be taken by Boys camera and from such photos it has been learned that the leader has an average velocity of propagation of $1.5 \times 10^5 m/s$. The leader negatively charged, may form branches on its downward path to the ground and consequently the positive charges will accumulate on the ground. From the ground, where there is an high concentration of electric field, starts a streamer called ***return stroke*** going upward and it will recharge the leader channel which has just been neutralized. As the return stroke approaches the cloud, it can hit other branches of the leader as it is possible to see in Figure 2.2.

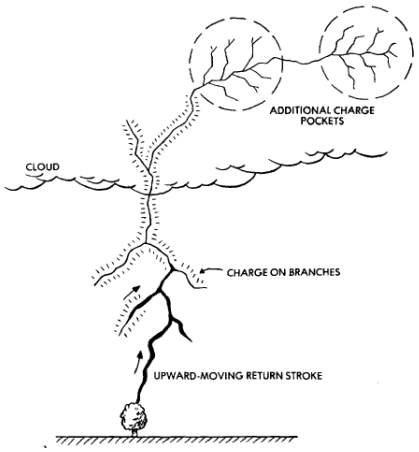

Figure 2.2: Upward moving return stroke [11]

When the return stroke passes these branches, the charge stored in them will contribute into developing lightning stroke and increasing the current helping it to reach the cloud. As the discharge continue the diffusion through the cloud, the currents of a few hundred ampere continue to flow in the leader of lightning flash. During the end, usually the discharge within the cloud reaches a different cell of the cloud or another region where is present another body of electrical discharge. At this point happens the ***restrike*** that starts with additional charge coming from the cloud to form a new leader called ***dart leader***, when it reaches the ground level, a return stroke occurs. The amplitude of this return stroke is high because the current come from an ionized region close to ground and the current rises more faster than does that of the initial stroke, presumably because the upward leader coming from the ground does not have to spread into virgin air. [11]

2.3 Types of Lightning

There are different types of lightning flashes categorize in:

- **cloud to ground** and **ground to cloud** lightning of either polarity,
- **cloud to cloud** lightning: that corresponds to a flash between region of opposite polarity in different clouds,
- **intracloud** lightning: that corresponds to a flash between region of opposite polarity within a cloud.

An aircraft may be involved with any of the three types, but cloud to ground and intracloud lightning are the most common types.

It might be noted that leaders sometimes start at the ground and work their way toward the sky: this it happens most frequently from very high buildings or towers. Generally, it possible to understand the flash categories from the direction of the lightning flash branches whether the leader started at the cloud or at the ground as represented in Figure

2.3

Figure 2.3: 1.Downward branching leader starts at the cloud. 2.Upward branching leader starts at the ground

In terms of engineering definition of current for what concern the **cloud to ground** flashes, it is possible to distinguish :

- **negative flash polarity** which lowers negative charges to the earth
- **positive flash polarity** which lowers positive charges to the earth

Chapter 2.2.1 described the phenomenon of **negative flash polarity** which helps to understand the return stroke current during an intense negative flash. It is possible to consider the following example and the parameters in Table 2.1. Zooming in the zone between 1 and 11, that corresponds to the one with major number of negative flashes strokes, the subsequent strokes have an higher rate of rise although lower peak amplitudes than the initial stroke and can be the causes to introduce an high amount of voltage in wiring. And the coupled voltage will be direct proportional to the rate of change of lightning current, as in Figure2.4. [21]

	min-max	**average**
Number of stroke	**1-11**	**3**
Total duration	**20 ms-1s**	**0.2 s**
Time interval between the strokes	**60 ms**	
Rise time first stroke	**2** μs	
Decay time first stroke	**40** μs	

Table 2.1: Typical return stroke current values

There is also an intermediate current component in which there is a lower level current of a few kA. After the presence of some strokes, there is a continuing current of 100 to 400 A, having a charge transfer that is common before a restrike starts again, note in particular after stroke 5.

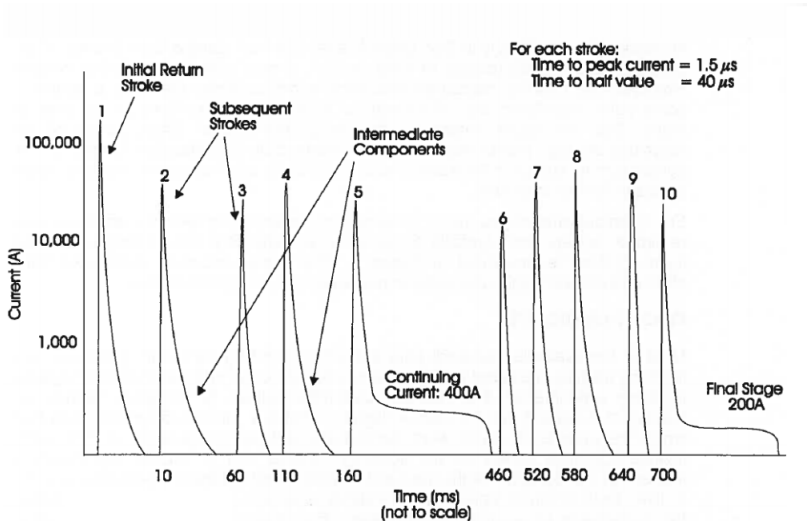

Figure 2.4: Model of Negative Lightning Flash Current Waveforms [11]

Some flashes with a **positive polarity** happen less frequently with a respect to the negative one and they correspond on an average of 10%. The most important difference respect to the negative one is that they consist in only one stroke with a slower rise time, high peak current and a long duration, as shown in Figure 2.5 [18]

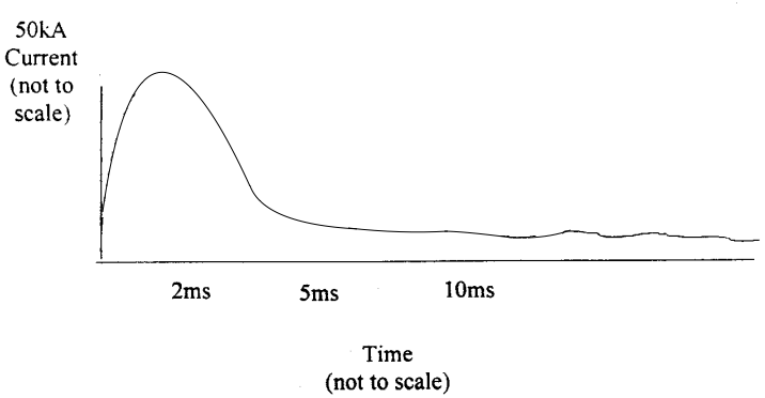

Figure 2.5: Model of Positive Lightning Flash Current Waveform [11]

In order to know the features of **cloud to cloud** flashes, specific studies have been done, by means of instrumentation integrated on aircraft and employed in France and USA; the result was that this kind of flashes are less high and with an high peak of current respect to the cloud to ground. For **intra cloud** flashes have been recorded streamers with a peak current more high than 60kA, even if that typically are between 20 to 30 kA.

Chapter 3

Aircraft Lightning interaction

3.1 Introduction

The following chapter is focused on the different kind of approaches with which an aircraft is struck by lightning flashes. A statistic amount of reports drafted by aircraft pilots provide the possibility to understand how the lightning flash interacts with the aircraft surfaces and the possibility to define the lightning strike zones on the surfaces of the aircraft. Strike occurrence data, based on turbojet or turboprop aircraft, has been collected for many years and assemble according the following categories:

- *Altitude*,
- *Flight path*: level flight or descent,
- *Meteorological conditions*,
- *Outside temperature*,
- *Lightning strikes effects*

It is important to highlight that the percentage that indicates that no aircraft is likely to receive more than one or two lightning strikes in a years. In particular the lightning strikes effects on aircraft will be discussed in the subsequent chapters.

3.2 Aircraft lightning strike mechanism

An Aircraft in particular during the flight phases of takeoff and landing, is exposed to both of **natural lightning** and **triggered lightning**. A naturally strike happens when a lightning leader propagating outward from the charge center of a cloud and it ultimate destination is at an opposite charge center in the cloud or on the ground. This difference of potential that exists between the leader and the opposite charge fix an electrostatic force field that is represented by using imaginary equipotential surfaces, as illustrated in Figure 3.1,

In kV per meter is expressed the field intensity and is greatest where the equipotential surfaces are closest to the aircraft.[24].

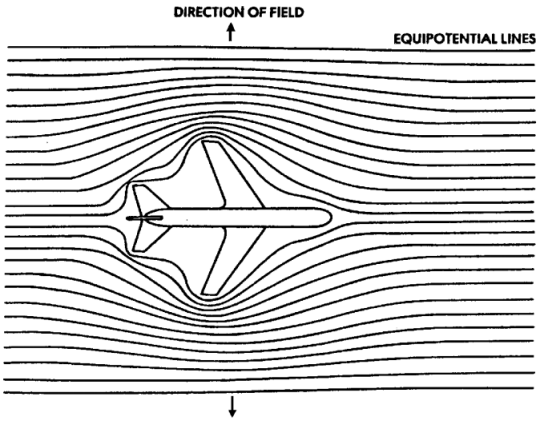

Figure 3.1: Compression of electric field around the extremities of an aircraft [24]

When the leader is in the neighborhood of an aircraft, the electric field in the extremities increased of about 30 kV/cm and electrical sparks will form, extending in the direction of the oncoming leader. Streamers may propagate onward from two or more extremities of the aircraft at the same time. The surface of the aircraft where the junction leader arises from this becomes the initial/entry attachment points, at the same time the other junction leader that arises in the other extremity, it is propagating away in direction with an opposite polarity charge, are called exit points. [12]

The **junction leader**, will be in contact with the nearest branch of the advancing leader and form a continuous spark from the cloud to the aircraft, as in Figure3.2 Instead, when the leader has reached its destination, a continuous channel between

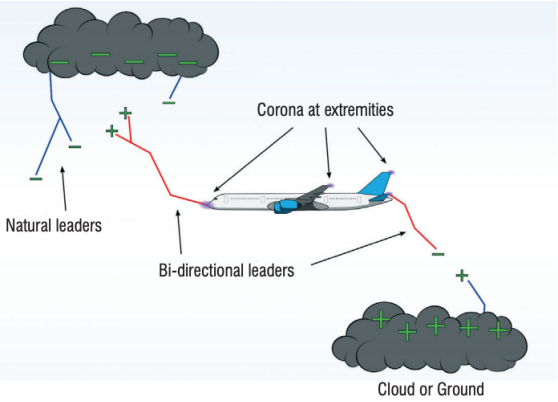

Figure 3.2: Leader approaching aircraft

charge centers has been formed, therefore will occur the recombination of positive and negative charges in order that the leader channel forming an high return stroke current. This stroke current and any ulterior stroke must flow through the aircraft, which it has become a conducting channel between the charge centers.

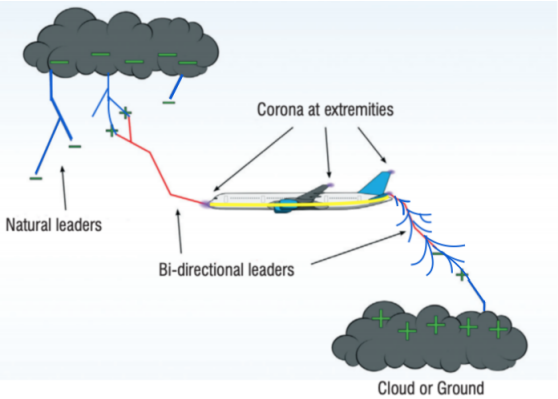

Figure 3.3: Leader approaching aircraft with the formation of the current channel

It is possible to consider also the case in which another branch of the leader reaches the ground before that there is the contact between this one and the branch from the aircraft, the return stroke will follow the original one, causing a die out of all the others branches. In this case the aircraft will not be involved in any damage.[7]

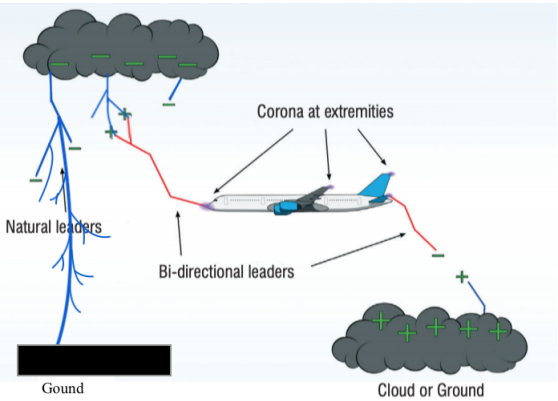

Figure 3.4: No Return stroke through the aircraft

It is important to underline that the aircraft triggered lightning occurs because of the aircraft presence and would not otherwise occur. When the aircraft has been struck, the current flows through the channel. The channel remains in its original location and considering the speed of the aircraft, it can move forward a significant distance during the life of the flash. Determined already the initial and exit points by the mechanism previously described, there are other attachment points on the surfaces, for example a nose or a wing, that corresponds to an attachment point, the motion of the aircraft through the lightning channel causes the channel sweep back over the surface. This phenomenon is the **swept-channel process**, as illustrated in Figure 3.5.

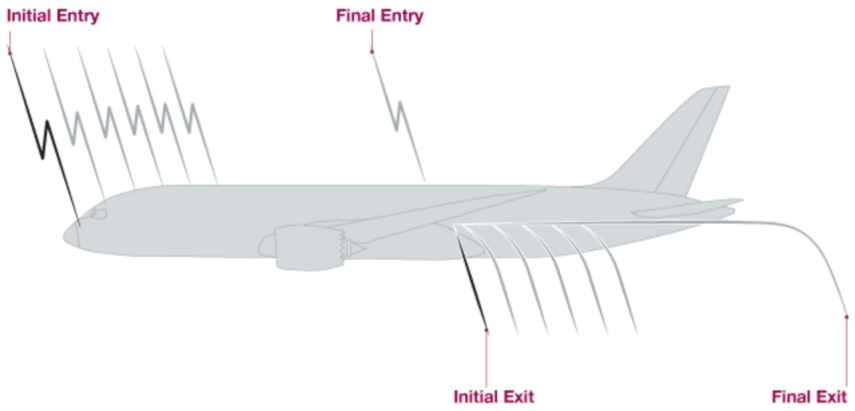

Figure 3.5: Typical path of swept-channel attachment point of an aircraft [13]

The characteristic of the surface can brings the lightning channel to reattach to and dwell at various surfaces locations for different period of time. This resulting in a series of successive lightning attachment points along the sweeping path. These following attachment points have been referred to as dwell points. Depending on the type of the aircraft skin material, it can be various the amount of damages produced at any dwell point by a swept channel[4].

3.3 Lightning attachment zones

Considering the lightning attachment mechanism, not all the surfaces of the aircraft are subjected to the same lightning environment components. In order to optimize lightning protection, zones definition and methods of locating them on particular aircraft are given in the documents: **ARP-5414 Aircraft Lightning Zoning** [4] **ARP-5412 Aircraft Lightning Environment and Related Test Waveform** [2]. So, an aircraft can be divided into the following zones:

- **Zone 1A**- *First return stroke zone*: all the areas of the aircraft surfaces where a first return stroke is likely during lightning channel attachment with a low expectation of flash hang on.
- **Zone 1B**- *First return stroke zone with long hang on*: all the areas of the aircraft surfaces where a first return stroke is likely during lightning channel attachment with a high expectation of flash hang on.
- **Zone 1C**- *Transition zone for first return stroke*: all the areas of the aircraft surfaces where a first return stroke of reduced amplitude is likely during lightning channel attachment with a low expectation of flash hang on.
- **Zone 2A**- *Swept stroke zone*: all the areas of the aircraft surfaces where subsequent return stroke is likely to be swept with a low expectation of flash hang on.
- **Zone 2B**- *Swept stroke zone with long hang on*: all the areas of the aircraft surfaces into which a lightning channel carrying a subsequent return stroke is likely to be swept with a high expectation of flash hang on.

- **Zone 3**- *Current conduction zone*: Those surfaces not in Zones 1A, 1B, 1C, 2A, or 2B, where any attachment of the lightning channel is unlikely, and those portions of the aircraft that lie beneath or between the other zones and/or conduct substantial amount of electrical current between direct or swept stroke attachment points.

It is important to consider that the location of the lightning strike zone of each aircraft is depending on the geometry and if a new or a modified aircraft is analogous to an existing aircraft whose zoning has been validated, the new or modified aircraft can be zoned in the same way as the existing one. Instead for what concern a completely new design, the entity of certification will use the zone location process catheterized by eight steps to determine the lightning zones. Taking into account the example of Figure 3.6, it corresponds of a map of the aircraft lightning zones, created by the aircraft designer that is used by the all aircraft design team during an aircraft development or modification; in order to understand and establish the protection schemes that will be appropriate protect the aircraft from dangerous condition due to lightning. [22]

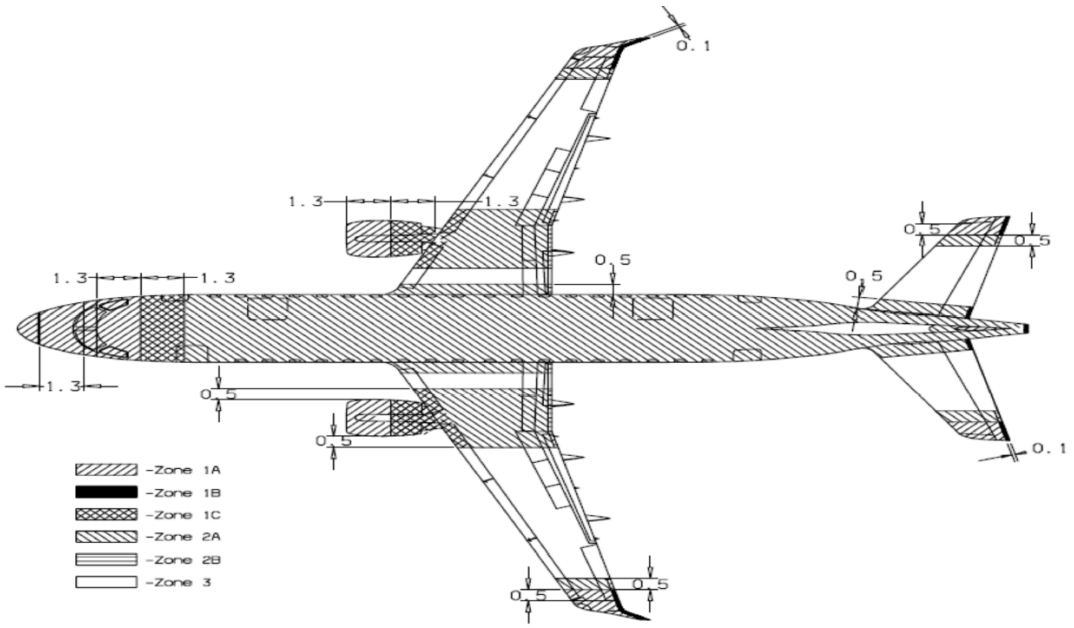

Figure 3.6: Example of lightning strike zoning for Transport-Aircraft [22]

Chapter 4

The Certification process

4.1 Introduction

Considering that an aircraft is usually struck by lightning once a year, this event it is considerable unpredictable and avoidable and can be mitigated if a specific protection is applied to avoid major safety issue for the aircraft. The purpose of this chapter is to describes the aircraft lightning protection included by the **Federal Aviation Administration (FAA)** in the ***Federal Aviation Regulations (FAR's)***.
For this reason aircraft manufacturers relying on regulatory documents, such ***Aerospace Recommended Practise (ARP)*** edited by **SAE international group**, which explains if their aircraft are adequately protected from the effect of lightning in compliance with the lightning certifications.[21] In the past decade, the aircraft protection requirements focus on a limited number of hazards, such fuel tanks, access panels or antennas while ignoring problems such as internal arcs and sparks sources as well as indirect effects on electrical and avionic systems.[6] But nowadays, aircraft lightning protection requirements and related standards have being updated periodically to reflect a refinement in the lightning environment and the demand of new aircraft design technologies, such as electronic control systems and advanced composite air frames. In the ARP 5412A [2], the waveforms represent idealized environments which are to be applied to the aircraft with the aim of analysis and testing. Must be taken in considerations that the waveforms don't have the task to replicate a specifics lightning event, but should be reproduce the same effects on the aircraft as those from natural lightning. In particular standard lightning environment include *voltage waveforms* and *current waveforms* components which represent the important characteristics of natural lightning flashes.

4.2 Idealized voltage waveforms

Taking into account of an increasing of electric field until the breakdown occurs. The breakdown is due of the puncture of solid insulation, such as the fiberglass skin of radome, or flashover through the air or across the insulating surface. What have just been mentioned correspond to the main issues which are at the base of the

test analysis which vehicles are subjected. Indeed, the voltage waveforms presented in the document[2], included several voltage waveforms intended to represent the electric field surrounding an aircraft immediately preceding lightning attachment. The influence of voltage waveform on the attachment points of aircraft models is characterized in particular for the waveform (Waveform A) with a fast rising and a production of a small number of attachment points, instead slow front waveform (Waveform D) produce a greater spread of attachment points. Follow are presented the different types of waveforms:

- **Voltage Waveform A**: rises with a rate of $1000kV/\mu s(\pm 50\%)$ until breakdown occurs due to the puncture of, or flashover, the object under test. At that time the voltage collapse to zero. If breakdown does not occur (open circuit voltage of a lightning voltage generator) the decay time of the voltage is not specified.

- **Voltage Waveform B**: is a $1.2\mu s \times 50\mu s$ electrical industry standard waveform for impulse dielectric tests. It rises to crest in $1.2\mu s(\pm 20\%)$ and decays to half of crest amplitude in $50\mu s(\pm 20\%)$. Time to crest and decay time refer to the open circuit voltage of a lightning voltage generator and assume that the waveform is not limited by puncture or flashover of the object under test.

- **Voltage Waveform C**: is a chopped voltage which the breakdown occurs at $2\mu s(\pm 50\%)$ and the amplitude of the voltage at time of breakdown and the rate-of-rise of voltage prior to breakdown are not specified.

- **Voltage Waveform D**: has a slow fronted due to a rise time between 50 and 250 μs so as to allows time for streamers to develop an object. It should give a higher strike rate to the low probability regions than otherwise might have been expected.

4.3 Idealized current component

The lightning injection current is not reproducible from one event to another, but can be observed typical signature on all events. This is why normalization standards have tried to define generic waveforms with which system must comply. From all the organs of certification as **RTCA**[23], **EUROCAE** [10], have been designed and defined the waveforms sequences. Following the documentation of [2], the external lightning environment is characterized by these current components: **A,** A_h**, B, C, D** and **H**, the **multiple stroke (MS)** and **multiple burst (MB)**, where **MS** is included of component **D** and **D/2** and **MB** is included of component **H** pulse sequences. It is possible to observe the entire waveform in Figure4.1, which is composed by 4 subsequent elementary waveforms. In particular for evaluating direct effects, it must be taken as a reference the Table 4.1, each having a large action integral. Instead for evaluating indirect effects are applicable the current components **A** and **D**, and waveform sets **MS** and **MB**, as referred in Table 4.2.
The *action integral* (AI), corresponds to the time integral of the current squared and represents the ability of the current to deposit energy in a resistive object. In this way, having a large action integral allows to characterize large current amplitudes or long persistence time.[11]

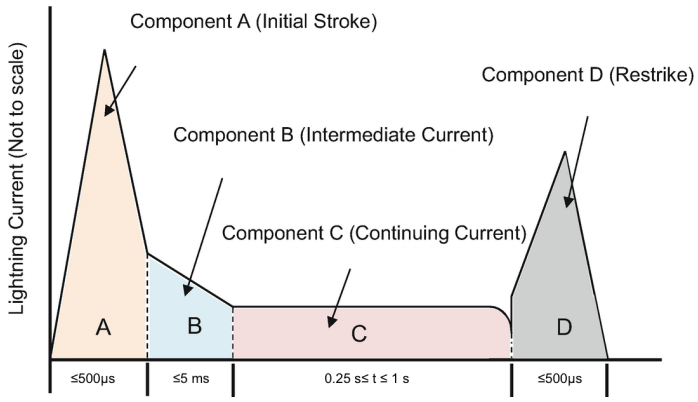

Figure 4.1: Typical lightning current components[10][23]

Direct Effects	Amplitude	Time duration
Component A- Initial Stoke	200 kA($\pm$10%)	$\leq 500\mu s$
Component B- Intermediate Current	2 kA($\pm$20%)	$\leq 5ms$
Component C- Continuing Current	200-800 A	$0.25 \leq t \leq 1ms$
Component D- Restrike	100 kA($\pm$10%)	$\leq 500\mu s$

Table 4.1: Table related to Current Components for Direct Effects Testing [2]

Starting to analyze in more detail, the current components:

- **Current Component A- Initial Stroke**: is a mix of positive and negative parameters of first return stroke, and it takes place when the aircraft flying at low altitudes. This waveform is used both for Direct and Indirect Effects.
  For Direct Effects, all the parameters summarized in Table 4.1, must be taken into account. For the analysis of Indirect Effects, on which the thesis studies are focused, it must be considered the double exponential waveform show in Figure 4.2. This waveform mathematically is a double exponential governed by the expression:
  $$I(t) = I_0(e^{-\alpha t} - e^{-\beta t}) \tag{4.1}$$
  All parameters, used to carry out the thesis, are summarized in Table 4.2

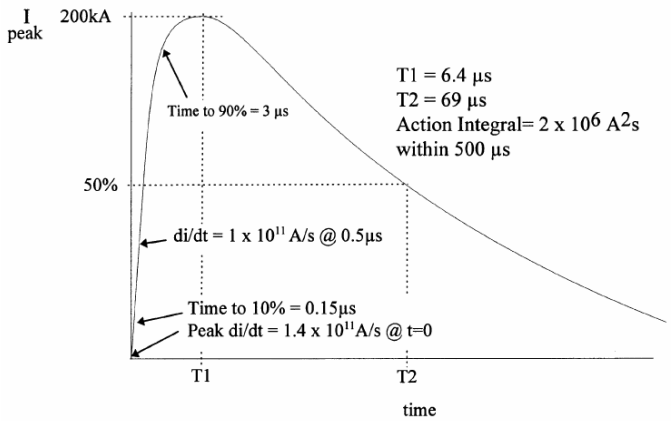

Figure 4.2: Current Component A- Indirect Effects [2]

- **Current Component A_h- Transition Zone Initial Stroke**: this waveform represents the estimated shape of first return stroke (Component A) at higher altitude; for analysis purpose a double exponential is used with the same Equation 4.1, but with different values summarized in Table 4.2.

- **Current Component B- Intermediate Current**: this waveform represents mainly the intermediate currents following some of the negative return stroke and/or restrike, for analysis purpose a double exponential is used with the same Equation 4.1, but with different values summarized in Table 4.2.
  This waveform typically is used for Direct effect analysis and should be unidirectional like a rectangular one, exponential one or linearly decaying.

- **Current Component C- Continuing Current**: the primary purpose of this waveform is charge transfer. The current represents the lightning environment, that might be caused by the long duration currents which may follow some restrikes as: of the negative cloud to ground lightning strikes and also of the return stroke of the positive cloud to ground flashes. This waveform typically used for Direct effect analysis and the geometrical forms it must have, are the same as those explained for the Component B.

- **Current Component D- Subsequent Stroke Current**: is used both for Direct and Indirect Effects. For Direct valuations this component represents a subsequent stroke. In particular, for Indirect effects, on which the thesis studies are focused, must be considered the double exponential waveform show in Figure4.3. This waveform represents the initial stroke in the **MS** and mathematically corresponds into a double exponential governed by the same expression used in the Equation 4.1, but with different values summarized in Table 4.2.

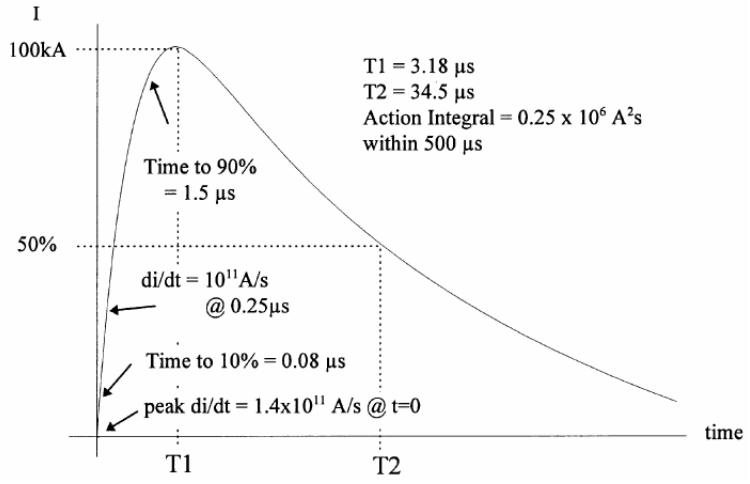

Figure 4.3: Current Component D- Indirect Effects [2]

- **Multiple Stroke Waveform Set**: is defined as a **current component D** followed by 13 components of D/2 distributed randomly over a period of up to 1.5 s according $10ms \leq \Delta t \leq 200ms$, as represented in Figure 4.4.

  The main purpose of **MS** is to evaluate system functional upset, more precisely of systems that can be sensible to effects of multiple induced transient

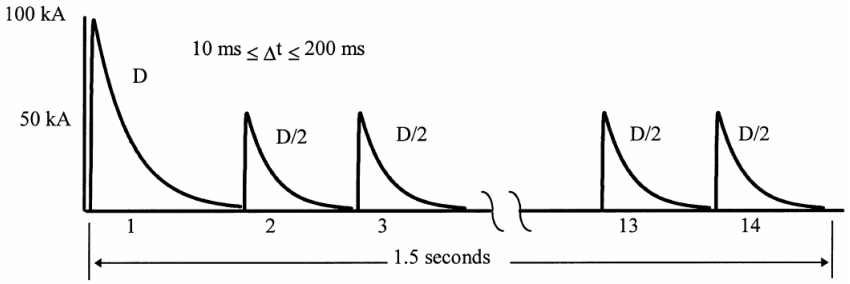

Figure 4.4: Example of a Multiple Stroke Waveform Set [2]

and it is not necessary that this set of waveforms is applied at the defined levels in a test. Instead, for what concern the internal environment due to a single component may be determined by test and **MS** combination of induced transients applied to the equipment. The **MS** waveform is used only for Indirect Effects evaluation and for analysis purpose D/2 waveforms parameters are identical to the current component D parameters with the exception of I_0, as referred in Table 4.2.

- **Multiple Burst Waveform Set**: consists of repetitive **Component H Waveforms**, which are characterized by a high rate of rise pulses whose amplitudes and time duration are much less than the one of a return stroke. It is important to take in consideration, that these impulses are always in groups at the starting of a lightning strike to an aircraft and in a randomly way for all lightning flash duration. Instead not will cause any physical damage to the aircraft, but only interference to certain systems due to the random and repetitive nature of these pulses. In general the recommended waveforms consist of a multiple of **Component H Waveforms**, characterized of 3 burst of 20 pulses each like in Figure 4.5 according $50\mu s \leq \Delta t \leq 1000\mu s$ and the 3 burst are distributed according $30ms \leq \Delta t \leq 300ms$, as in Figure 4.6.

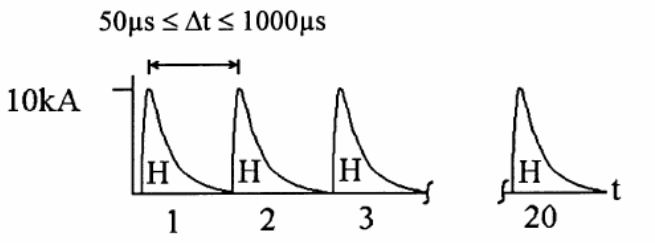

Figure 4.5: Multiple Burst Waveforms Set (it is highlighted that one burst is composed by 20 pulses) [2]

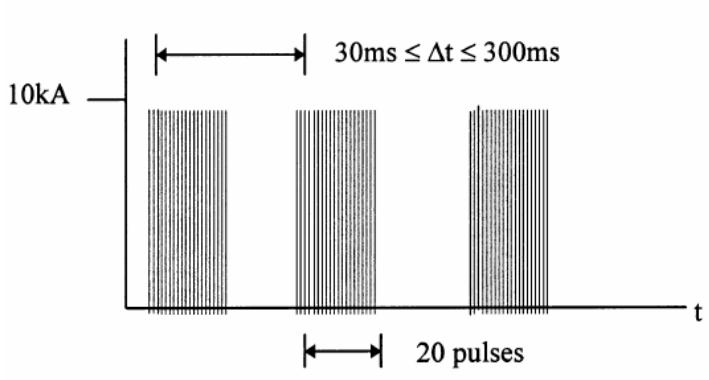

Figure 4.6: Multiple Burst Waveform Set [2]

The **MB** waveforms set is used only for Indirect Effects evaluation, as in Figure 4.7, and mathematically corresponds into a double exponential governed by the same expression used in the Equation 4.1, but with different values summarized in Table 4.2

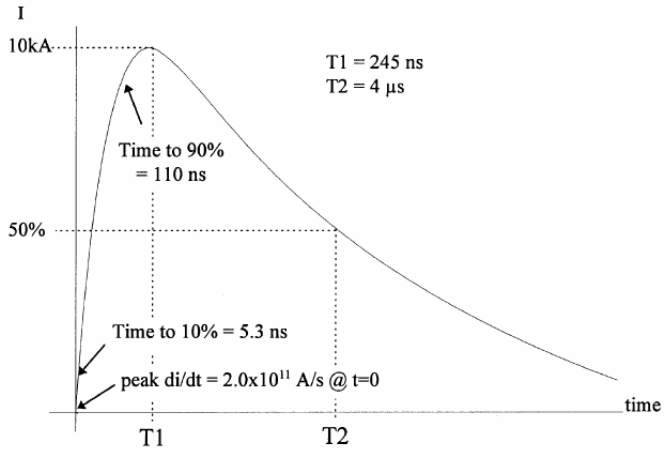

Figure 4.7: Current Component H- Indirect Effects [2]

Following is reported in Table 4.2, that contains a summary of lightning current components and of the parameters necessary for the double exponential definition.

Parameter	**Current Components**						
	A	A_h	B	C	D	D/2	H
$I_0(A)$	218.810	164.903	11.300	400	109.405	54.703	10.572
αs^{-1}	11.354	16.065	700	N/A	22.708	22.708	187.191
βs^{-1}	647.265	858.888	2.000	N/A	1.294.530	1.294.530	19.105.100
$I_{peak}(A)$	200.000	150.000	4.173	400	100.000	50.000	10.000
$di/dt_{max}(A/s)$	1.4×10^{11}	1.4×10^{11}	N/A	N/A	1.4×10^{11}	0.7×10^{11}	2.0×10^{11}
Action Integral (A^2s)	2.0×10^6	0.8×10^6	N/A	N/A	0.25×10^6	0.0625×10^6	N/A

Table 4.2: Table related to all Parameters of Idealized Current Components [2]

Summarizing, these waveforms can be applied for the evaluation used for both direct and indirect effects, but in appropriate way the waveforms for direct effects include voltage waveforms **A, B, C, D** and current components **A,** A_h**, C** and **D**,

together include the important characteristics of a severe natural lightning flash current although not all the components may strike everywhere the aircraft. Instead, waveforms for appropriate evaluation of indirect effects, include current components **A, D** and **H** which are individual components of the single stroke, **MS** and **MB** waveform sets. When the area of interest includes more than one zone, the evaluations of protection must be carried out utilizing the zone or zones characterized by the most critical environments. For most applications, the airframe is located in Zone 3 as well as one or more of the other zones (ex. Zone 1A,2A or 2B). In the following Table 4.3, it is possible to observed the relations between the application of the lightning environment waveforms and of the components of specific lightning strike zones (Chapter3.3). [11] [2][4].

Aircraft Zones	**Voltage Waveforms**				**Current Components**						
	A	**B**	**C**	**D**	**A**	A_h	**B**	**C**	**D**	**MS**	**MB**
1 A	X	X		X	X		X			X	X
1 B	X	X	X	X	X		X	X	X	X	X
1 C	X					X	X		X	X	X
2 A	X						X		X	X	X
2 B	X		X				X	X	X	X	X
3	X		X		X		X	X	X	X	X

Table 4.3: Application of Lightning Environment to Aircraft Zones [2]

Chapter 5

Lightning Effects on Aircraft

5.1 Introduction

Taking a look at the past after the beginning of powered flight, the Organizations have been focus their studies and tried out to find some solutions, considering the aircraft was hit by lightnings sometimes with very catastrophic results. The first aircraft cables were unable to conduct the currents of lightning stroke, causing cables explosion, caught fire of fuel tanks or even if several structural damage did not occur, pilots were shocked or burned by lightning currents, coming from their feet via control pedals or by hands via the stick. But going on with the years and with the advent of new types of aircraft, the catastrophic effects due to lightning were reduced and the ***Subcommittee of Aircraft Safety, Weather and Lightning Experts*** formed by the **National Advisory Committee for Aeronautics (NACA)** in 1938, it had the task of defining the additional necessary protection measures. During the successive years other organizations, such as **U.S National Bureau of Standards**, **Lightning and Transient Research Institute** began researches into Lightning effects on aircraft.
Certification bodies have categorized the overall lightning effects on the aircraft into three main categories: **Lightning Direct Effects (LDE)**, **Lightning Indirect Effects (LIE)** and **Effects** on the **Fuel System** . In particular this chapter is focus mainly on the **Direct Lightning Effects** and **Indirect Lightning Effects** and what types of consequences the aircraft is plagued with. There are two trends, in the design of aircraft, which can worsen the problems of the lightning effects; the first one is the increasing of using solid state components in aircraft electronics and electric power systems and even if these are more efficient, lighter, but they are inherently more susceptible to overvoltage produced by indirect effects. The second trend is the increasing of using reinforced in plastic and non conducting material in place of aluminium skins, a practise that reduces the electromagnetic shielding increasing the level of surges induced in wiring. With the increase of electronic systems in order to guarantee greater flight safety, in 1968 the **FAA, National Aeronautics and Space Organization (NASA)** and the **Department of Defence** initiates researches programs to measure how predict and how protects against the lightning effects.[12]
Taking as reference the Figure 5.1, it is possible to understand which are, by a

general view, the **Lightning Direct Effects (LDE)** and the **Lightning Indirect Effects (LIE)**. Considering that the **Indirect Effects** manifest themselves mainly in the electrical wiring of the aircraft and that they can be present anywhere in the aircraft also at equipment locations far from the lightning attachment points. Instead, the **Direct Effects** occur more often near the lightning attachment points or within structures or fuel tanks that lie within lightning current paths between strike entry or exit points.

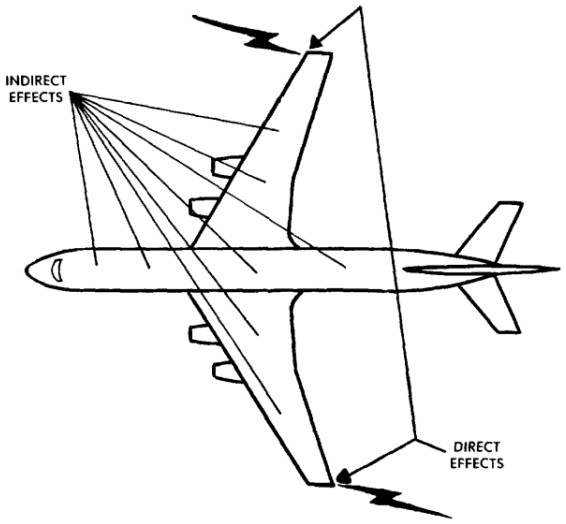

Figure 5.1: Areas of Direct and Indirect Effect [12]

5.2 Lightning Direct Effects (LDE)

The lightning strike commonly attaches to an aircraft nose, wing tips, vertical fin tip, horizontal stabilizer tips, propellers, antennas, pitot booms or pylon-mounted. These already mentioned are the places where the lightning arc attaches in a direct way to the aircraft, causing physical damages effects called **Direct Effects**, which correspond into skin hole at the point of flash attachment, welding or roughening of moveable hinges and puncturing or splintering of non-metallic structures.[11] The degree of exposure to lightning effect that correspond to the definition of **Susceptibility** of components, strongly depends on their location on the aircraft and using the lightning strike zone definition of Chapter 3.3, it is possible to established their vulnerability. For this reason aircraft protection techniques have been developed for protecting them from either type of lightning effect and in the particular case of *Direct Effects* should be include the following:

- In general electrical cables should not be exposed to the direct effect of lightning, but when this is unavoidable these cables should be covered by enclosures of conductive material with good mechanical and electrical properties.

- The interfaces between the vehicle surfaces and the elements of the vehicle, should be able to conducting the lightning current without destructive effects on structures and on the electrical systems.

- It should be present appropriates non-detrimental conductive paths (lightning bonds) between structures, components, joints, extremities to conduct/attenuate, or able to direct in a proper and safely way the applicable portion of the lightning currents and voltages.

- Design in proper ways the containers, tanks, lines and vents as not to be reached by any effects of a lightning flash because could be dangerous for the flammable fluids or gases contained in these solids.

Following are presented some common examples which occur on aircraft, in order to understand this kind of effects and the attention that need the aircraft designer when project the aircraft.

5.2.1 Direct Effects on Skin Structures

The outer skins of the aircraft and the internal framework characterized by ribs, bullheads and spars, that are the components in which the lightning current flows between the entry and exit point of the aircraft and tends to spread out between attachment points, making the aircraft an entire conductor. Any conductive material, metal or conductive composite with which most of these structures are fabricated becomes part of the conductive path for lightning current. Despite the current density is high in a single point of the surface of the aircraft, rarely this causes a physical damage, instead it is what does happen when there is not a good electrical bond between the structural elements.
From the effects which suffers the skin, both metallic and CFC-composite, it is possible to include:

- *melting or burning* at the lightning attachment points and it is possible to evidence the presence of pit marks along the fuselage or holes in the final part of the edges or empennage tips. Most of the time the holes are present in skins of 1mm (0.040") thick instead in case of trailing edge, where the leader attached the skin for longer time, it could happen a melting or burning of this thicker surfaces.

- *magnetic force* damage could be the result of the intense magnetic field which accompany the lightning current near the attachment points. This kind of damage is not enough significant to require an abortion of flight, but if severe bending metal is involved the damage is not more repairable.

- *resistive temperature rise* is due by lightning currents that deposit the energy in the conductor. When the lightning occur, the most part of metal is able to tolerate it without overheating, but this is not true for all. For this reasons there are methods for determines temperature rises in cases of specific materials.

- *shock wave and overpressure*, occur when the lightning stroke current flows in the channel leader, for a time of $5 - 10\mu s$, causing an expansions of it with an increasing in velocity, until will propagate to the surface of the aircraft. Taking into account the distance between the channel and the surfaces (windshields or the navigation light), the result will be an overpressure of several 100 atmosphere at the surface that will cause an implosion.

Once presented the problematic effects and for the particular case of *melting or burning*, it is possible to see some examples of lightning testing on skins, in which are highlighted the types, evaluated the several thickness and other conditions like the thickness of protection painted material.
In case of a skin panel in Aluminium, which gives a very high degree of conductivity, have been encountered damages in Zone 1A, as in Figure 5.2. Instead, considering a

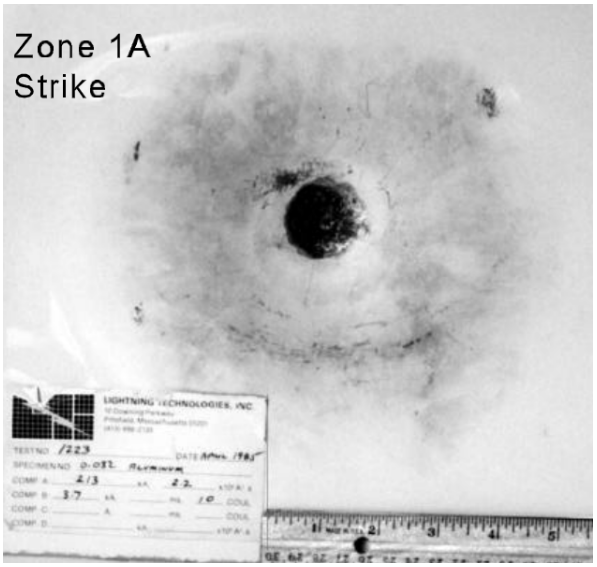

Figure 5.2: Aluminium panel (0.032") thick [24]

0.040" painted aluminum panel covered by aluminium tape, it is possible to see from the Figure 5.3 the completely reduction of the damage. As already seen in Figure

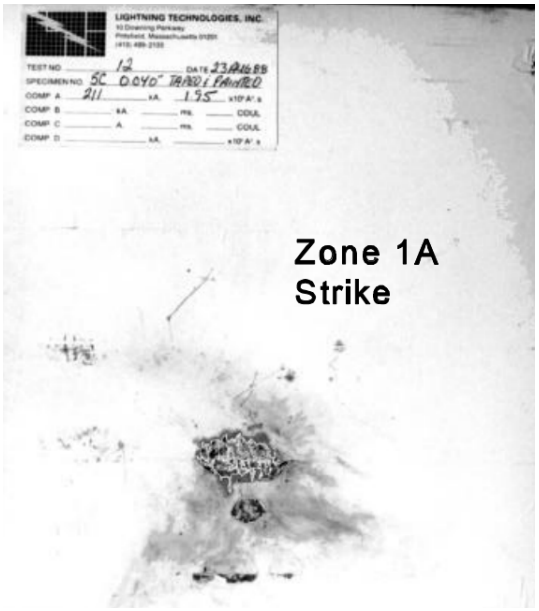

Figure 5.3: Painted aluminium panel covered by aluminium tape (0.040") thick [24]

5.3, the protection added to Aluminium skins increased the resistance to melting and burning, this because it is part of the methods implemented for the protection of Aluminium. For the particular case of Aluminium have been implemented four

methods, which are highlighted in Figure 5.4 for the completely reduction of the damages.

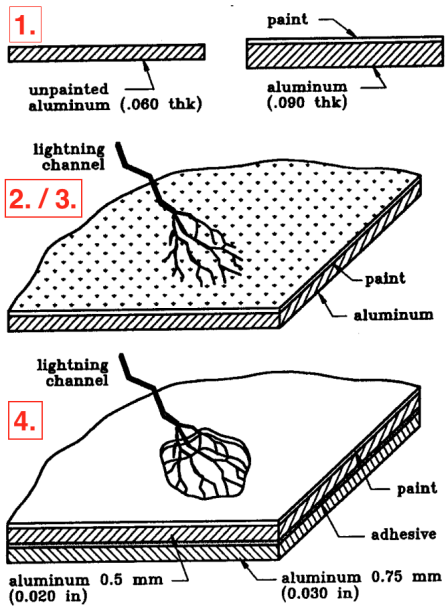

Figure 5.4: Methods for protecting against melting and burning [24]

1. Consist of the increase of skin thickness;
2. Insertion between the surfaces of a barrier of dielectric;
3. Addition in the upper surface of conductive particles, which lead to the lightning flash a major diffusion in these new multiples conduction paths.
4. Insertion of a thermal barrier between skin and inner layer.

Moreover, have been done also other studies on protection's techniques for the Non conductive composites and carbon fiber composites (CFC), which characterize other skin materials utilized for the realization of the aircraft.

5.3 Lightning Indirect Effects (LIE)

Indirect effects are the result of interactions of the electromagnetic fields accompanying a lightning flash to the aircraft, thus creating a transient internal environment for the lightning for the duration of the flash. [8]
The **Lightning Indirect effects**, occurs when in the electrical equipment of the aircraft there is a dysfunction or some damage due to the strike of lightning flashes. The lightning current travel on the skin's surface of the aircraft, with a strong magnetic flux and in accordance with changing due to the rapidly lightning current stroke. So, these **Lightning Indirect Effects (LIE)**, have the capability to induce transients into wires or in equipment under the skin, in particular from the in Figure 5.5, is represented the current path through the aircraft. Before that the electronics

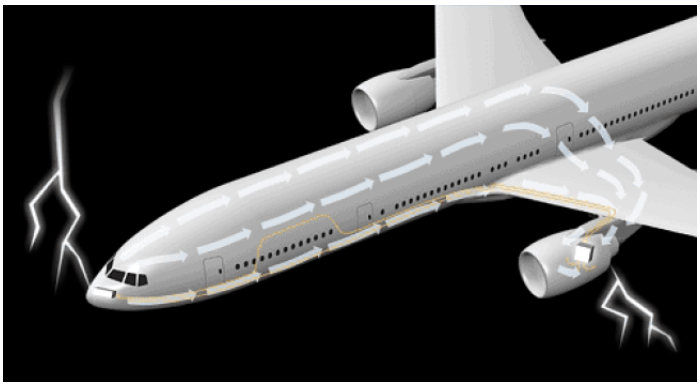

Figure 5.5: Typical current path of **Lightning Indirect Effect** [5]

in aircraft was miniaturized, indirect effects from external environment such precipitation and lighting were not a big problem, but with the advent of micro-electronics increased the sensibility to transient voltages. In order to avoid these problems in cables and in equipment caused by indirect effects several solution could be applied as good grounding, shielding, a use of surge suppression devices and every circuit that is critical or essential to continued safe flight and landing of an aircraft, must be verified by the manufacturers according by the regulations set by **FAA**.[12][11]
It is possible to notice that the practices already cited, involved the control of the lightning indirect effects, are also good for control of EMI- Electromagnetic Interferences and EMC- Electromagnetic Compability.
A strong influence on the indirect lightning effects was given by ***NEMP- Nuclear Electromagnetic Pulse***, in particularly for what concern the test technique developed in which current and voltage are injected into electronic equipment and into wiring. Other studies have been done on lightning indirect effects, in particular on *AEHP-Atmospheric Electricity Hazard Program*, conducted by *US Air Force*, *Boeing Military Airplane Company*. A reviewing on standard lightning test design and advisory documents, was edit by a **SAE- Society of Automotive Engineers** with the aim of coordinating US and European agreements between vary certifying agencies and at the end completed by **FAA**. Considering that NEMP is a phenomenon at which an aircraft will never be subjected, has a lot of similarities with lightning on an aircraft but also some differences like a shorter duration, not higher amplitude but more energy at higher frequency. In particular it is possible to observe from the Figure 5.6 that lightning has more energy than NEMPS at lower frequencies.

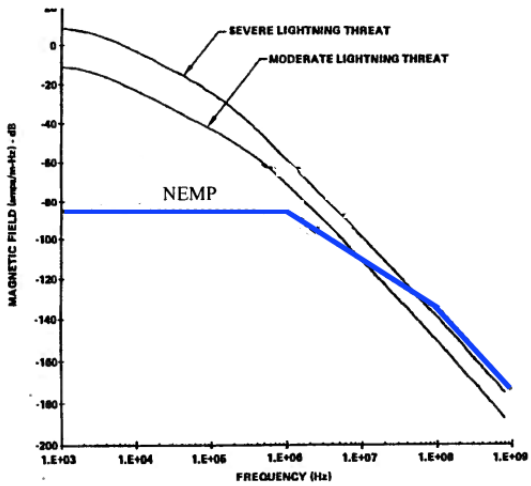

Figure 5.6: Comparison of spectra of lightning and NEMP [11]

5.3.1 Induced Effects

Theoretically, it is possible consider a metal aircraft as a Faraday screen that implies the need to distinguishes the electrical environments form the inside to the external of the aircraft. There are important mechanisms that concern on the *coupling of electrical energy* to the interior of the aircraft. The most characteristic parameters for lightning due to induced voltages are; the wiring length, shielding and the location of wiring respect to the apertures. The induced effects are also presents when externally aerials or navigation lights could be susceptible to direct injection of current, thus damaging avionics at which the aircraft wiring are connected. As consequence the cross-coupling and the relative inductance of the cables ensure a little currents through the fuselage. In order to avoid the strike to the external components should be ensured the housing into the main metallic structure of the aircraft is well bonded and the wiring are insulated from it [11]. The basic coupling methods are presented and analyzed below:

- **Magnetic induced Voltage** : the coupling into the wiring, occurs principally because of the magnetic field due by the lightning current flowing in the airframe. A continuous changing of the field will passes as a loop through the wiring and the structure causing the induced current/voltages. Figure5.7

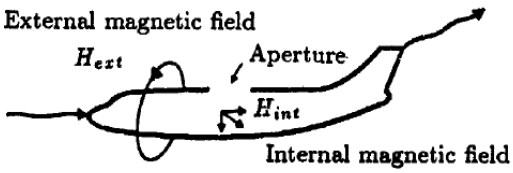

Figure 5.7: Magnetic field coupling in a aircraft[11]

Taking into account the positions of equipment that is not so important for the induced voltage, but what can make a large difference is the route of wiring between them. Considering an aluminum aircraft that is not a closed structure, but characterized by the presence of holes, electrical apertures ex. doors and windows, should gives in phase of design a high level protection for internal wiring. Instead areas realized in composite materials, do not allow the same shielding effect of Aluminium and it is possible to consider them as electromagnetic apertures during the lightning effects. Remembering the Lenz's law, a changing magnetic field that goes through a loop, generates an open circuit voltage in that loop, given by:

$$V = \frac{d\phi}{dt} \tag{5.1}$$

where $\phi = 4\pi 10^{-7} H \times A$, is the total magnetic flux passing through the loop of area A and H is the magnetic field strength.[11] Taking as example the Figure5.8, corresponds to a representative circuit equipment where the wires are bonded at each end with the metallic structure of the aircraft. ϕ is depen-

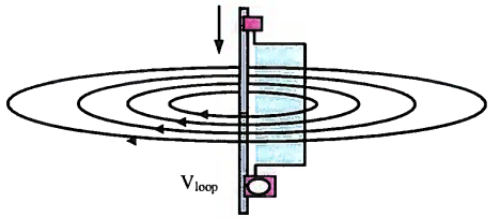

Figure 5.8: Magnetic flux that induced a voltage in a wire connected at the two extremities of the metallic structures [14]

dent on the dimension of the loop, if the cables are close to the structure, it will be minimized or it's not present the voltage induced.

It is possible to observe the behaviour of the magnetic field inside a metallic fuselage as in Figure 5.9, but in proximities of the apertures (ex. multiple windows) some line of flux penetrate inside.

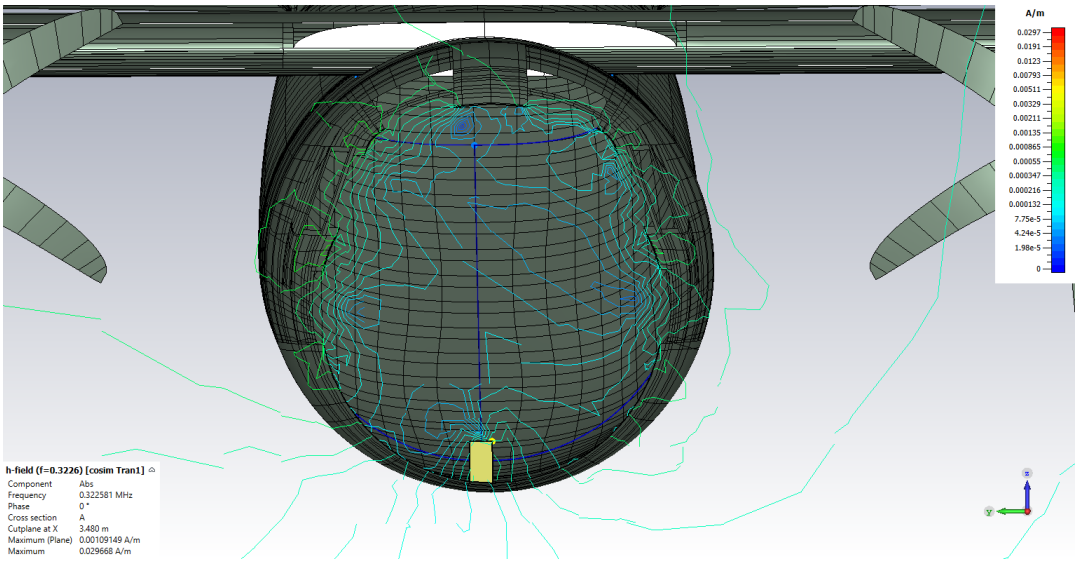

Figure 5.9: Magnetic field lines in a fuselage with windows.

In general in the aircraft the wiring are place adjacent to the metallic skin in order to minimize the loop size and the induced transient levels.[14]

- **E-Field coupling**: consists into involve the E-Field that pass through apertures, like in Figure 5.10, to the interior of aircraft.
  At this mechanism is possible to associate a capacitive coupling, where one

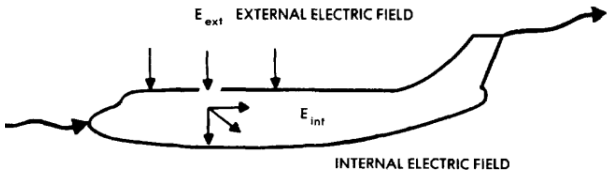

Figure 5.10: Electric field coupling in a aircraft[11]

"plate" of the capacitor is external to the aircraft, and the other is the aircraft, including the wiring exposed beneath open apertures has charge induced appropriate to this electric field. The current will flows in the exposed wirings, if the E-field changes in a rapid way, the magnitude of the coupling can be related to the magnitude of E-field. In metal aircraft, this type of coupling is present through the apertures, since any thickness of metal gives good shielding against the electric field, unlike with pieces in composite this may or not be happen.

- **Resistive Voltage**: is another coupling mechanism related to the electric field produced along the inner surface of the aircraft, with the flow of current through resistance. Figure 5.11

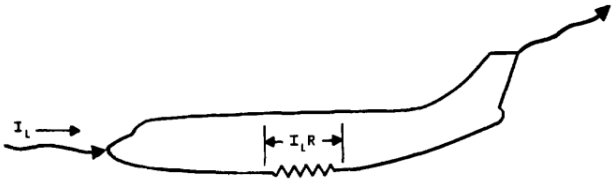

Figure 5.11: Resistive coupling in a aircraft[11]

In a more practical way, it possible to consider that due to the current passage, there is a resistive voltage rise, which corresponds to a source that is applied to an external circuit, in this case the aircraft's wiring. This process could be exploit with the classic IR mechanism. For example if the lightning, strikes a light in a wing, the current will flow through the resistance and the voltage rise having the same waveform of the lightning flash, but is not always true because of the inductance and capacitance of the wire. Also, it is possible to cite the fact that, this effect of joint resistance on circuit is in a high way influenced by the manner in which the circuit is grounded.

- **Skin Effect**: it has a considerable relevance on the structures, especially the one fabricate in carbon fiber composites. In a conductor the current does not flows in a uniform way within the cross section of the metal, but flows on that surface of the conductor which is closest to the return path and hence is close to the magnetic and electric fields accompanying the current. The penetration of current depends from materials resistivity and frequency, considering an Aluminium skin of an aircraft, it has a low resistance that enable skin effect to keep the current and fields outer surface. For pure Aluminum, taking a very high frequency at which there is significant lightning energy in the high current pulses of lightning, it is possible to calculate the skin depth in this way:

$$\delta = \sqrt{\frac{\rho}{\pi \mu_o f}} \tag{5.2}$$

For pulse of current, like lightning with a very wide spectrum, it is more convenient to work in the time domain.[14][11] [18]

It is possible to reduce the induced transients due to the lightning effects; with the use of shielding as to reduce the peak voltages, where aperture effects are the main responsible for the induced coupling. Remembering the Example done in Figure 5.8, at the same wire is applied a shield and if is bonded back at the two extremities, then the shield will conduct part of the lightning current along it and if the shield is a perfect conductor, there not be the presence of the flux and the wires will not be affected from induced voltage, taking as reference the Figure 5.12. The shielding cables for the lightning effects are inefficient as long as they are bonded back at both ends, in fact they typically have a resistance that limits the flow of current on the shield, but some flux is able to penetrate the loop causing the induced voltage generated on the side of the screen, given by:

$$V = I_{screen} \times Z_T \tag{5.3}$$

where Z_T is the screen transfer impedance.

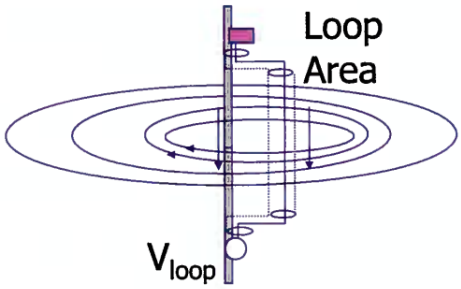

Figure 5.12: Resistive coupling in a aircraft[11]

5.3.2 Certification of Aircraft Electrical/Electronic System for the Lightning Indirect Effects

It was redacted by the **SAE Aerospace Recommended Practice (ARP)** a guidance for showing the compliance with the regulations for hazards caused by lightning environment to electronic and electrical systems, that are presents in the external/internal portions of the aircraft. Mainly the equipment hazards addressed include those due to indirect effects on the equipment and the associated wiring that is mounted on the aircraft exterior as well as indirect effects on equipment and its associated wiring located within the aircraft interior. In order to certificate an aircraft with respect to the indirect effects of lightning, the applicants must follow this iterative process characterized by seven activities:

1. **Control the safety analysis with respect to the indirect effects of lightning on the aircraft**: in particular is valuated the behaviour of **FHA-Functional Hazard Assessment**, in order to classify and identify that any indirect effects of lightning as a common mode. The failure conditions reported in the Table5.1 below, are useful to help the applicant to understand their severity:

Severity classes	Description of the Effects
Catastrophic	Failure Conditions which would impeded safe flight and landing
Hazardous/Severe-Major	Failure Conditions which would reduce the capability of the aircraft or the one of the crew to cope with hostile operating conditions to the extend that there would be: - Great reduction in safety margins or functional capabilities; - Physical danger or higher workload for the flight crew could not be able to perform their tasks; - Serious injury to a small number of occupants.
Major	Failure Conditions which would reduce the capability of the aircraft or the one of the crew to cope with adverse operating conditions to the extend that there would be: - Significant reduction in safety margins or functional capabilities; - Significant increase in crew workload or in conditions impairing crew efficiency; - Discomfort to occupants and possibly injuries.
Minor	Failure Conditions which would not significantly reduce aircraft safety and which involve crew actions that are well within their capability, for example: - Slight reduction in safety margins or functional capability ; - Slight increase in crew workload like the routine flight plan changes; - Some inconvenient to occupants.
No Effects	Failure Conditions which do not affect on safety and on the operational capability of the aircraft or increase in crew workload

Table 5.1: Failure conditions classifications [3]

It is important to consider that the development assurance level related, in Table 5.2, to the failure conditions classifications, would also be assessed when performing the **FHA**.

Level A	Electrical and electronic system whose failure would causes or contributes to a failure of functions resulting in a Catastrophic failure conditions for the aircraft
Level B	Electrical and electronic system whose failure would causes or contributes to a failure of functions resulting in a Hazardous/Severe major failure conditions for the aircraft
Level C	Electrical and electronic system whose failure would causes or contributes to a failure of functions resulting in a Major failure conditions for the aircraft
Level D	Electrical and electronic system whose failure would causes or contributes to a failure of functions resulting in a minor failure conditions for the aircraft; once a system has been confirmed, the certification authority will no apply further application of this required
Level E	Electrical and electronic system whose failure would causes or contributes to a failure of function resulting in a no effect conditions for the aircraft; once a system has been confirmed, the certification authority will no apply further application of this required

Table 5.2: Assurance levels related to Failure conditions classifications [3]

2. **Determine the lightning strike zones for the aircraft**: already discussed in Chapter 3.3.

3. **Establish the airframe lightning current paths for the zones**: in the interaction of the lightning flash with the external environment of the aircraft are already represented in Chapter 4.3, the waveforms of the lightning current components at the aircraft surfaces.

4. **Establish the effects of the internal environment**: consist of the electromagnetic fields and structural IR voltage already presented in Chapter 5.3.1. In order to qualify a system, should be determined the lightning induced voltage and current waveforms and the **ATL- Actual Transient Level** that can manifest at the interfaces of the electronic devices. Should be notice that when were defined the induced transients in term of open circuit voltage and short circuit current appearing at wiring/equipment interfaces, the "v" and "i" will be correlated to the source impedance of the interconnecting wiring.

5. **Establish the TCL-Transient Control Level and the ETDL-Equipment Transient Design Levels**: The **TCL** philosophy is possible to understand looking at the Figure 5.13 and are set to be $\geq$ than the maximum **ATL**. The **ETDL** and **TCL** are set by airframe manufacturers, in order to establish the right combination of them basing on the penalties of vehicle or interconnecting wiring protection or equipment hardening. The difference between **ETDL** and

TCL is the *Margin*. The **ETDCL**, corresponds to the amplitude of voltage or current that should have the equipment to stand and remain operative. The **ETSL-Equipment Transient Susceptibility Level** corresponds to the amplitude of voltage or current applied on the equipment in order to cause it is upset and can no more perform it is function. The **ETDLs** establishes the characteristics of the electronic/electrical equipment and are represented as standardization of them in order to simplify compliance evaluations.

6. **Verify compliance**: of the **ATLs** that are present at wiring/equipment interfaces must not cross the **TCLs**, and that the equipment can tolerate the **ETDLs**.

7. **Corrective Measures**: improve the methodology of the lightning protection when test not achieve the right goals, by optimizing the use of installation design techniques and equipment design.

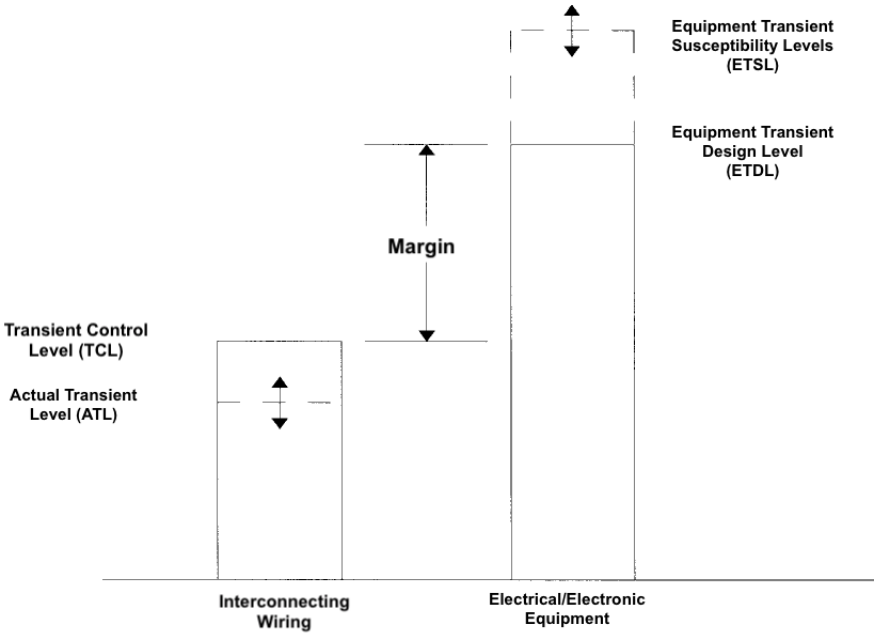

Figure 5.13: Relationship between Transient Levels [3]

Chapter 6

Simulation Methodology for the evaluation of the Lightning Indirect Effects (LIE)

6.1 Introduction

The already discussed effects and certifications on the **Lighting Indirect Effects**, were considered as a starting track to introduces the principal focus of the thesis, that discusses about of a ***Simulation Methodology for the evaluation of Lightning Indirect Effect on a 3D Digital Mock-up Model of a Transport-Aircraft***.
Firstly in order to facilitate the issue, as initial approach it has been done on a simplified 3D structure as the one of a **Cylinder**. In order to investigate and simulated virtually the Lightning Indirect effects on a simplified structured, the tool **CST Studio Suite** was used, exploiting the capabilities of two interacting software packages:

- **CST MICROWAVE STUDIO**, dedicated for fast, accurate **3D EM** analysis and design in the high frequency range. It simplifies the process of creating the structures by providing a powerful-graphical solid modeling. After the model has been constructed, an automatically meshing procedure is applied before a simulation engine is started. An advanced visualization engine and flexible post-processing allow to analyze and improve the design in a relevant efficient way. The software contains different simulation techniques, to best suits the various applications, as time domain solvers, frequency domain solver, integral equation solver etc. This thesis principally was conducted using the **Time domain solver**, which can obtain the entire broadband frequency behavior of the simulated device from a single calculation run. From the two time domain solvers that this package offers, in which in both were used the *hexaedrical mesh*, for the conducted studied, the the *Transmission-Line Matrix (TLM)* method was used.

- **CST CABLE STUDIO**, is an electromagnetic simulation tool especially designed for the fast and accurate investigation of real-world cables in complex

electromagnetic environments. Moreover, it gives the possibility to investigate multi-scales problems for instance, cables with dimensions down to micrometer range built in cars or towers. For the particular case of the thesis for the aircraft, with overall dimension in meter. It gives the possibility to use different types of cables as: single wires, twisted cables, ribbon cables and coaxial cables / shielded wires. It is very useful, because generates equivalent circuits from the cable harness, based on classical transmission lines theory and meshes in automatically the cable harness along its length and calculate the transmission line parameters.

Being the simulation campaign certification-oriented, referring to the thesis, in case of the aircraft mock-up, several test were done and different entry and exit points configurations were tested, according to the zones of major probability of lightning attachment. Instead, in the particular case of the simplified **Cylinder** structure, it was considered only one configuration related to the entry/exit point.

6.2 Virtual Testing of LIE on a simplified Cylindrical structure

The thesis focuses on the evaluation of the Lightning Indirect Effects (LIE) on a simplified 3D Digital Mock-up Model of a Transport-Aircraft, but as starting point was used the **CST Studio Suite** to conduct some simulation on a simplified **3D structure** as the one of a **Cylinder**, so that it represents the fuselage. In particular this first 3D model represented in Figure 6.1 was used as sketch for all the successive examples.

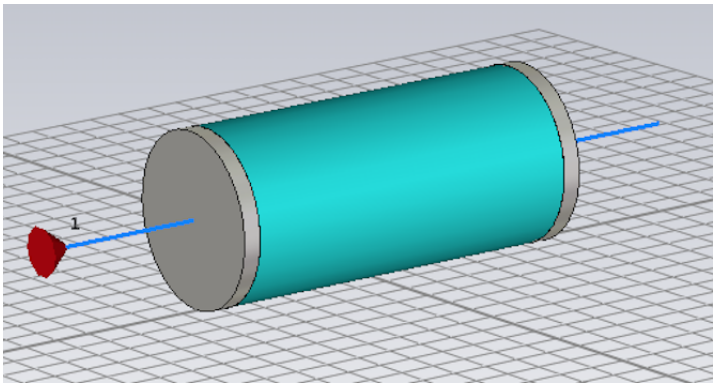

Figure 6.1: Structure of a 3D Cylinder

The materials used to realized the **3D Cylinder** are :

- **PEC***, for the two caps (*end_cap*1) and (*end_cap*1_1), respectively with the **dimension** 0.5 m of radius;
- **Thin panel of graphite**, for the whole structure with:

Dimensions	*Values*
Thickness	1 mm
Length	2 m
Real part of ϵ	1
μ	1
Electric Conductivity	20000 S/m

Table 6.1: Dimensions and values that characterize, for the case in question, the Graphite

PEC*-Perfectly Electric Conducting

PEC materials are those that are through of as exhibiting infinite conductivity, they do not produce losses although the material, it is an idealization and is very useful for very good conducting materials, in particular it should be presents as PEC materials that can be simulated much faster than "real" materials with finite conductivity.

6.2.1 Model Setup

There are several important factors to be considered in lightning analysis:

- **Transient current**:
  The lightning produces a high intensity transient current according to the Standard waveforms already cited in Chapter 4.3. The Transient current can be simulated directly using Time-domain TLM as illustrated in Figure 6.2, that corresponds to the double-exponential **Component A**, used for the LIE. In order that the simulation starts, the **Component A** is inserted at the entrance to the **lightning channel** by the **Current Port** shown in Figure 6.1. In order that the double-exponential will be sets, the following dimensions were used, in the Table 6.2:

Name	Value
$t_{amplitude}$	218810
t_{fall}	88.07
t_{rise}	1.55
t_{total}	100

Table 6.2: Parameters to set Double-exponential **Component A**

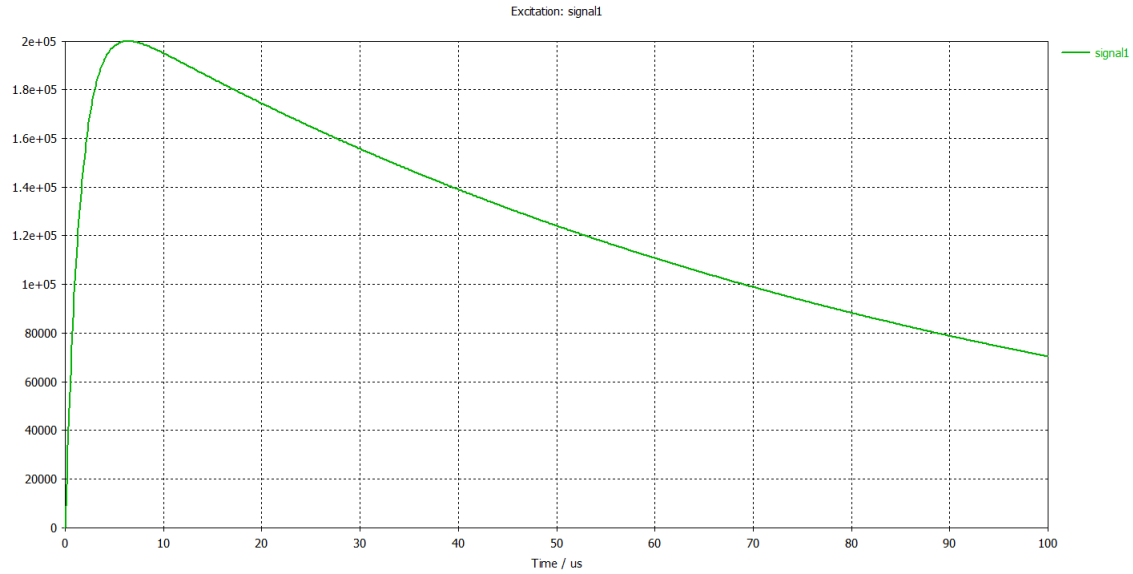

Figure 6.2: Double-exponential component A

- **Frequency Spectrum**:
  It is possible to use the *Discrete Fourier Transform (DTF)* in order to transform the signals in **time domain** into those in the **frequency domain** and eventually evaluated the energy spectrum. The lightning is a relatively low-frequency phenomenon (below 10 MHz) with respect to HIRF (up to 40 GHz) and as it is illustrated in Figure 6.3, this spectrum corresponds to the (DTF) of the double exponential of the component A.

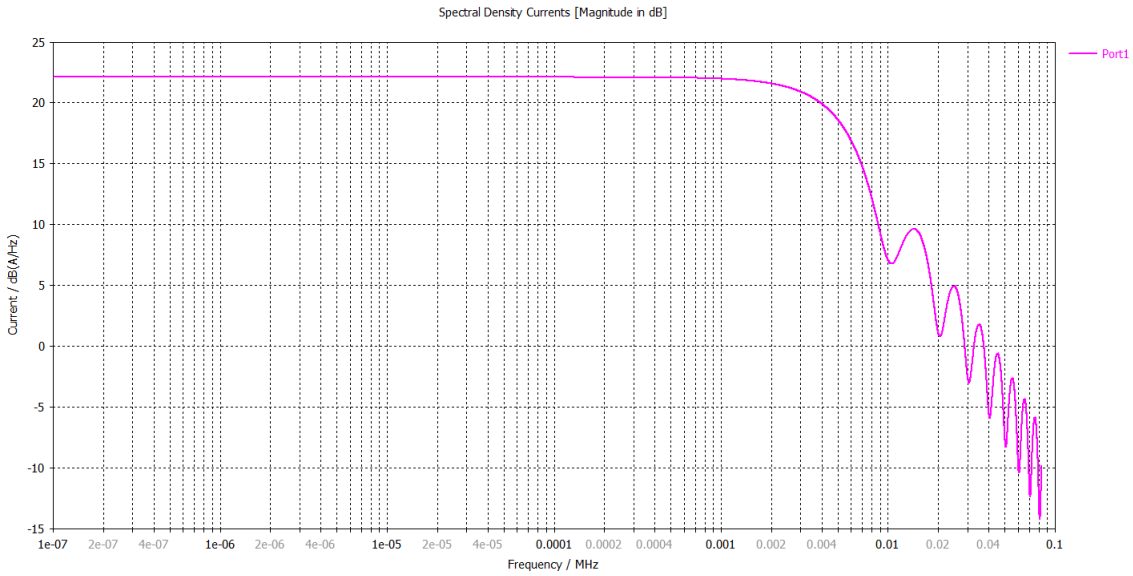

Figure 6.3: Frequency spectrum

6.2.2 Simulation Settings

- **Boundaries**
  Boundaries setting is important because the program is only capable of calculating problems that have finite expansion and so, it should specifies the boundaries conditions, by the dialog box. The boundary conditions are automatically set to "open", as illustrated in Figure 6.4, extending the touching geometry virtually to infinite allowing to any fields radiated from the structures to be absorbed, connecting the entry and exit wires to the open boundaries avoids artificial reflections. By default the TLM-solver uses 377Ω surface impedance for open boundaries.

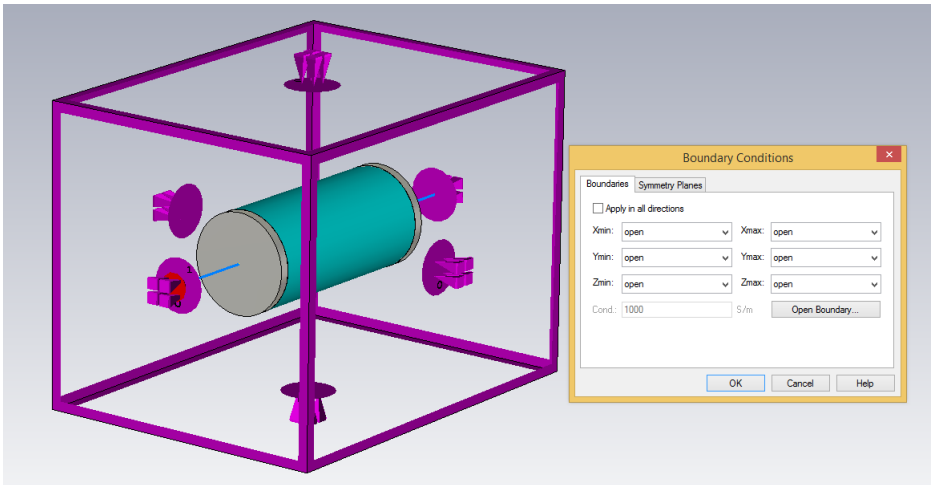

Figure 6.4: Frequency boundaries

- **Hexahedral Meshing:**
  Corresponds to the way in which the structure under study is discretized and this strongly influences the accuracy of the results. The computed results, converge towards the "continuous world" results when the mesh size get smaller and smaller until the discrete lengths vanish or, being more exact, became differentials. So, generally speaking the structure and the fields are simulated best with a finer mesh. The mesh generator determines the important features of the structure and automatically create a mesh, which represents the interested structure and the field equally well. In particular for structured hexahedral meshes cell size can be defined independently in x,y,z directions, it is simply the length of the x,y, z edge of the cell. In the particular case of high-frequency EM simulations, the maximum cell size is often defined with respect to the wavelength, in order to provide an optimal spatial sampling rate for the fields inside the structure. Increasing the number of cells per wavelength this leads to a higher accuracy, but also increases the total calculation time and overall simulation speed. So, in general is important to try to find a good compromise between them.

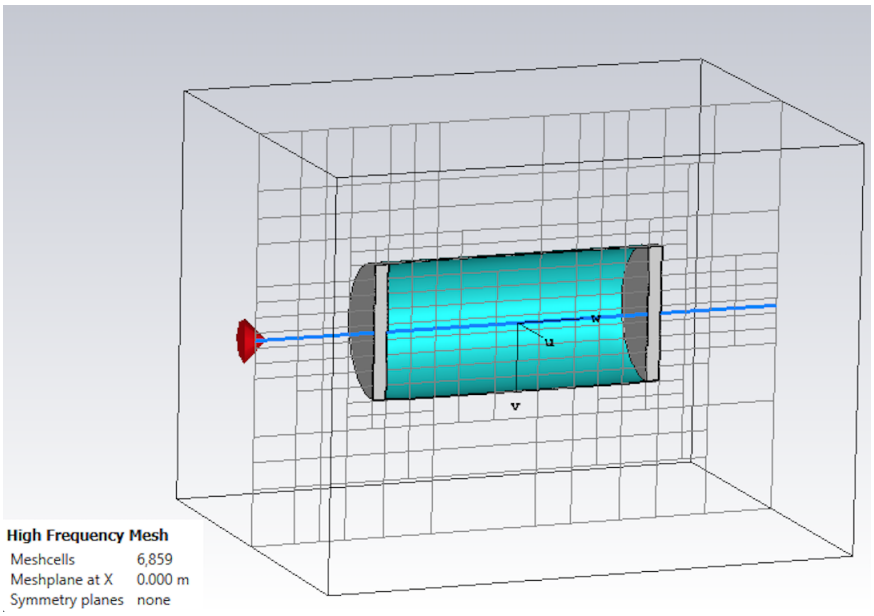

Figure 6.5: Mesh

- **Insertion of Astrostrike:**
  Consists in a new material that will use as Lightning protection, and usually is add on top of other materials as a stack. In the following Table 6.3 are resumed all the characteristics:

Dimension	***Values***
Thickness	1 mm
Width	5 mm
Real part of ϵ	1
μ	1
Electric Conductivity	$5.8e^7$ S/m

Table 6.3: Parameters for the Astrostrike.

6.2.3 Process steps

At the beginning was realized a Cable, always inside of the Cylinder structure, using the intrinsic functionality of the tool Full-Wave TLM. Then, it was realized a new project by the use of **CST Cable Studio** in which was inserted a *Coaxial_Cable_prova* as it is possible to see from the Figure 6.6.
This cable was realized thanks to the function of "Cable Bundle" from a "Curve", taking into account that the wire was the one internal to the Cylinder of the file realized in **CST MICROWAVE STUDIO**.
CST CABLE STUDIO uses the powerful 3D solid modeling front end of **CST MICROWAVE STUDIO** to set it up or to import arbitrary metallic 3D shapes, ranging from the simple ground planes to complex chassis structures as the aircraft. Moreover, the powerful 3D full-wave solver from **CST MICROWAVE STUDIO** is used to calculate the electromagnetic field in the environment cables. All this was done because the target of interest was to make a comparison between this two file CST CABLE STUDIO *EMC_lightning3cable* and the measure done with TLM.

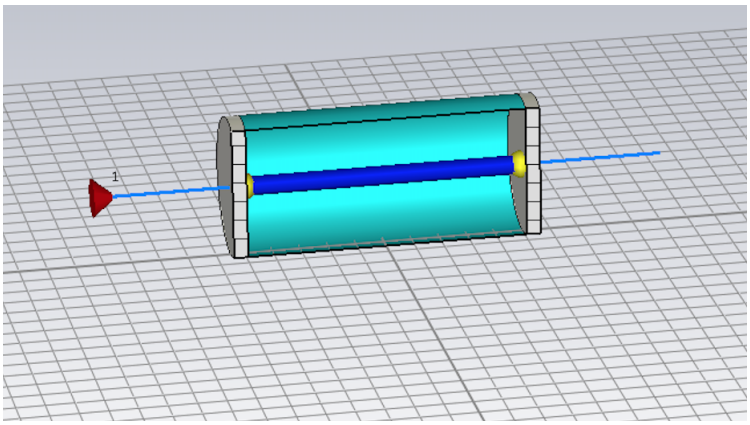

Figure 6.6: Cable inside the Cylinder.

In the following Figure 6.7 is represented the Cross Section Cable and in the Table 7.3 all its characteristics:

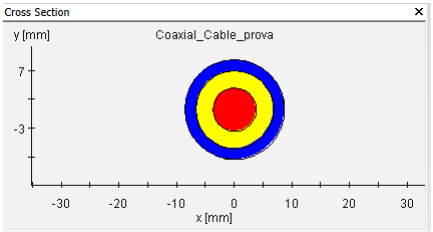

Figure 6.7: Cable Cross Section

	Shape type	Material	Diamiter	Thickness
wire	Circle	CU	7.514 mm	
insulator inside	Wrap	Air		3mm
screen	Circle	CU	17.3 mm	
insulator outside	Wrap	Air		0.01mm

Table 6.4: Cross-Section of wire

In the interface of **CST CABLE STUDIO**, it is important to highlight that there is a main view composed of :

- 3D
- Schematic

by selecting the Schematic tab, one can change the view in which is possible to define and edit loads on equivalent circuits of the cable harness by the help of the schematic editor. If further enables the circuit simulation of the whole system in time and frequency domains, while maintaining a tight interface with the 3D transient solvers to easily exchange impressed current and voltages.

For this specific case in question, it is possible to observe the schematic illustrate in the Figure 6.8:

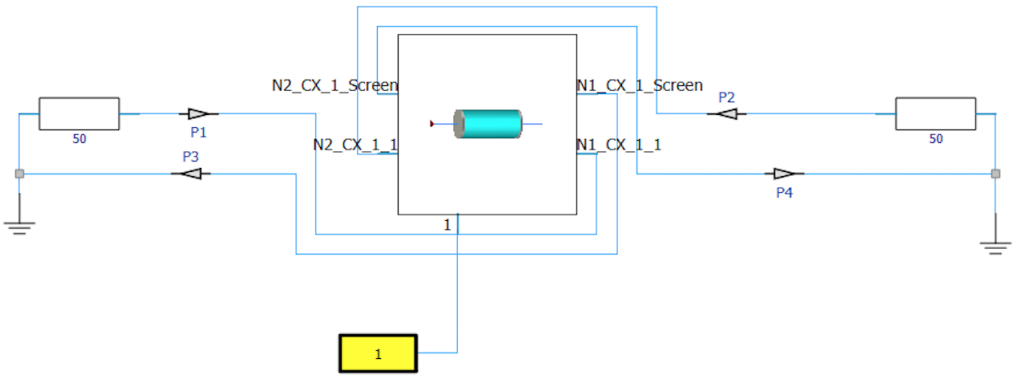

Figure 6.8: Cylinder Test-case Schematic

Thanks to the use of a **Discrete Current Port** , by which is injected the lightning waveform into the Cylinder, it is possible to observe the results obtained after the Simulation had run.
It is important to highlight that the results were divided:

- Current in the wire (*CORE*), as in Figure 6.9;
- Current in coax shield (*SCREEN*), as in Figure 6.10.

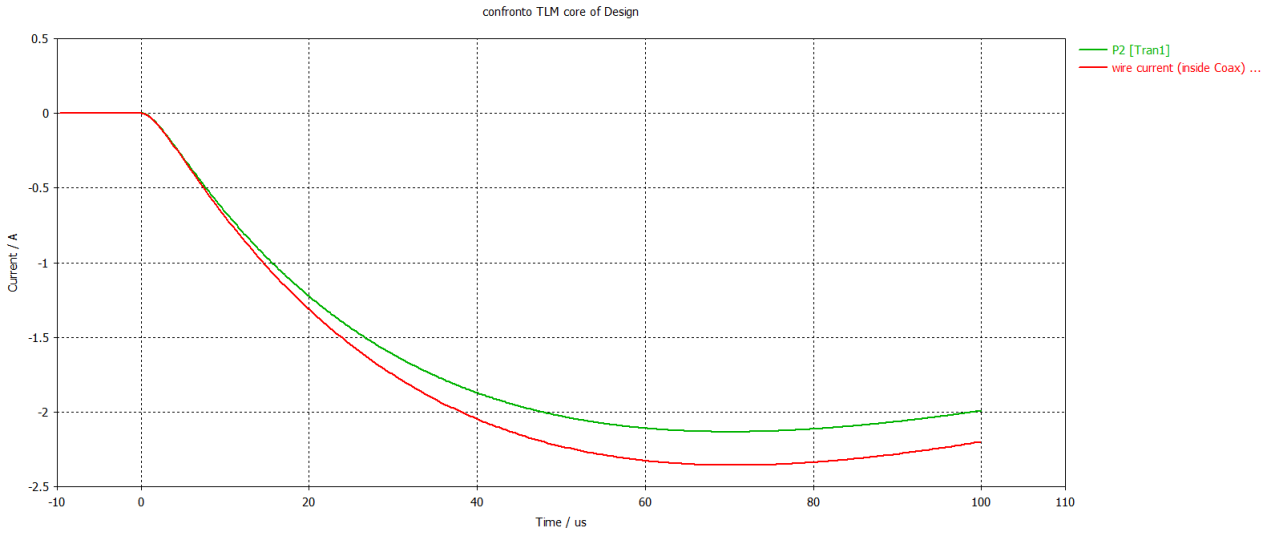

Figure 6.9: TLM vs Cable (*CORE*)

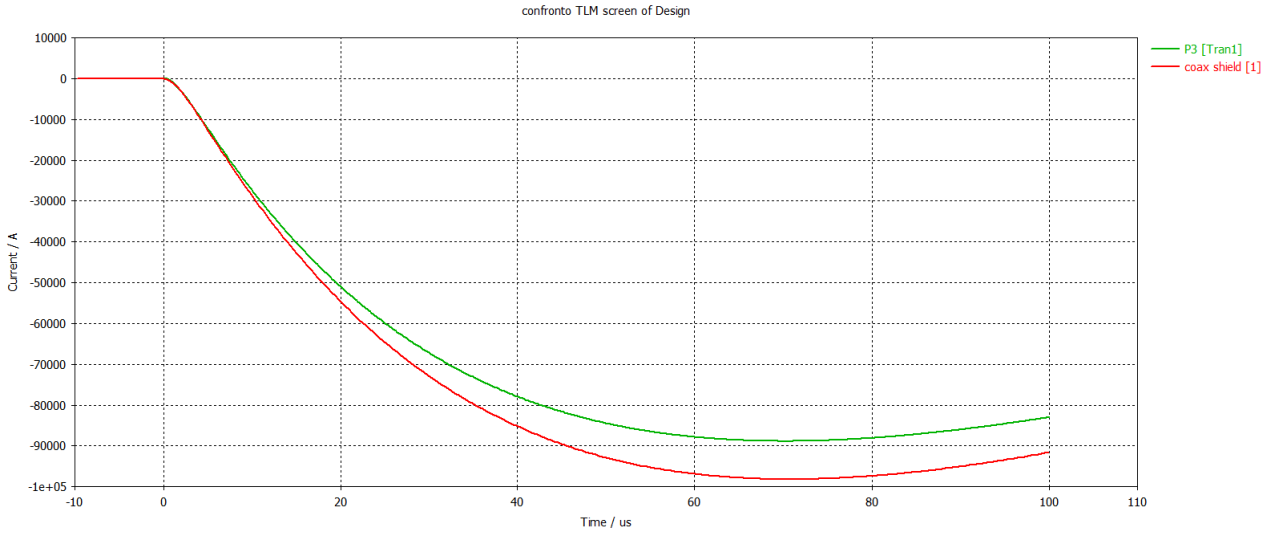

Figure 6.10: TLM vs Cable (*SCREEN*)

It is possible observe that the results of the two solvers configuration are almost equivalents for this simplified cases, however was taking in consideration in this thesis to use the **CST CABLE STUDIO** that is equipped of superior features.

Subsequently different cases were realized whose target was to understand the impact of the presence or not of the astrostrike (expander copper mesh) on the induced current. Then, in order to getting closer to the model of the aircraft, a cylinder with three apertures in each side was realized, as it is possible to see in Figure 6.11. These apertures aim the task of representing the windows of an aircraft and also in this case understand what the presence or not of the astrostrike will led. The astrostike protection was applied on the graphite cover.

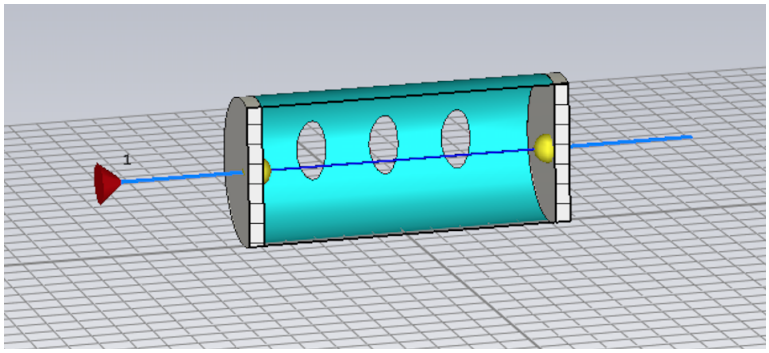

Figure 6.11: Cylinder with three windows each side

Following are present different cases and the results, in term of induced current in the internal cable, grouped in the in diagrams in Figure 6.12 and Figure 6.13:

- *Cylinder* **without** *windows* & **without** *Astrostrike* ,
- *Cylinder* **without** *windows* & **with** *Astrostrike* ,
- *Cylinder* **with** *windows* & **without** *Astrostrike* ,
  Material : thin graphite
- *Cylinder* **with** *windows* & **with** *Astrostrike* ,
  Material : a layer of thin graphite + a layer on top of Astrostrike

In the following Figure 6.12 6.13, the purple line P4 TRAN corresponds at the third case (with windows and without astrostrike).

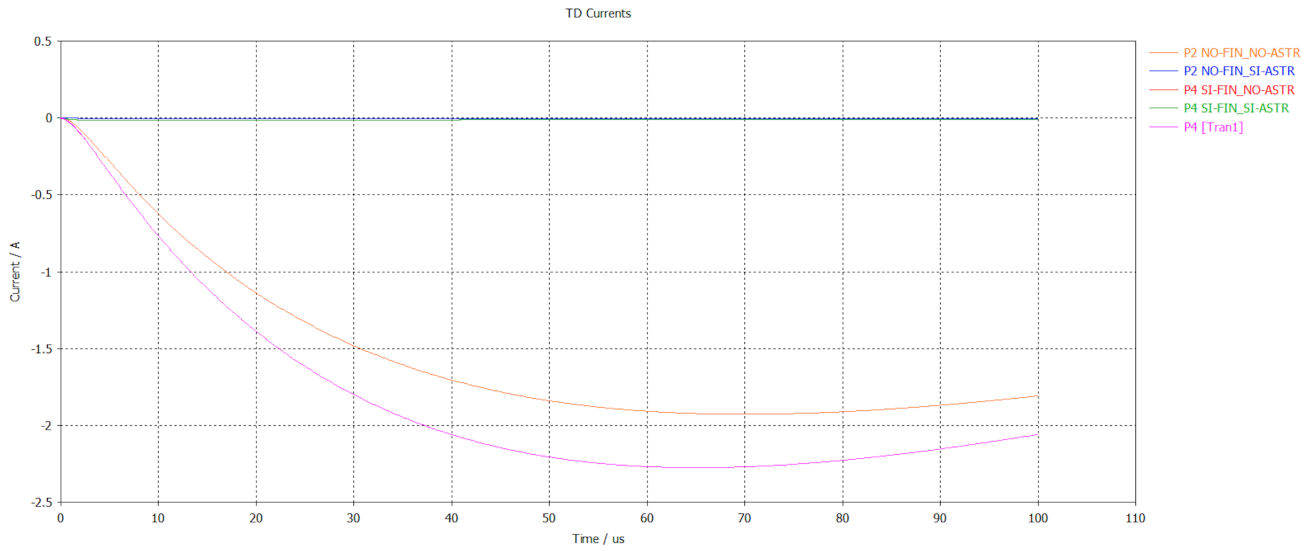

Figure 6.12: Final results for Core

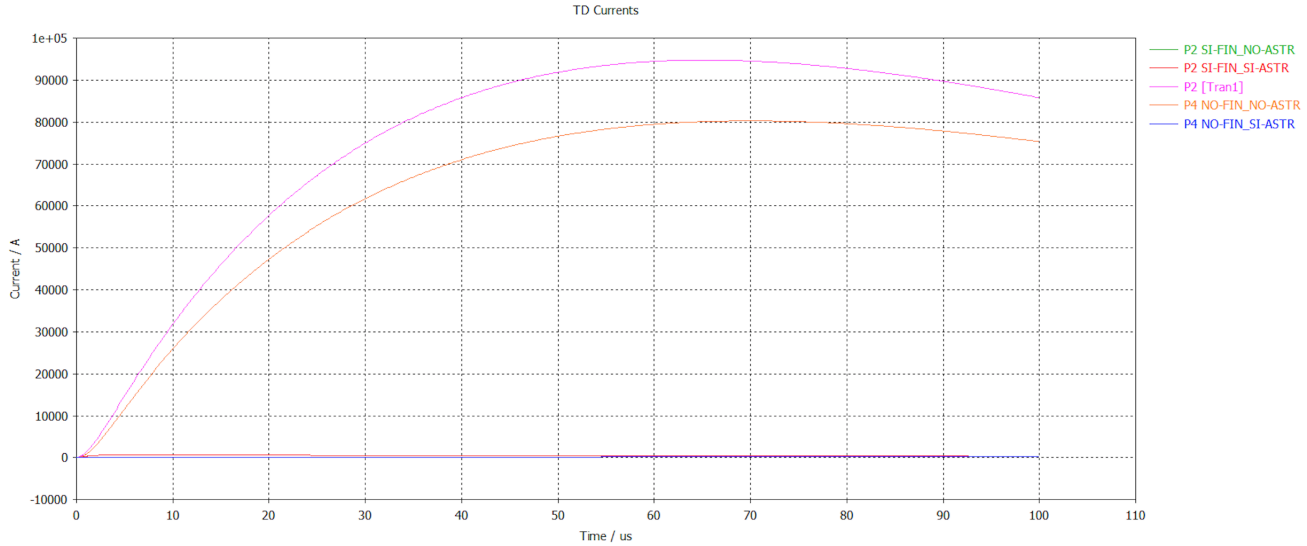

Figure 6.13: Final results for Screen

At the end is it possible to confirm that the presence of the astrostrike is more impacting in term of lightning protection respect to the only presence/absence of the windows.

Another example was done in order to get closer and closer to the model of the aircraft:

- In a part of the Cylinder with the windows was used as material the Al like in Figure 6.14 (left)
- In a part of the Cylinder with the windows was used as material the Al and was possible to insert a ground plane just 10 cm below the cable as in Figure 6.14 (right)

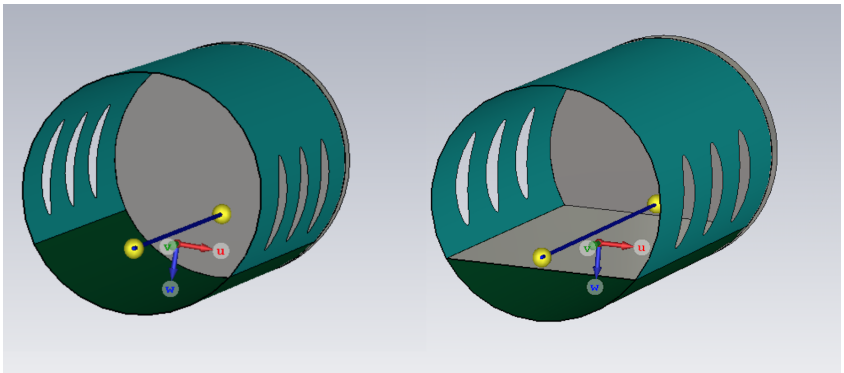

Figure 6.14: Two different cases for the Cylinder

below it is possible find the results reported in Figure 6.15 and Figure 6.16:

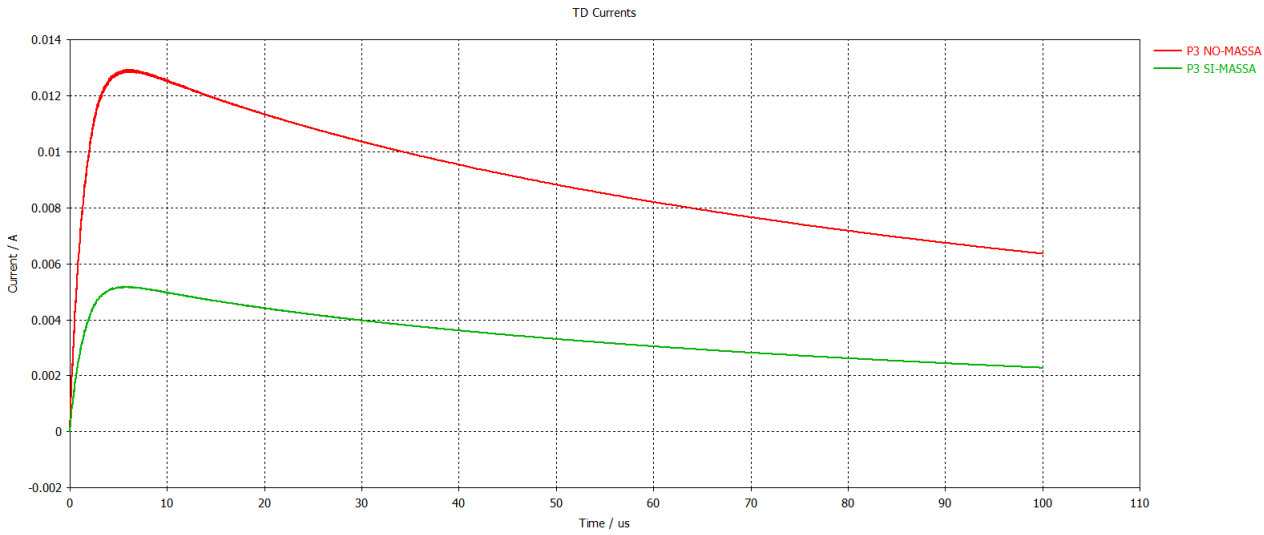

Figure 6.15: Final results for Core

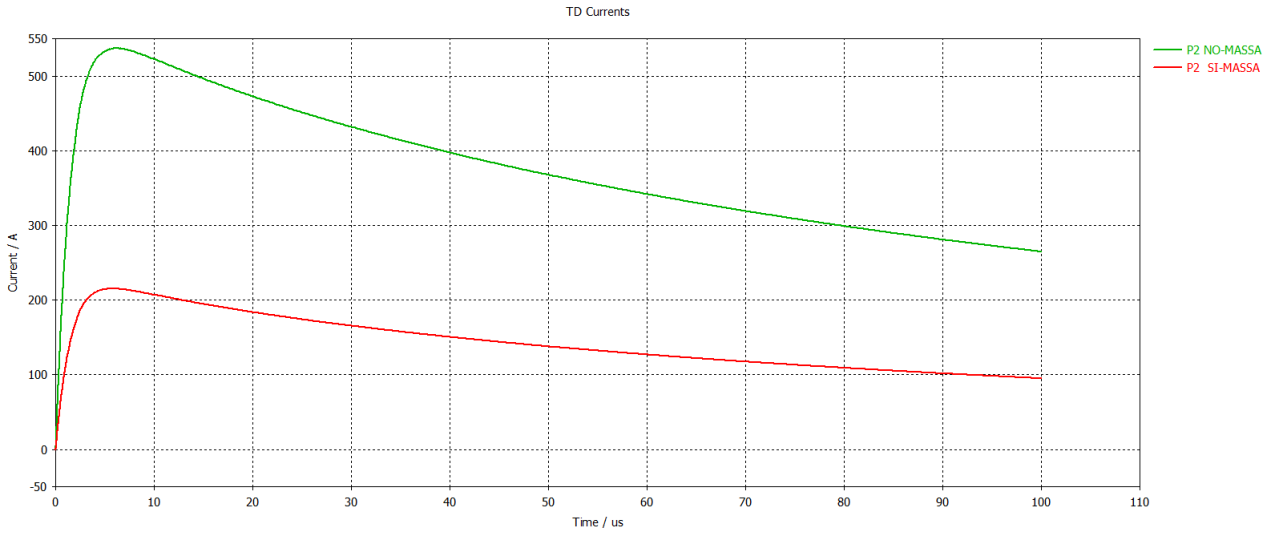

Figure 6.16: Final results for Screen

This results are meaningful, because of the presence of the ground floor reduces the coupling effects as expected and will be used as a starting point for going to grounded the screens of cables in the aircraft structure.

6.2.4 Slot Effects and its problems

It was conducted another study on the Cylinder, in which some slots have been made, in order to understand if it could be a problem in terms of coupling in the internal cables. In particular four cases, are considered:

1. ***Cylinder*** with an **horizontal** slot of length 1400.00 mm and width 0.50 mm as illustrate in Figure 6.17:
   Material: all PEC.

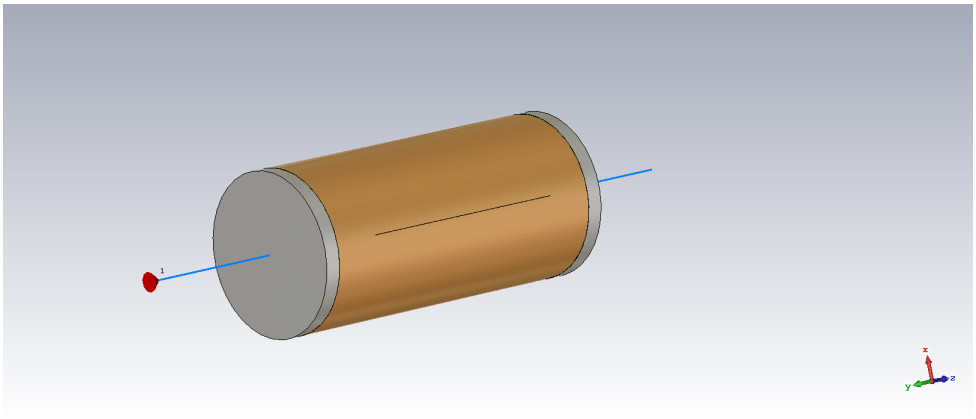

Figure 6.17: Cylinder with one horizontal slot

In the Figure 6.18 below is plotted the current vs time of:

- Input signal that is nothing more than the waveform of the lightning strike,

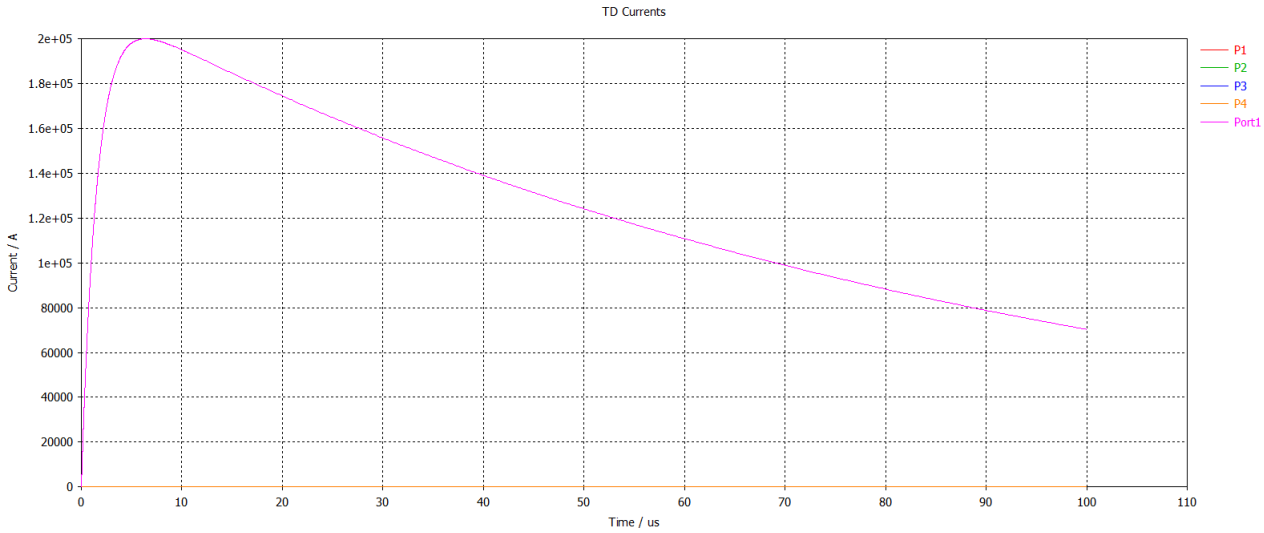

Figure 6.18: Current vs Time of cylinder with one horizontal slot

- Current in the internal wire that is zero due to the all surfaces in PEC.

So, it is possible to understand and to confirm that a *single* slot, does not cause any problem, in particular it's not like it could cause any holes. And as it is possible to notice in the Figure 6.19, the mesh was done in a perfect way.

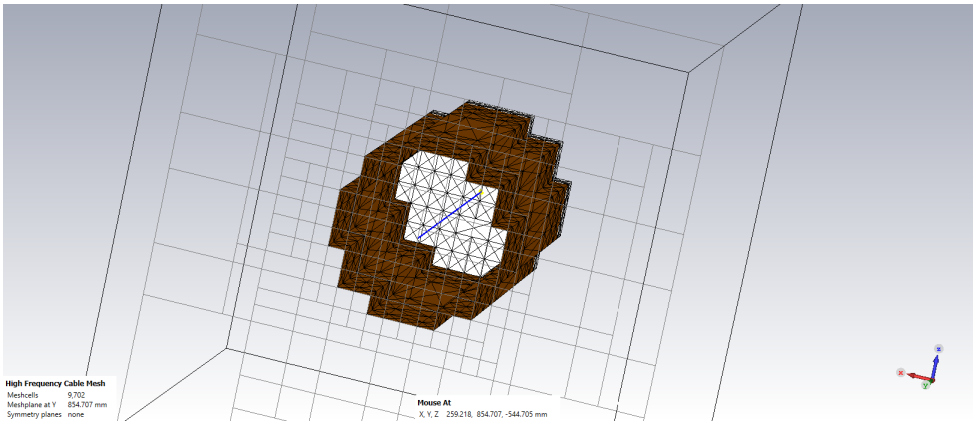

Figure 6.19: Mesh of ***Cylinder*** with one horizontal slot.

2. ***Cylinder*** with an **horizontal** slot of length 1400.00 mm and width 2.10 mm and on the other side a **vertical** slot of length 435.89 mm and width 2.00 mm as illustrated in Figure 6.20
   Material: Aluminium, that is a lossy material characterized by the dimensions present in Table 6.5.

   The Simulations after that having run, resulted that there was not any problems regarding holes as in the previously case, even if there was add a new slot on the opposite side respect to the horizontal one.

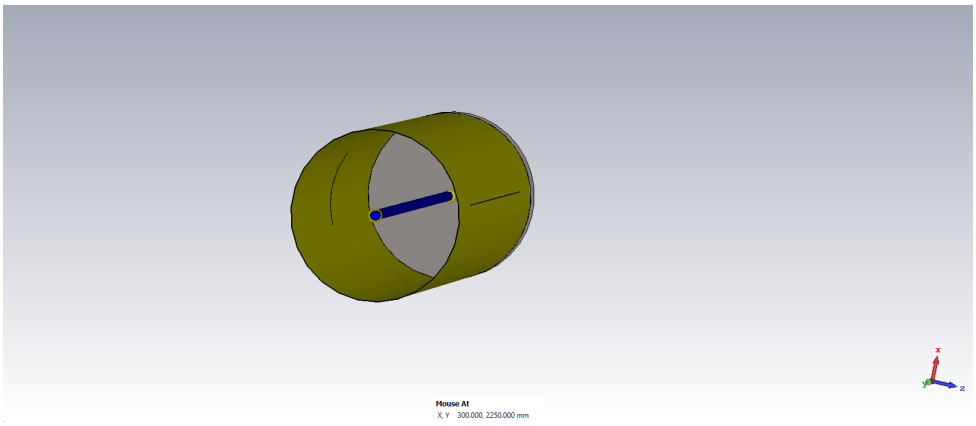

Figure 6.20: ***Cylinder*** with one **horizontal** slot and one **vertical** slot on the other side.

Dimension	***Values***
Diffusivity	9.75309 $e^{-5}m^2/s$
Young's Modulus	69 kN/mm^2
Heat Capacity	0.9 kJ/K/kg
ρ	2700 kg/m^3
μ	1
Electric Conductivity	3.56e^7 S/m
Poisson's ratio	0.33

Table 6.5: Dimension of Aluminium

3. ***Cylinder*** with three **horizontals** slots of length 1400.00 mm, width 0.50 mm and separated from each other of a distance of 152.03 mm, on the other side with three **verticals** slots of length 800.00 mm, width 0.50 mm and separated from each other of a **distance** of 150.00 mm.
   Material: PEC.

4. ***Cylinder*** with three **horizontals** slots of length 2000.00 mm, with 2.10 mm and separated from each other of a distance of 50.00 mm, on the other side with three **verticals** slots of length 800.00 mm, width 0.50 mm and separated from each other of a **distance** of 50.00 mm, as illustrated in Figure 6.21
   Material: PEC.

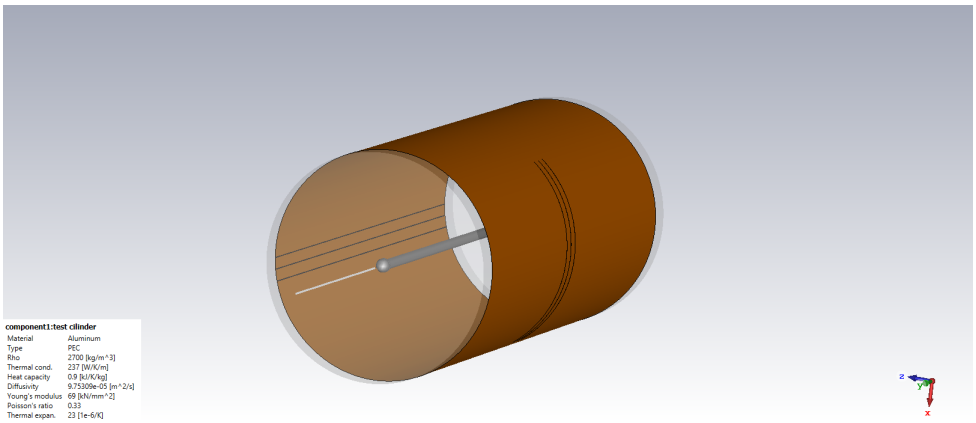

Figure 6.21: ***Cylinder*** with three **horizontals** slots and three **verticals** slots on the other side, each slots is separated of a low distance

The difference between the 3 and 4 case is the distance between each slots, in particular in the 4th case it is possible to understand that due to the low distances between each slots will incurs in problems of coupling and indeed in the Figure 6.22 is illustrated the presence of current in the internal wires.

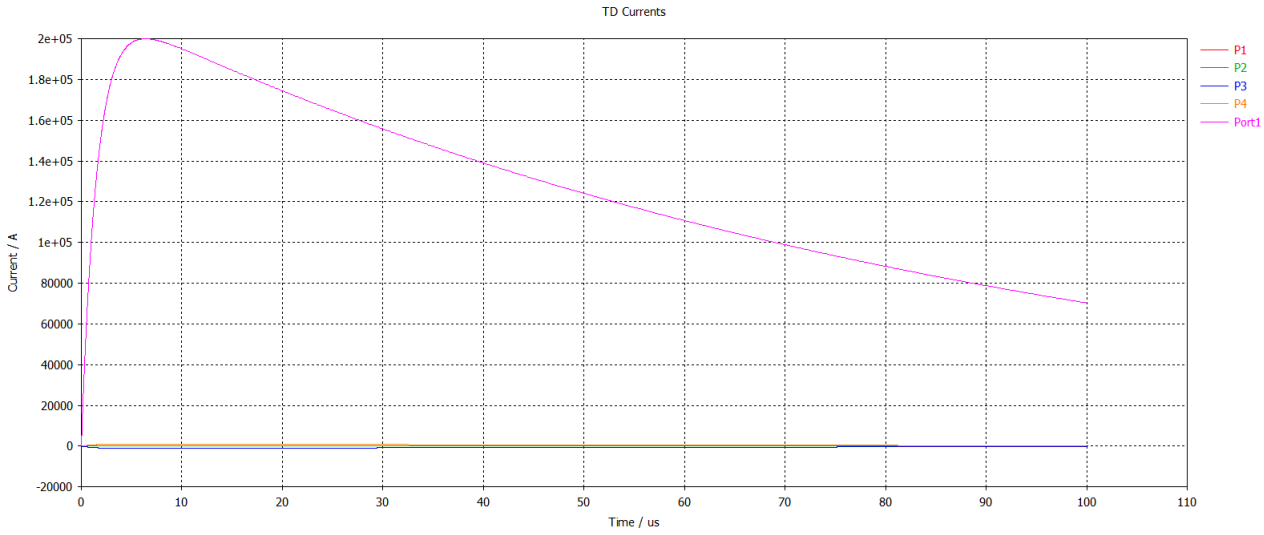

Figure 6.22: Current vs Time of ***Cylinder*** with three **horizontals** slots and three **verticals** slots on the other side, each slots is separate of a low distance

This is can be explained by the fact that the minimum cell size for the mesh is about 99.2 mm. Indeed, in this last case in which the slots were separated each from other of a distance of 50 mm, the slots are seen by the mesher as a big hole causing an excessive coupling in the wire inside the cylinder. All this is possible to see thanks to the mesh view as illustrated in Figure 6.23.

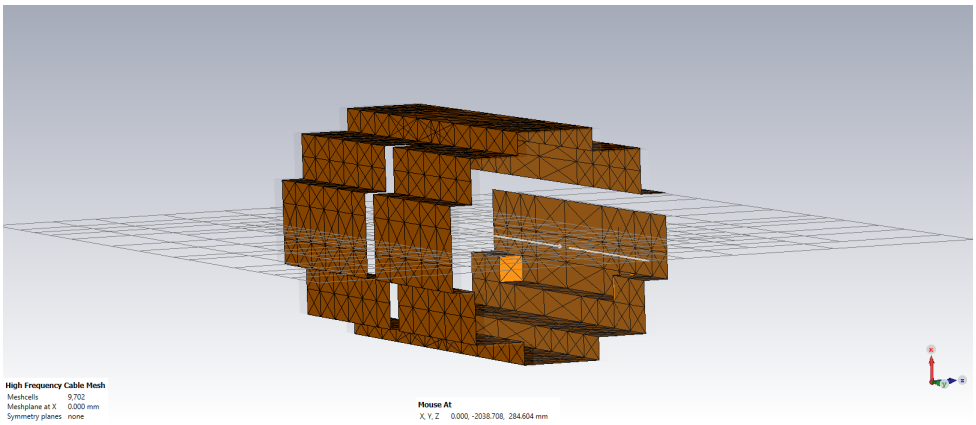

Figure 6.23: Mesh of a ***Cylinder*** with three **horizontals** slots and three **verticals** slots on the other side, each slots is separate of a low distance.

Chapter 7

The effects of Lightning on a simplified 3D Digital Mock-up Model of a Transport-Aircraft

7.1 Introduction

In order to define and tune the Virtual Testing methodology for the evaluation of Lightning Indirect Effects (LIE), **Leonardo S.p.A** has provided a **3D CAD/CATIA V5** file, representative of a simplified ***3D Digital Mock-up Model of a Transport-Aircraft***. The model was characterized by the external surfaces of the aircraft and the main internal structures with dimension around and over 10 cm including equipment, floor, windows, ribs, spars, longerons, pipe and so on. Considering the Lightning as a Low Frequency phenomena, all the mechanical components whose size was less than approximately 5 cm (screws, rivets, strips, nuts, bolts e.g.) commonly present for structural analysis, have been removed before the importing in CST environment.
Despite **Leonardo S.p.A** had provided a representative and simplified file characterized only by the external surfaces of the aircraft, some problems of misalignment of adjacent surfaces have been found, after importing the file from **CATIA V5** into **CST Studio Suite**. In order to overcome and identifies the misalignment, it was thought to split the cad in the following sub-parts:

- **Cockpit**;
- **Fuselage**;
- **Wings**;
- **Vertical stabilizers**.

7.2 Cockpit

It was imported from the **3D CAD/CATIA V5** into **CST Studio Suite** only the structure of the cockpit and at the beginning it appears as in Figure 7.2:

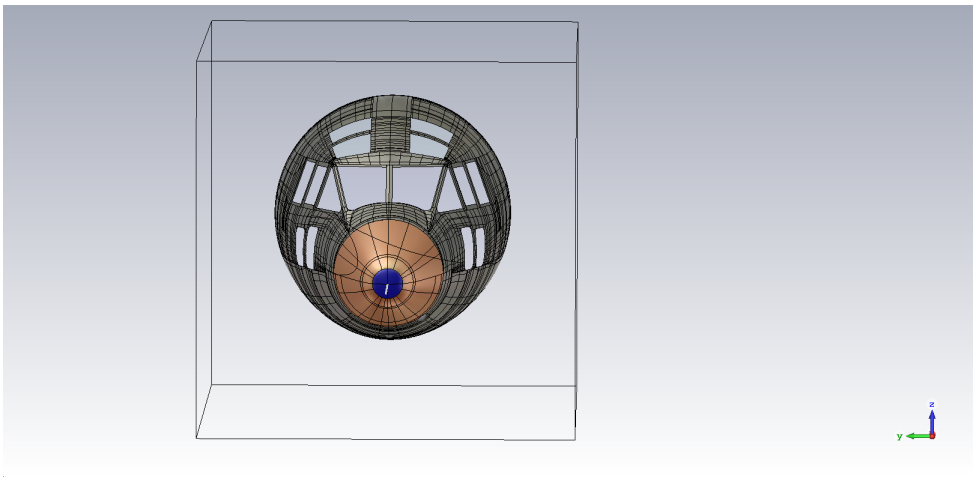

Figure 7.1: Cockpit at the beginning in CST environment

In order to Test the validity of the Cockpit model (no surfaces misalignments) with respect to the Lightning Indirect Effects, the following structures were added to obtain a completely closed structure:

- Realized all the windows in **PEC**
- Realized a back surface in **PEC**

and this it was done to obtained a completely closed structure as it is illustrated in the Figure 7.2.
When the Simulation had run in order to obtain the results, by looking at the *Mesh*

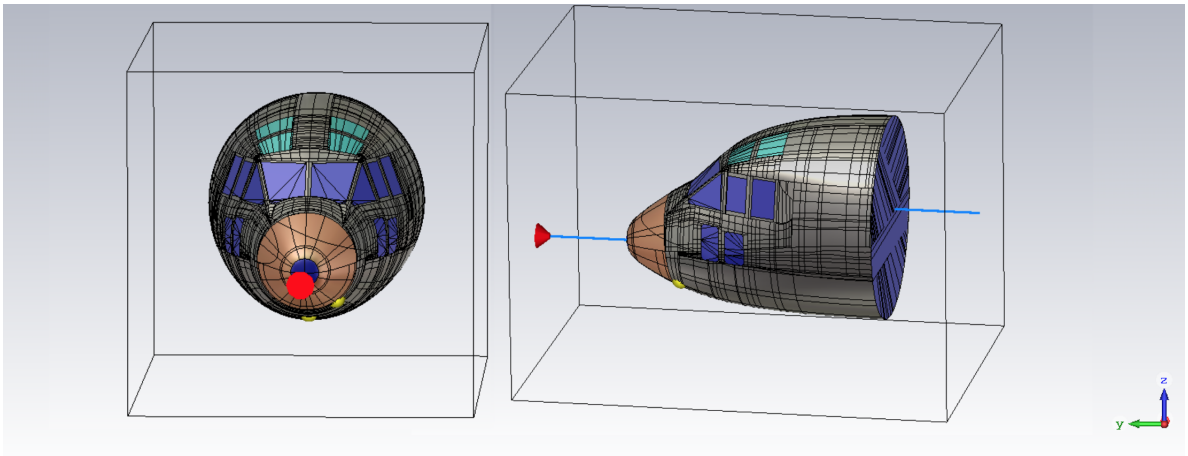

Figure 7.2: PEC structure of the Cockpit completely closed

view, it was noticed the presence of multiple big holes in the structure as highlighted in the Figure 7.3. This corresponds to the problem already found for the simplified example of a Cylinder caused by the importing cad from CATIA to CST, where these misalignments were interpreted by the mesher as empty cells.

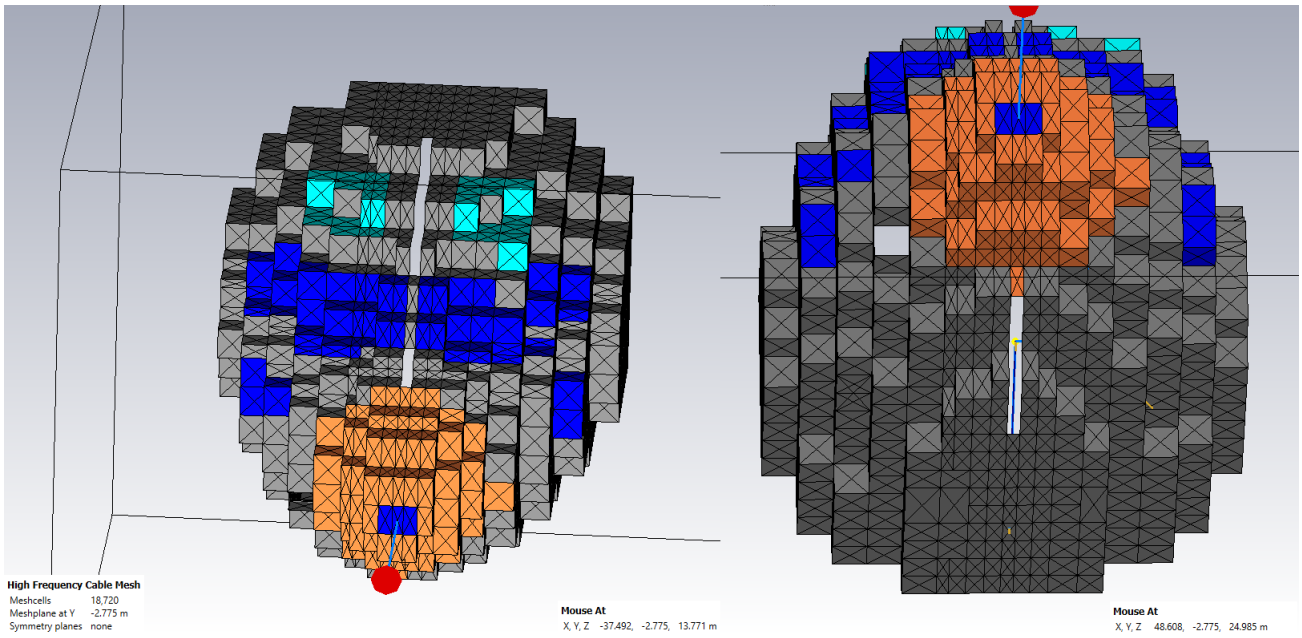

Figure 7.3: Front view and bottom view of Cockpit Mesh with the presence of holes

In order to overcome this problem, all the possible spaces between the surfaces were covered by creating some patches "ad hoc" thanks to the use of command **LOFT**.
To evaluate the promptness of the model, two fictitious cables were realized and grounded internally to the cockpit as illustrated in Figure 7.4

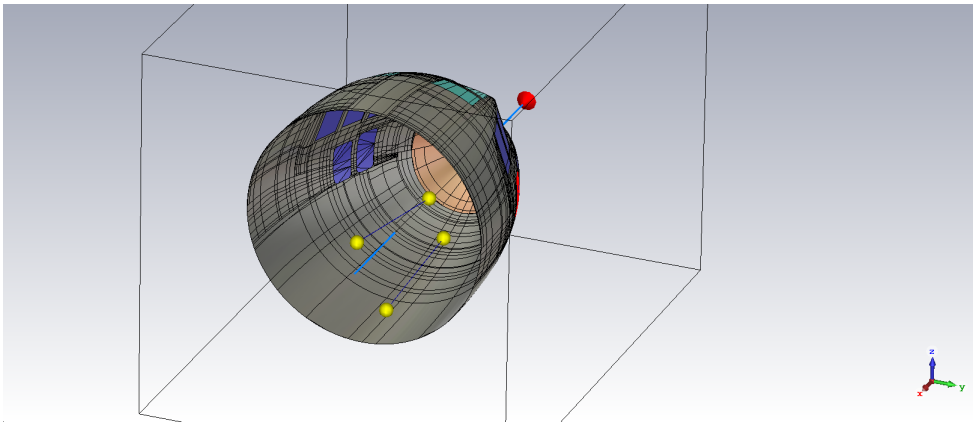

Figure 7.4: Cockpit with two Cables

This two cables **CG_1** and **CG_2** were characterized by one Coax Cable and two single wires, in the Figure 7.5 are illustrated the signal that characterize the cables and their relative Cross Sections.

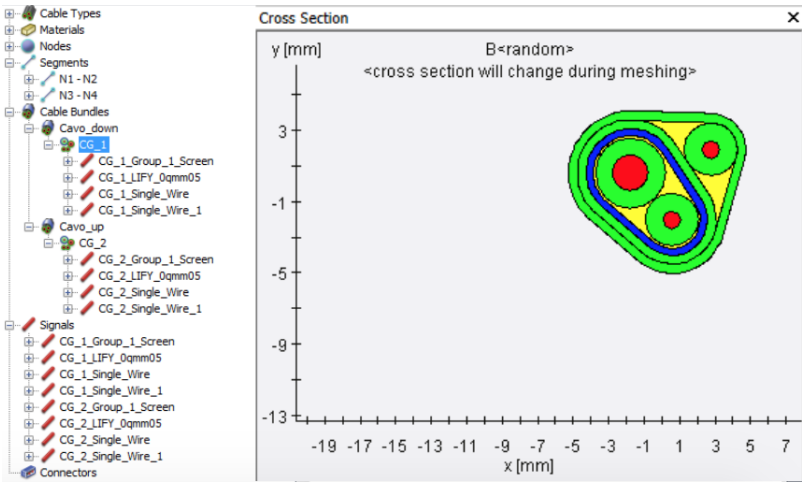

Figure 7.5: Cables cross section

Once all the tricks were used to overcome the presence of the holes, after observing the new mesh in Figure 7.6, the problem can be considered solved.

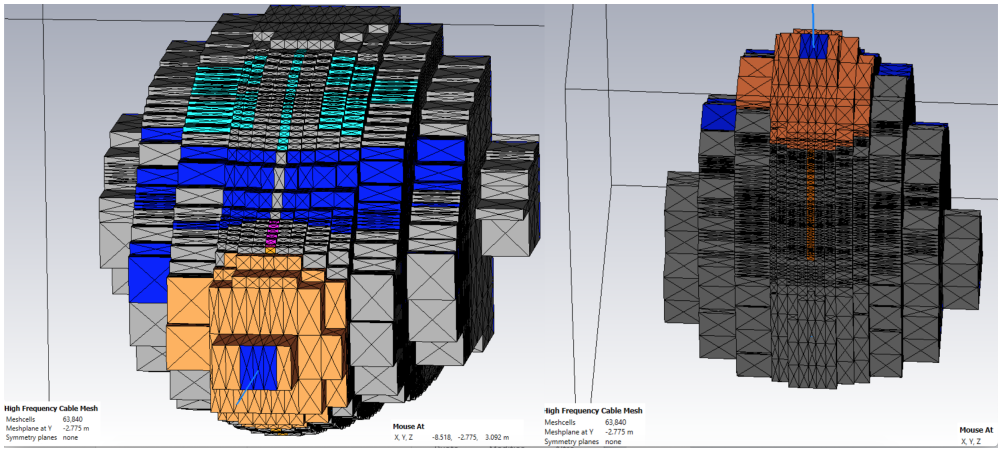

Figure 7.6: Front view and bottom view of Cockpit Mesh without presence of holes

By looking at the current into the cables, it is understood that despite the current flow on the skin of the cockpit, there is not any field penetration nor current coupling into the two cables, as expected.

The same validation process done for the cockpit was repeated for all the sub-parts already mentioned in 7.1 and it was confirmed that not unwanted field penetration was found in all sub-parts.

However, it is important to mention the technical approaches that have been taken to test the fuselage. For the Fuselage were designed the following structures:

- Realized all the windows in **PEC**;
- Realized a front surface in **PEC**,

and this was done in order to obtain a completely closed structure to validate it respect to the Lightning Indirect Effects.

Finally, in Figure 7.7 and Figure 7.8, it is shown the Magnetic Field *Isolines* outside the closed structures. As already explained in Chapter 5.3.1, for a closed

structure, no Induced Effects due to the lightning (H-Field penetration and current coupling), are present in the Cockpit and in the Fuselage.

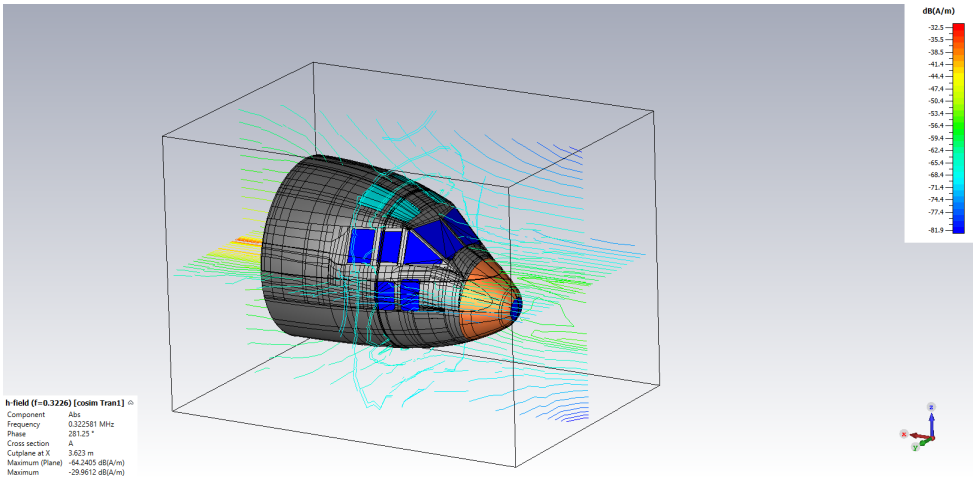

Figure 7.7: H-field of Cockpit

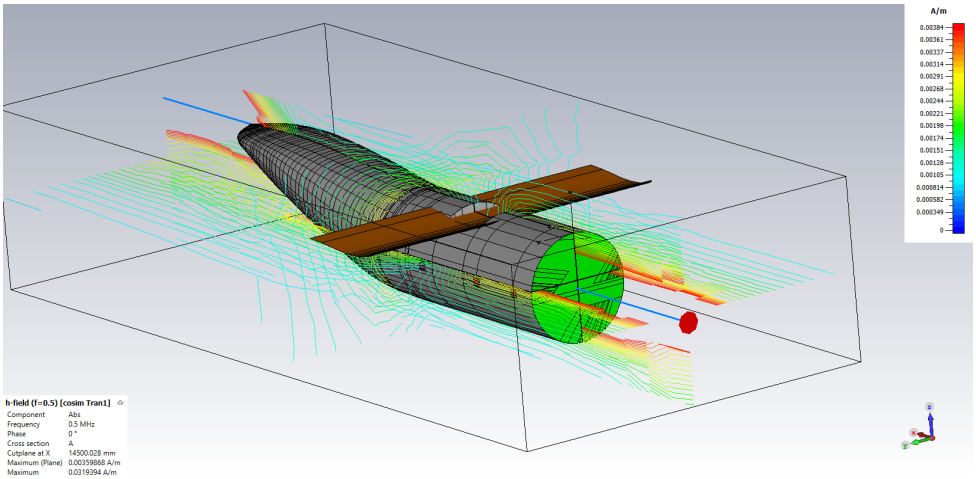

Figure 7.8: H-field of Fuselage

7.3 Wings

The total structure of the wings was used as test object of interest for different studies as:

- Realization of a **fictitious Cables Network** inside the structure;
- Study and design of a **CFC material**.

Let's start to analyze in detail the structure of the wings as illustrated in Figure 7.9, Figure 7.10 and Figure 7.11.

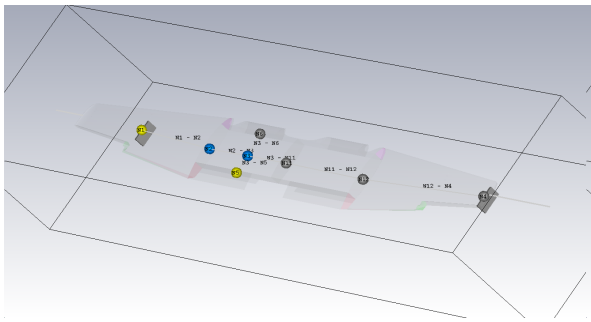

Figure 7.9: Route of *Cable Bundle* B_1

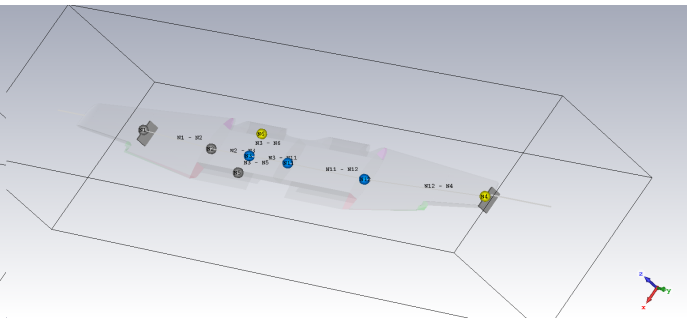

Figure 7.10: Route of *Cable Bundle* B_2

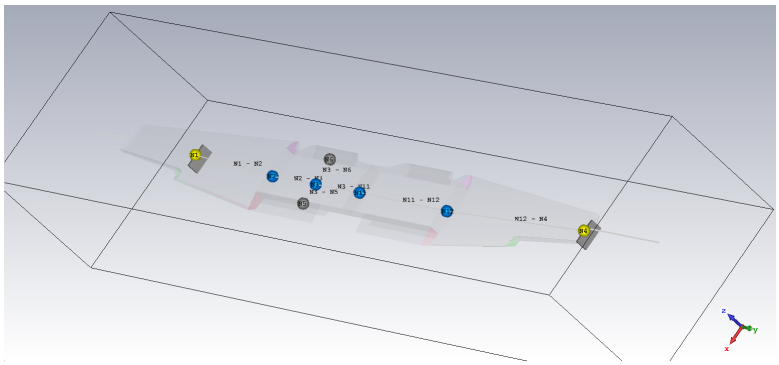

Figure 7.11: Route of *Cable Bundle B*

The factious the cable network interested into the wings structure is characterize by 3 different cable routes:

1. The first cable bundle (B) that goes from one tip to the other both positioned at the ends of wings.
   This cable route passes through the following nodes: **N1, N2, N3, N11, N12** and **N4**, as displayed in Figure 7.11
   The *Cable Bundle* B, is characterized by a Coaxial cable CX_1 and a Single wire SW_1,

2. The second *Cable Bundle* (B_1), that goes through the nodes **N1-N2-N3-N5**, that it is composed by a single wire SW_2, as presented in Figure 7.9.

3. *Cable Bundle* B_2, that goes from the nodes **N4-N12-N11-N3-N6**, and that is composed by a Single wire SW_3, as presented in Figure 7.10.

By observing the structure in Figure 7.12 it is possible to notice the internal presence of bulkheads, that could lead to wrong cable screen currents (because could be used as grounding point) for the cables running through them.

Taking into account that the material used was **PEC** for all the surfaces, in order to appreciate the penetration though the apertures, in particular the upper surfaces covering the node **N2-N5** were excluded from the mesh as shown in the Figure 7.13.

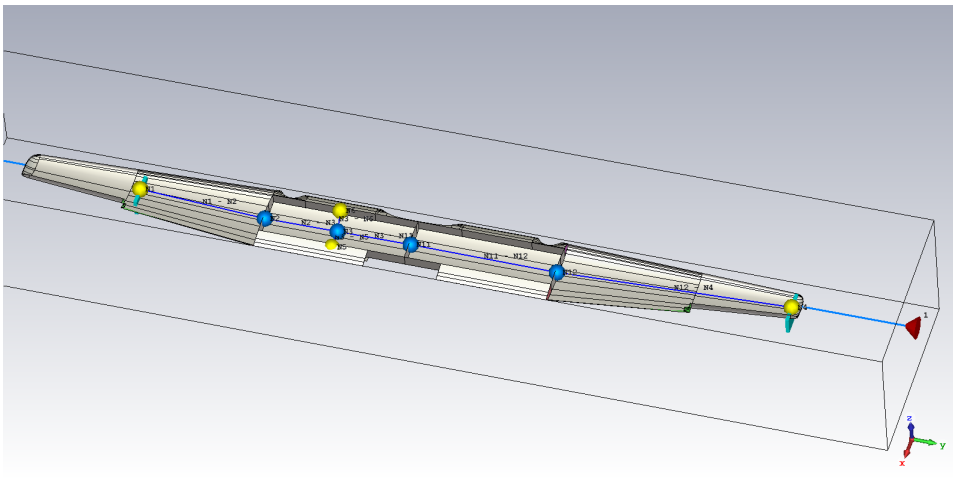

Figure 7.12: Internal wings structure

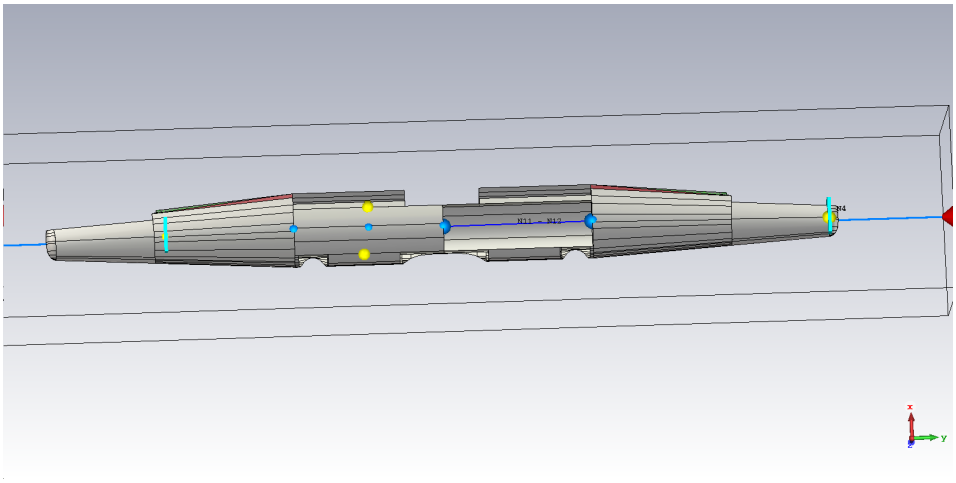

Figure 7.13: Type model of Wings structure simulated

In correspondence of the Nodes **N1** and **N4** are presents respectively two Connectors **C1** and **C4**, represented by the little light blue boxes, at which were assigned different plugin (generator of new sub-connectors) for each signals as in Figure 7.14:

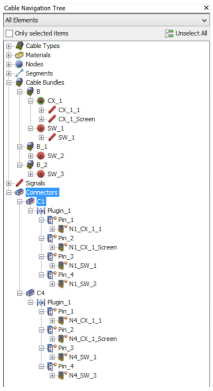

Figure 7.14: Connectors with the relatives signals in the plugin

The main focus of this section is understand what happen if the screen of a cable

is grounded or not when goes across a bulkhead. In particular, the two following configurations were examined :

- *Configuration 1*: the screens of the coaxial in the *Cable Bundle* B, is not grounded, as in Figure 7.15
- *Configuration 2*: grounding of the screens of the *Cable Bundle* B, in correspondence of the nodes properly positioned on the bulkheads as in Figure 7.16. Precisely the screens of the *Cable Bundle* B, that goes from the Connector **C1** to **C4**.

The node used as grounding points are **N2, N5, N6, N11, N12** and from the schematic illustrated in Figure 7.16, it is possible to see which screen of the cables that goes through those nodes is grounded.

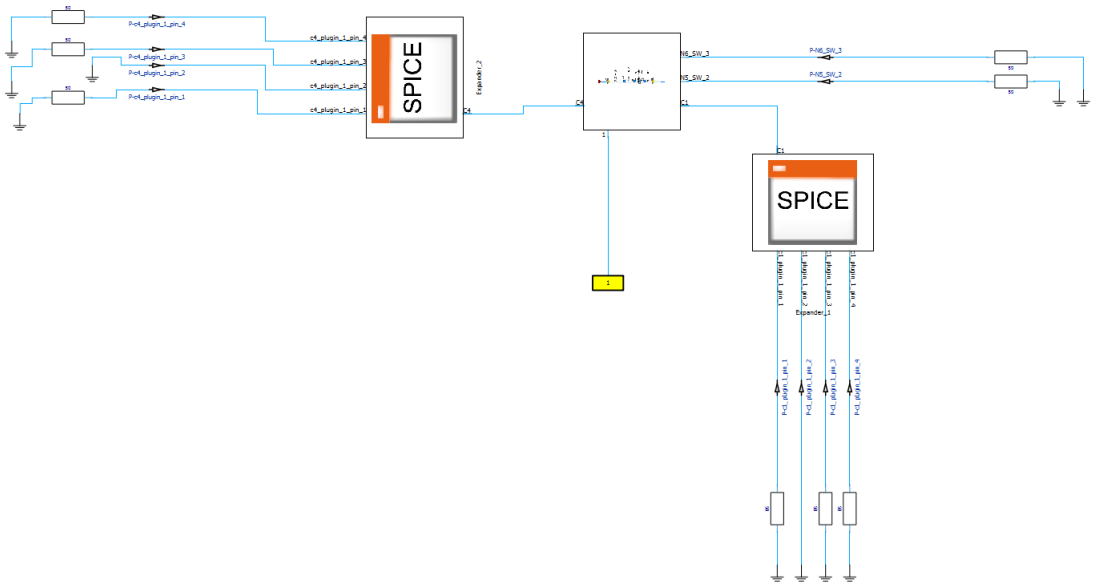

Figure 7.15: Schematic of *Configuration 1*, no grounding on the bulkheads

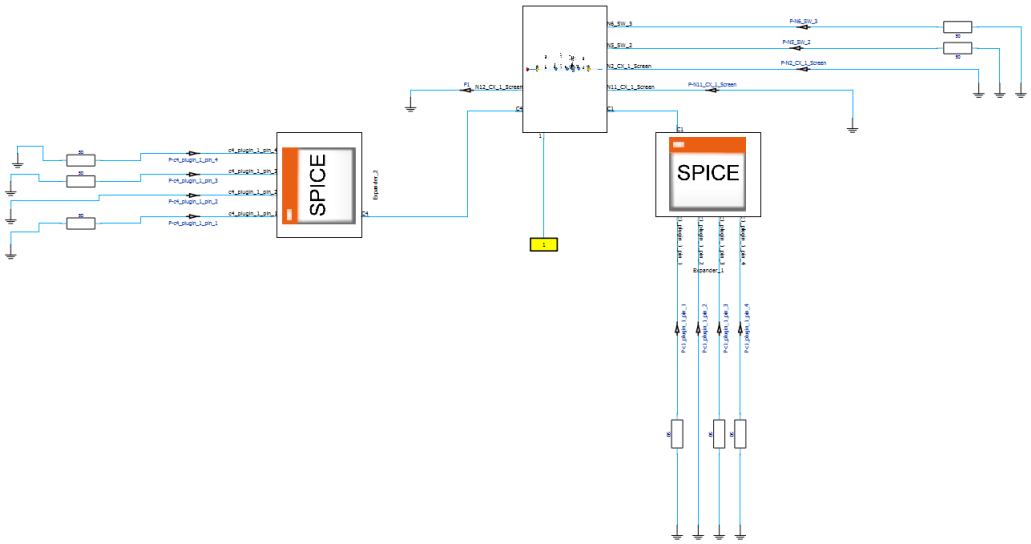

Figure 7.16: Schematic of *Configuration 2*, grounding on the bulkheads

After that the Simulations have been run, it is possible to focus our attention on the current flowing through the screen in Figure 7.17 and core in Figure 7.18, respectively. The measurement probe were put at Connector **C1** or **C4** for the two configurations (screen grounded at the bulkheads and not).

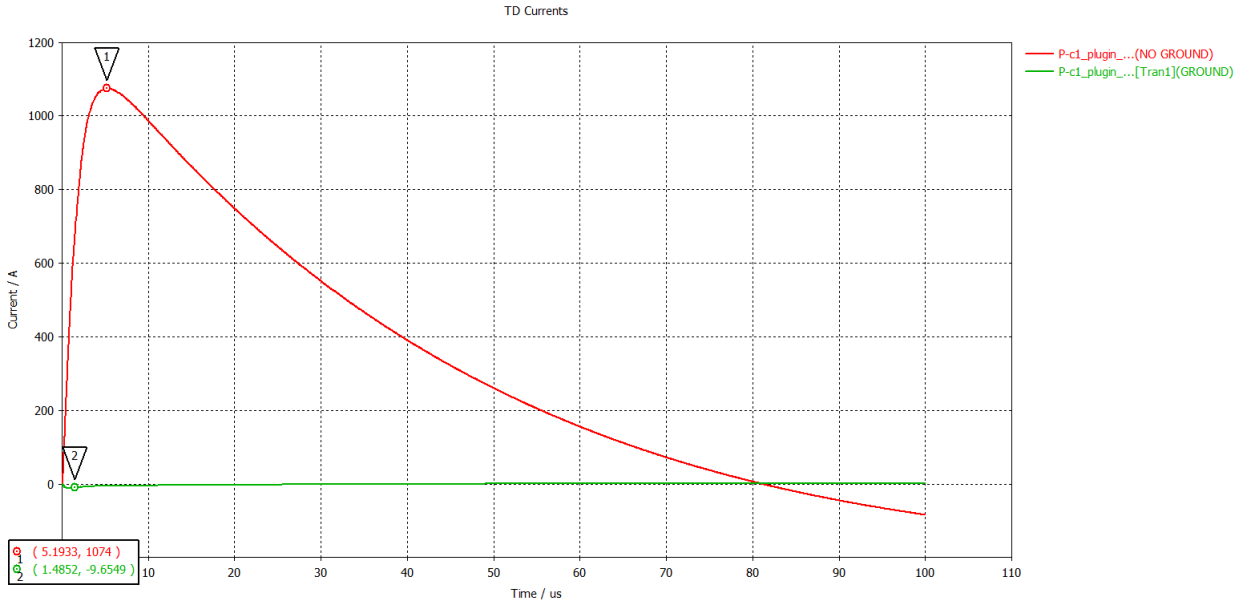

Figure 7.17: Screen Current vs time at Connector **C1**; Comparison between *Configuration 1* and *Configuration 2*

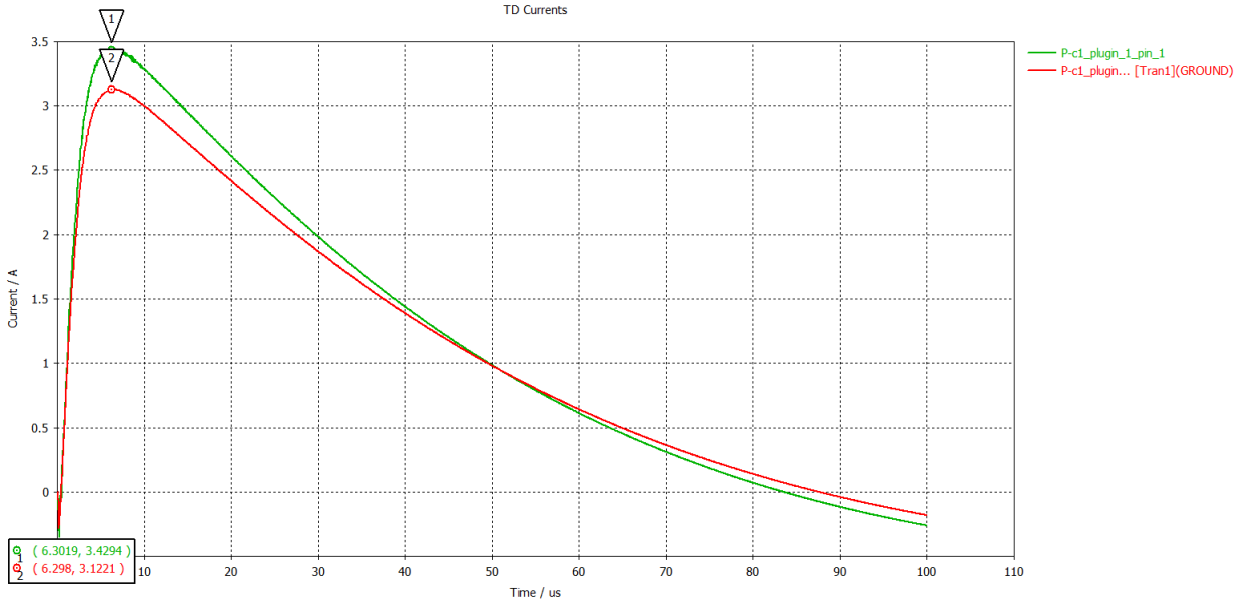

Figure 7.18: Core Current vs time at Connector **C1**; Comparison between *Configuration 1* and *Configuration 2*

It is highlighted that by grounding the screens in the intermediate bulkheads, the screen current at the C1 connector is drastically reduced (from 1000 A to 11 A).

Instead, for what concern the current flowing through the core, it is not observed a strong attenuation as in the screen case, because from the point of view of the core is not impacting if the screen current is discharged over the bulkheads or over the connectors.

Considering the results obtained with the grounding of the cable screens over the bulkheads (reduction of screen current at the connector points), this second configuration will be adopted for all the subsequent simulations.

CFC Material

The second topic, faced in this section (by using the structure of the wings), was related to the used of a **CFC Material**, in place of an ideal PEC. In this case it was thought to use a CFC material for the whole wings structure, excluding the wings tips and the bulkheads, that are still modeled as PEC, as illustrated in Figure 7.20.

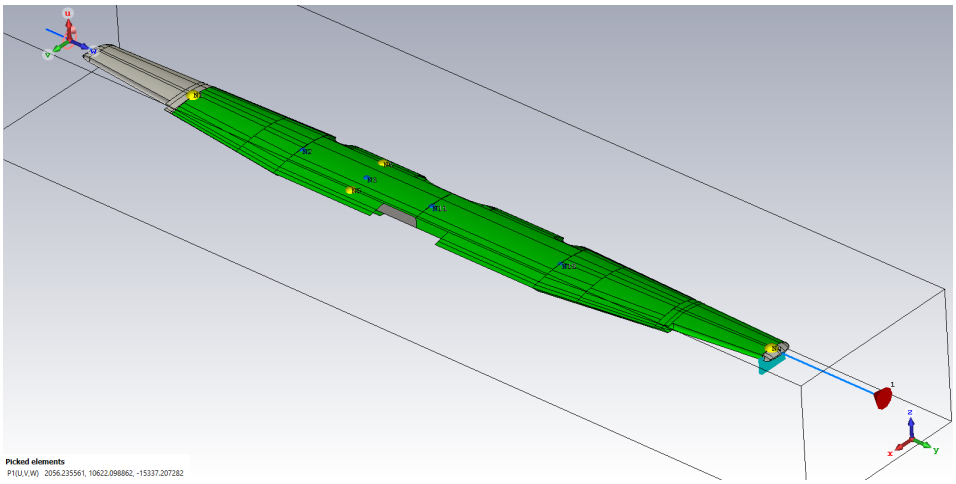

Figure 7.19: Wing structure in CFC

The thin panel of **CFC** is realized for a **total thickness** of 5 mm obtained by a stack-up of a *first layer* of thickness of 4.75 mm with an **Electric Conductivity** of $2.5e^4$ S/m and a *second layer* of Copper mesh of thickness of 0.25 mm. Since this second layer (the Copper mesh) is an anisotropic material (different conductivity in x,y,z directions), in order to model correctly the material, a **local solid coordinates system SCS**, was attached on each solid surfaces, realized in **CFC**. The **SCS** is used with anisotropic materials for features which depend on the orientation of solid. When the "view of **SCS**" is activated, the appropriate systems are drawn in shades style with axis labels u',v',w', for each solid owning a local solid coordinate system, as shown in the Figure 7.20.

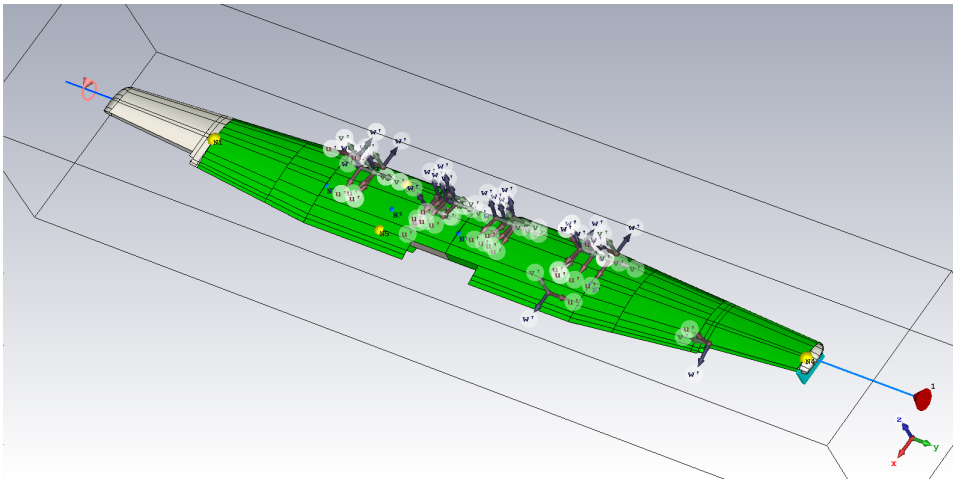

Figure 7.20: Wing structure in CFC and Copper Mesh: **local coordinates system SCS view**

After having run the Simulation, were obtained results and for what concern the current of the screen for the cable that goes through the bulkheads, the amount was really significant. In particular the Figure 7.21 shows, the current flowing on the screen at the connector **C1** (pin 2). [The simulations were done until $100\mu s$]

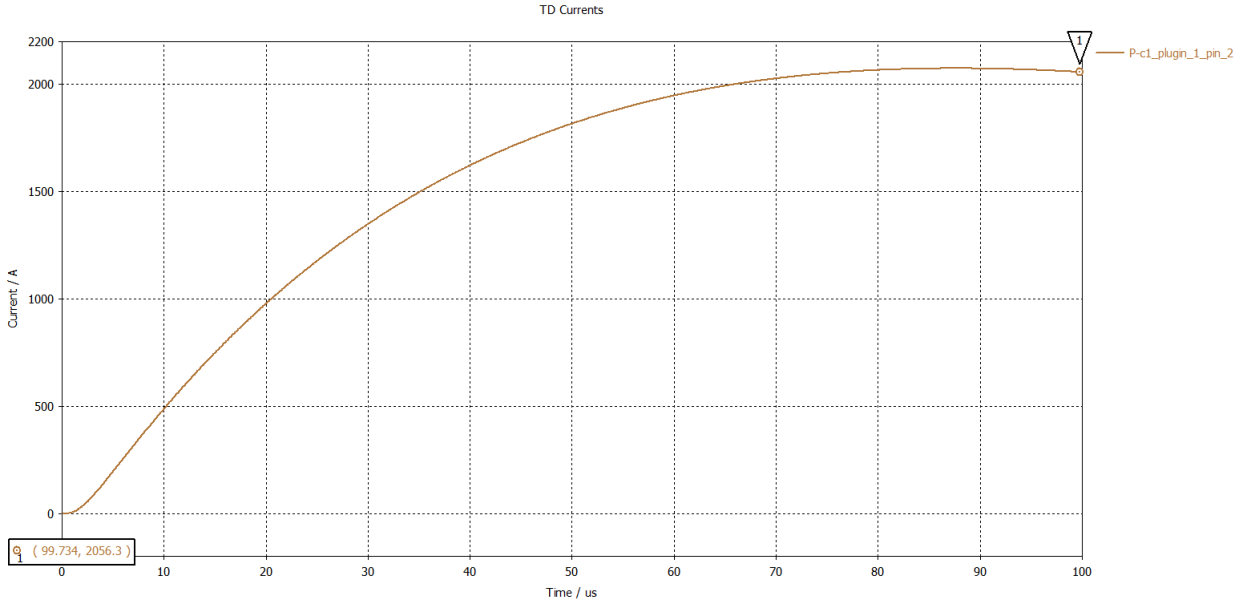

Figure 7.21: Wings Cfc structure: Current vs time (connector **C1** (pin 2))

Reasoning on the fact of having to apply in the subsequent steps the material **CFC** for the whole aircraft, would be unthinkable to apply for all the solids that constitute the aircraft the **local solid coordinates system SCS**.
So, in order to simplify this problem was thought to realize an equivalent model of CFC that takes into account the effect of copper mesh, From the references [19] [26], the values of **CFC** with an **Electric Conductivity** of $2.5e^4$ S/m were taken.

In particular from the Figure 7.22, it is possible to see the current flowing on the screen of the connector C1 at the pin 2 for different **CFCs** conductivity with respectively :

Electric Conductivity	$2.5e^4$ S/m
Electric Conductivity	$1.1e^5$ S/m
Electric Conductivity	$0.935e^5$ S/m

Table 7.1: Different values of Electric Conductivity

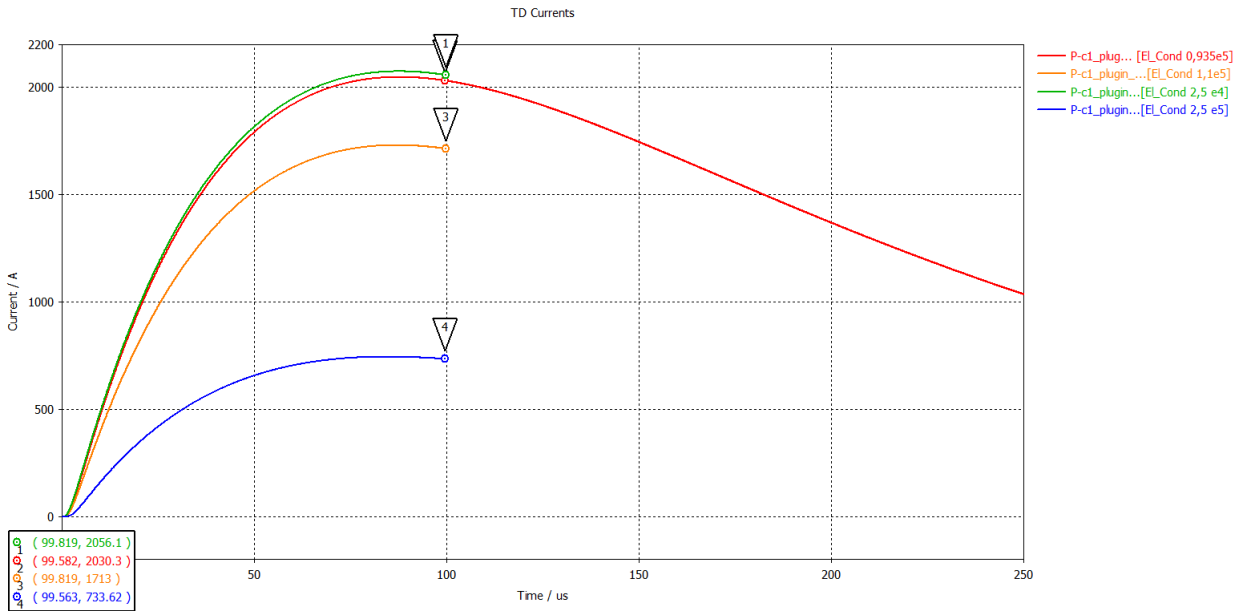

Figure 7.22: Current vs time for the case using different Electric Conductivities

By analyzing in detail all the results obtained for different **Electric Conductivities** of the **CFCs**, it is possible to highlight that the curve that comes closest to the one of CFC with an Electric Conductivity of $2.5e^4$ S/m (Green Curve), which is the equivalent model of CFC, is the one that have an Electric Conductivity of $0.935e^5$ S/m (Red Curve). In particular, this equivalent model of CFC having an Electric Conductivity of $0.935e^5$ S/m that takes into account the effect of copper mesh, it was used later to test the all surfaces of the Mock-up of Transport-Aircraft .

For both the Cockpit, fuselage and also for the wings structures, the results obtained for the H-field, E-field and Surface current were observed. In particular as well as the possibility of obtaining the intensity of the field using the "*Isoline*" view, it is possible to use the "*Contour*"view, which it allows to have an idea of the intensity of the field at a certain frequency on the structures, as shown in the Figure 7.23.

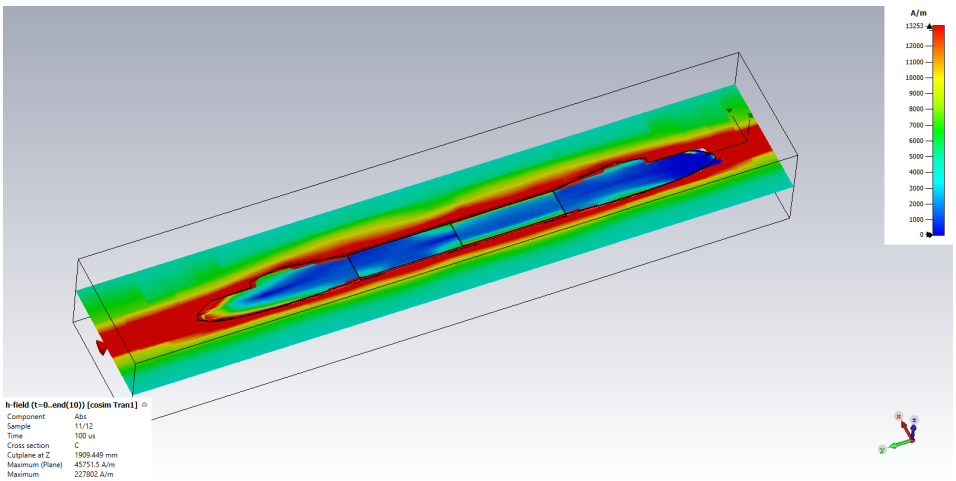

Figure 7.23: H-field for the structure of Wings

7.4 Final Virtual Testing on the entire 3D Digital Mock-up Model of Transport-Aircraft

After having conducted all the simulations for the individual parts of the plane, the next step was to assemble them. So, the entire 3D Digital Mock-up Model of a Transport-Aircraft was the subject of the other simulation activities :

- Virtual simulation using for the *total structure* the **Material** PEC.
- Virtual simulation using for the *main structure* the **CFC material** having an *Electrical Conductivity* of $2.5e^4$ S/m.
- Virtual simulation using for the *main structure* the equivalent model of **CFC material + Copper mesh** having an *Electrical Conductivity* of $0.935e^5$ S/m.

7.4.1 Definition of Entry/Exit point of the lightning current

Once defined the definitive structure of the 3D Digital Mock-up Model of a Transport-Aircraft, in order to consider all the possible about the indirect effects of lightning, it was conducted a study on nine configurations, which differs one from each other on the different entry and exit point of the lightning current that strike the aircraft.

Through the Figure 7.24 below and in the summary Table 7.2, it is easier to understand the nature of the different configurations based on the ***Entry*** and ***Exit*** points.

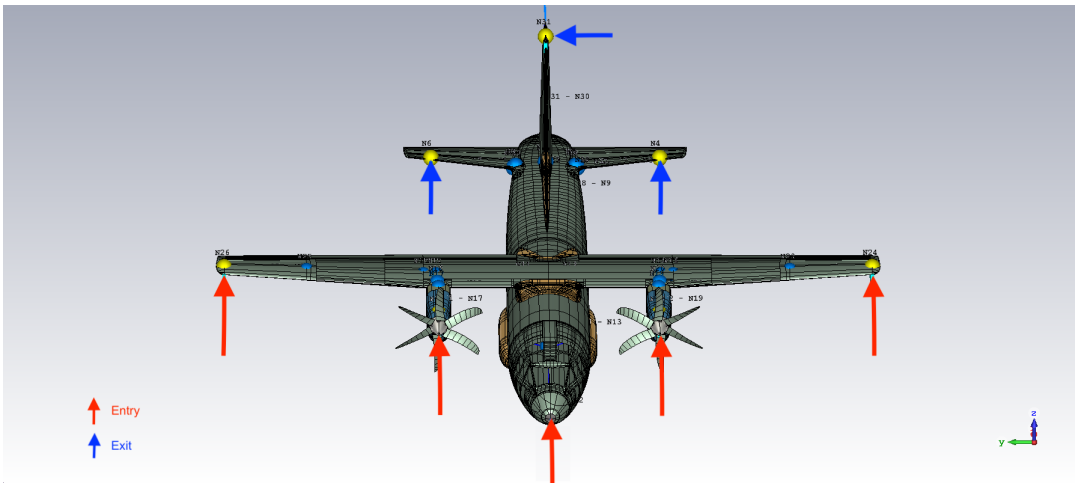

Figure 7.24: *Entry* and *Exit* of Lightning attachment points

Configuration	*Entry*					*Exit*				
	Nose Radom	Engine		Wing Tip		Fin Tip	Empennage Tip		Wing Tip	
		R	L	R	L		R	L	R	L
A1	X					X				
A2	X						X			
A3	X							X		
A4	X								X	
A5	X									X
A6				X		X				
A7					X	X				
A8		X				X				
A9			X			X				

Table 7.2: A1 to A9 Configurations

7.4.2 Cable Bundles network

Previously, the induced effects on a randomly selected cable network was computed, singularly for the each different sub-parts, that makes up the plane, applying the Transmission Line approach, without considering at the same time the whole on-board electrical system.
Once all the sub-parts of the Aircraft were reassembled, the next step it was to develop in order to derive an equivalent sketch of the complex network, constituted by a simplified representative cables network, along the entire surface of the aircraft.

In order to define a Cable Bundle, it was done using as traces the existing "*Curves*", realized "ad hoc" in 3D along all the internal skin surface of the aircraft, as shown in Figure 7.25.

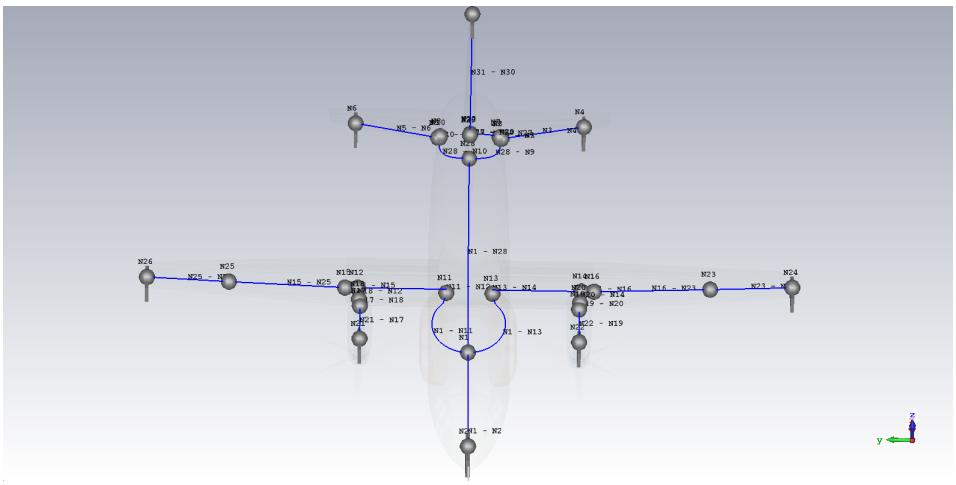

Figure 7.25: Initial Curves definig the Cables Bundle Network

In particular, the Cable Network is composed by seven coaxial Cables Bundle that, starting from a central avionic cabinet, located in the cockpit volume, branch off into the aircraft, reaching the corresponding seven termination points (providing connections to the equipment) located in:

1. **Right Wing Tip**,
2. **Left Wing Tip**,
3. **Right Engine**,
4. **Left Engine**,
5. **Right Empennage Tip**,
6. **Left Empennage Tip**,
7. **Fin Tip**.

Where taken from the "Library" of the simulation tool for each of this Cables Bundle a **Coaxial Cable** *RG*58, characterized by a ***CX_Core*** and ***CX_Screen*** and by the parameters listed in the following Table 7.3.

Coaxial Cable *RG*58

	Shape type	**Material**	**Diameter**	**Thickness**
wire	Circle	Cu	0.47 mm	
insulator inside	Circle	PE	1.475 mm	
screen	Braid	Cu	0.122 mm	
insulator outside	Wrap	PVC		0.5mm

Table 7.3: Cross-Section of wire

In particular, concerning the Screen, it can be characterized by its **Transfer Impedance** shown in Figure 7.26, that is a frequency dependent function and includes the relationship between the current on the outer side of the screen to the coupled voltage between the inner wire/wires and the inner side of the screen.

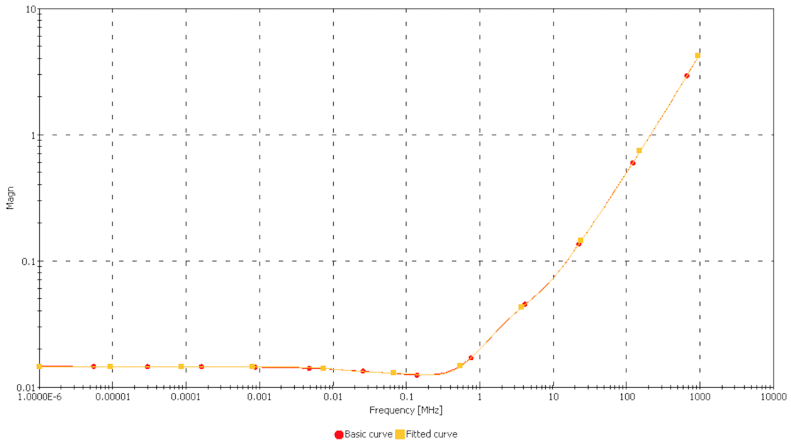

Figure 7.26: Transfer Impedance of the screen of the **Coaxial Cable** *RG*58

From the Figures: 7.27, 7.28, 7.29, 7.30, 7.31, 7.32,7.33 below, it possible to see how the cables network along the all main parts of the aircraft is distributed.

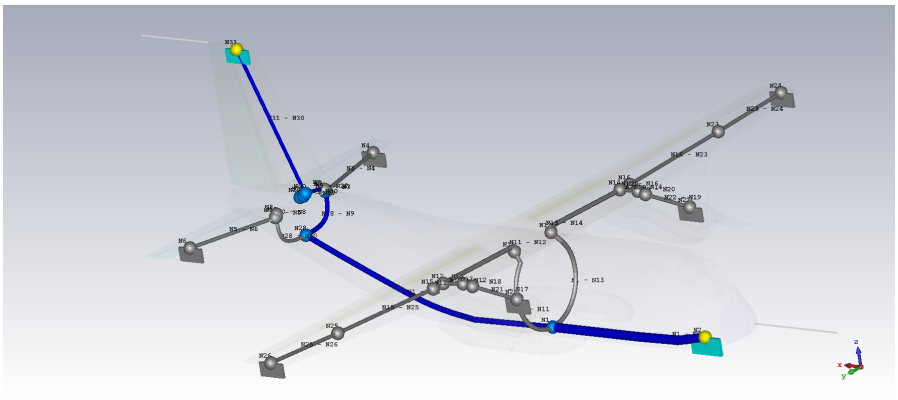

Figure 7.27: Cable Bundle of Fin Tip

Looking at the figures above, it is possible to see how the cables network was designed, starting from a Central Equipment, from which are sorted the various cables, that will reach the other equipment.

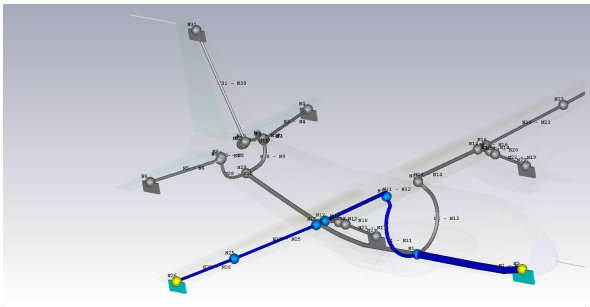

Figure 7.28: Route of *Cable Bundle of Right Wing Tip*

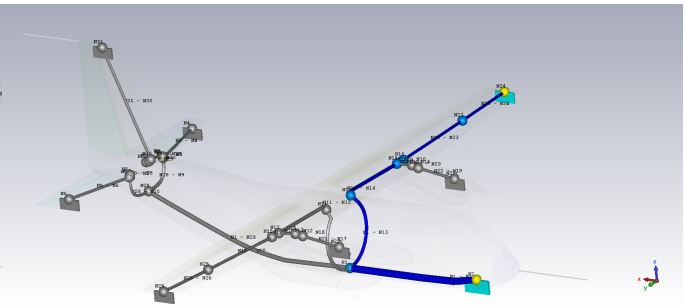

Figure 7.29: Route of *Cable Bundle of Left Wing Tip*

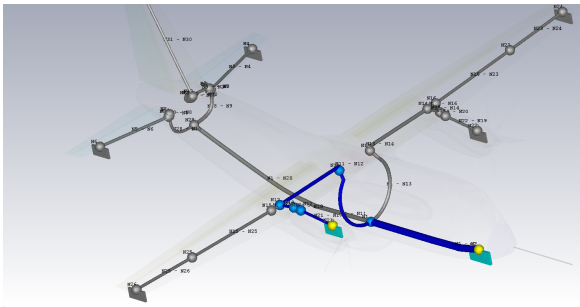

Figure 7.30: Route of *Cable Bundle of Right Engine*

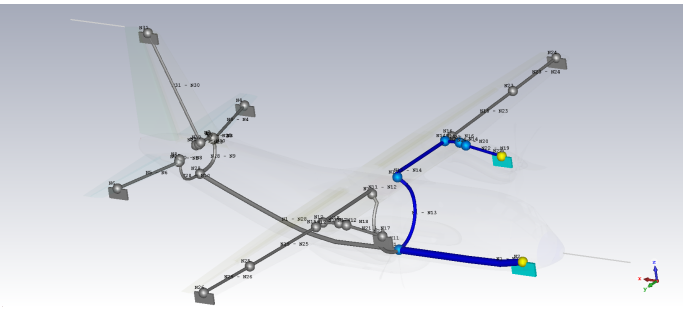

Figure 7.31: Route of *Cable Bundle of Left Engine*

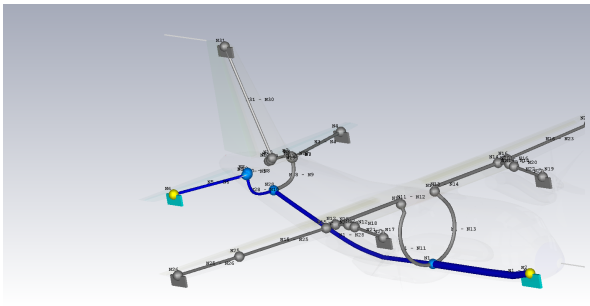

Figure 7.32: Route of *Cable Bundle of Right Empennage Tip*

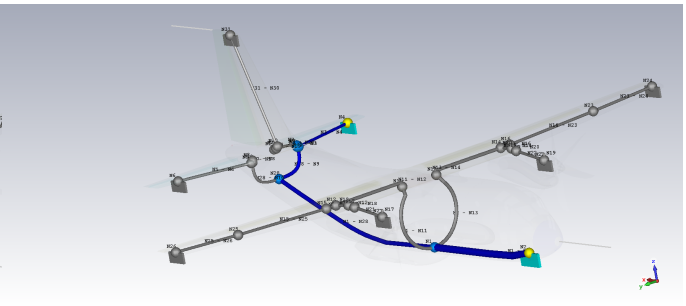

Figure 7.33: Route of *Cable Bundle of Left Empennage Tip*

LRU-Installation

Each Cable Bundle originates in each Equipment/Connector of critical apparatus, represented in Figure 7.34 by the light blue block, and ends at one or more Equipment/Connectors.

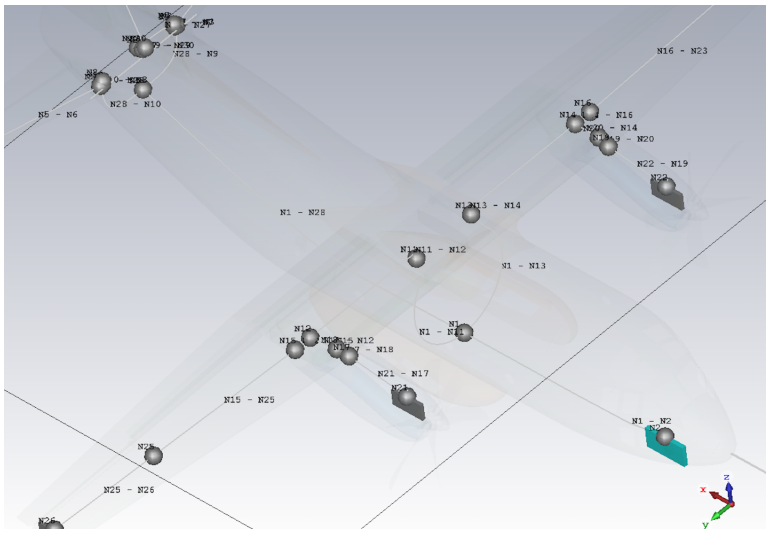

Figure 7.34: **C_Central** Connector

In particular each Equipment/Connectors, have been characterized by different plugin at which one is attached the respective ***CX_Core*** or ***CX_Screen***.
Were considered eight C_Connector:

- **C_Central**;
- **C_Right_Wing**;
- **C_Left_Wing**;
- **C_Right_Engine**;
- **C_Left_Engine**;
- **C_Right_Empennage_Tip**;
- **C_Left_Empennage_Tip**;
- **C_Fin Tip**.

In the following Figure 7.35, it is presented for example how the **C_Central** Connector was edited:

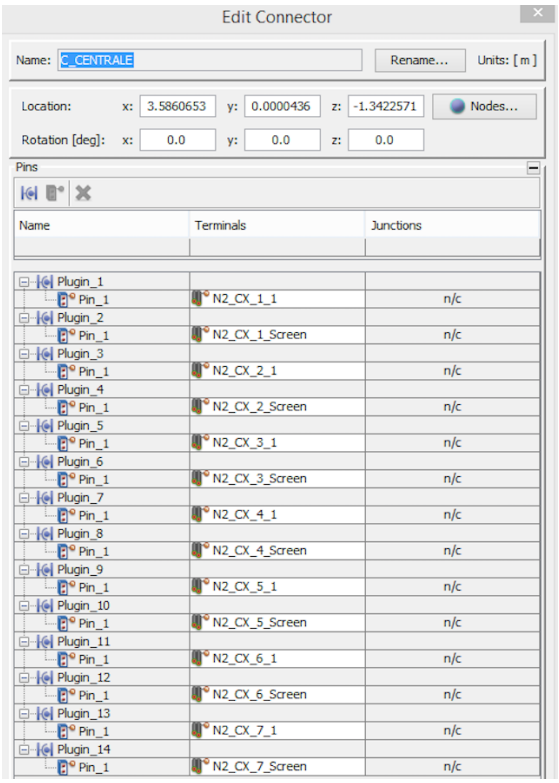

Figure 7.35: Edit of the **C_Central** Connector

Nodes and Segments

Each Cable Bundle, in **CST CABLE STUDIO**, it could be considered as a union of different **segments**, each of them starting and ending at two points called **Nodes**. During the cable network design, wherever the cable was crossing a surface a specific Node, was settled in correspondence of the intersection between the cable and the surfaces. Those Nodes actually represents an ideal bulkhead connectors, thus providing a grounding point for the the cable screen . It is possible to individuates the Nodes and the compensation Segments for each Cable Bundle that goes from one Connector to another.

Right Wing	Left Wing	Right Engine	Left Engine	Right Empennage Tip	Left Empennage Tip	Fin Tip
N2	N2	N2	N2	N2	N2	N2
N1	N1	N1	N1	N1	N1	N1
N11	**N13**	N11	N13	N28	N28	N28
N12	N14	N12	N14	N10	N9	N9
N15	**N16**	**N18**	**N20**	**N8**	**N7**	N27
N25	N23	**N17**	**N19**	**N5**	**N3**	**N29**
N26	N24	N21	N22	N6	N4	**N30**
						N31

Table 7.4: Cable network nodes (in orange the ones grounded in the schematic)

In fact in the Schematic as in Figure 7.36 , in correspondence of the previously orange mentioned Nodes, the screens of the cable were grounded, as displayed in Table 7.4.

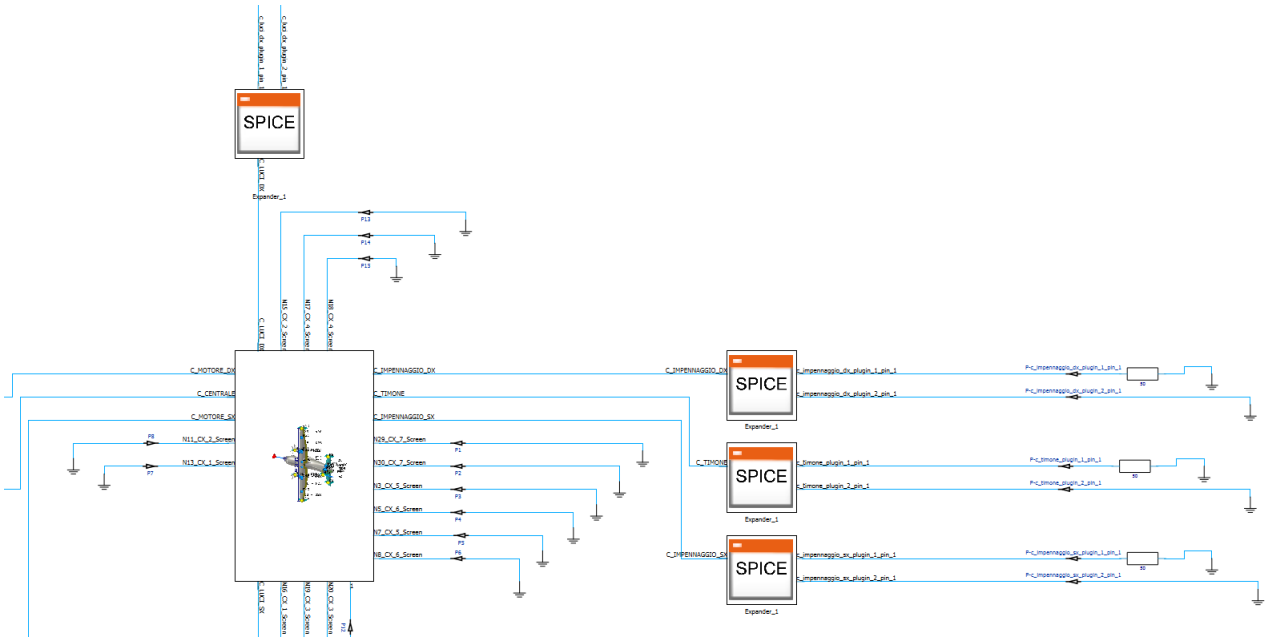

Figure 7.36: Explicit nodes present in the schematic

7.5 Materials Configuration

The main specifics of the three configurations already mentioned in the Introduction 7.4, in this Section are reported. In particular were divided the Components in:

- **SKIN_WINGS**;
  - **Right Engine Skin**,
  - **Left Engine Skin**,
  - **Fixed Wing Structure Skin**,
  - **Movable Wing Structure Skin**.
- **Fairings_Skin**,
- **Cockpit_Skin**,
- **Fuselage_Skin**,
- **Empennage_Skin**

1. First case of 3D Digital Mock-up Model of a Transport-Aircraft, as represented in the Figure 7.37.
   The **Material PEC** was globally used for the *total structure*.

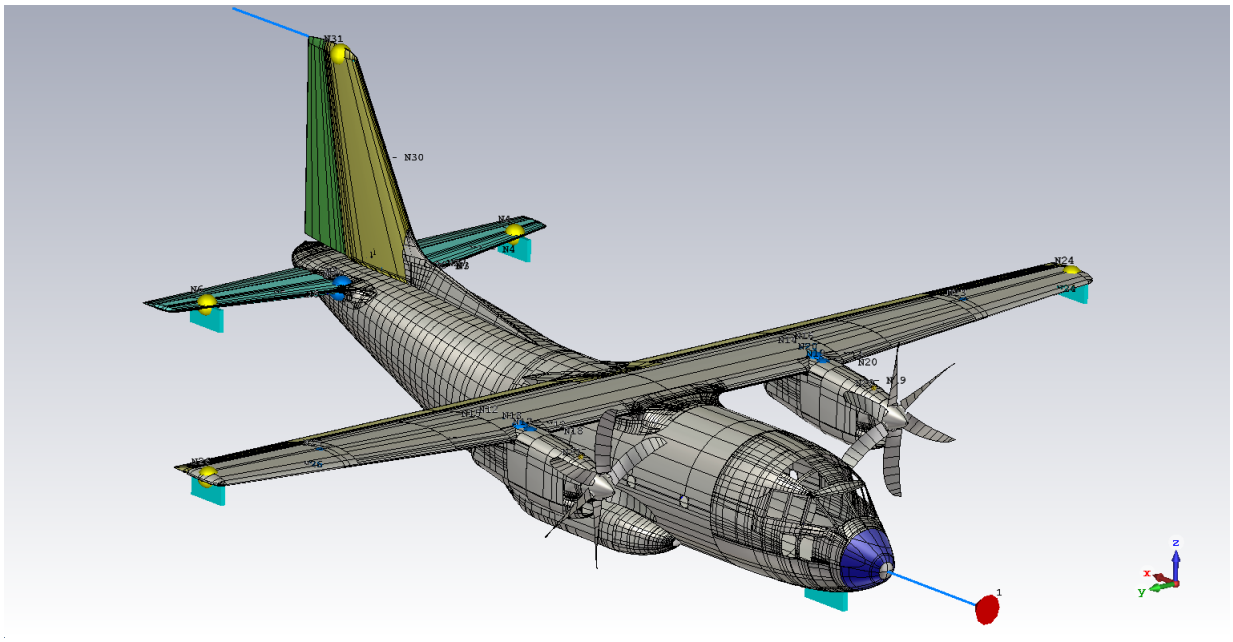

Figure 7.37: First case of 3D Digital Mock-up Model of a Transport-Aircraft

2. Second case of 3D Digital Mock-up Model of a Transport-Aircraft, as represented in the Figure 7.38 and it is possible to understand that the material used for the skin surfaces is mainly CFC with a standard electrical conductivity:

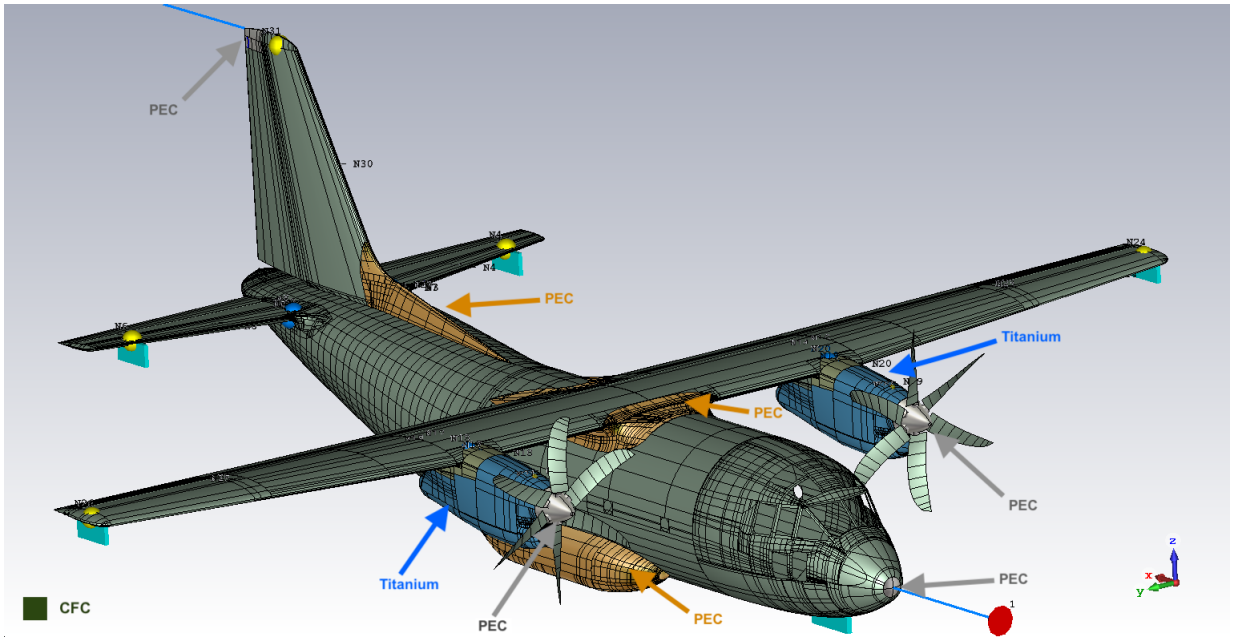

Figure 7.38: Second case of 3D Digital Mock-up Model of a Transport-Aircraft

This particular case of the Figure 7.38 corresponds to the **Configuration A1** and must be specified that for all the configurations the surfaces of the aircraft at which matches the *Entry/Exit Lightning attachment points* have to be in **PEC**. For the *main Structure* the Material used was **CFC**, having an *Electrical Conductivity* of $2.5e^4$ S/m.
For the **Right Engine Skin** and **Left Engine Skin**, it was used as **Material**

the **Titanium**, with the characteristics represented in the following Table 7.5.

Material	Titanium
Type	Lossy Metal
Electric Conducivity	$5.5e^5$ S/m

Table 7.5: Characteristic of Titanium

3. Third case of 3D Digital Mock-up Model of a Transport-Aircraft.
   In this case was used the same Material and colors as represented in the Figure 7.38. The difference respect to the Second case is related to the materials used for main structure of the Aircraft, in particular here was used as **Material CFC + layer of Copper Mesh**, having an *Electric Conductivity* of $0.935e^5$ S/m, the reason for having chosen this value was already motivated in the Section 7.3.

7.6 Mesh View

The Mesh generator is able to take into account different materials like perfectly conductive, real conductor, dielectric, composite etc. From the Figure 7.39 it is possible to see all the Mesh proprieties used:

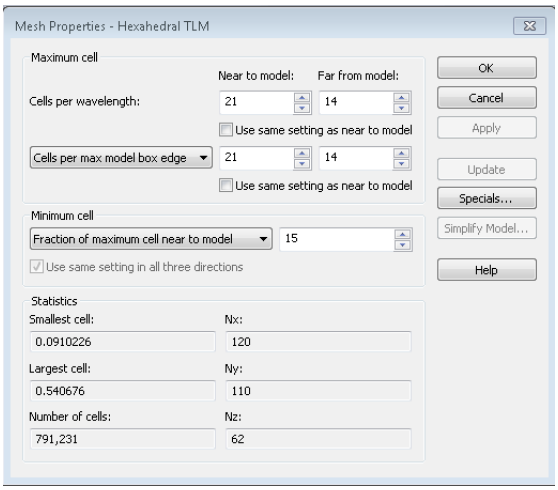

Figure 7.39: Mesh Proprieties

It is possible to highlight how the mesh is refined in a lot of surfaces thanks to the high resolution given by the already settled dimensions of the mesh, as the following Figure 7.40

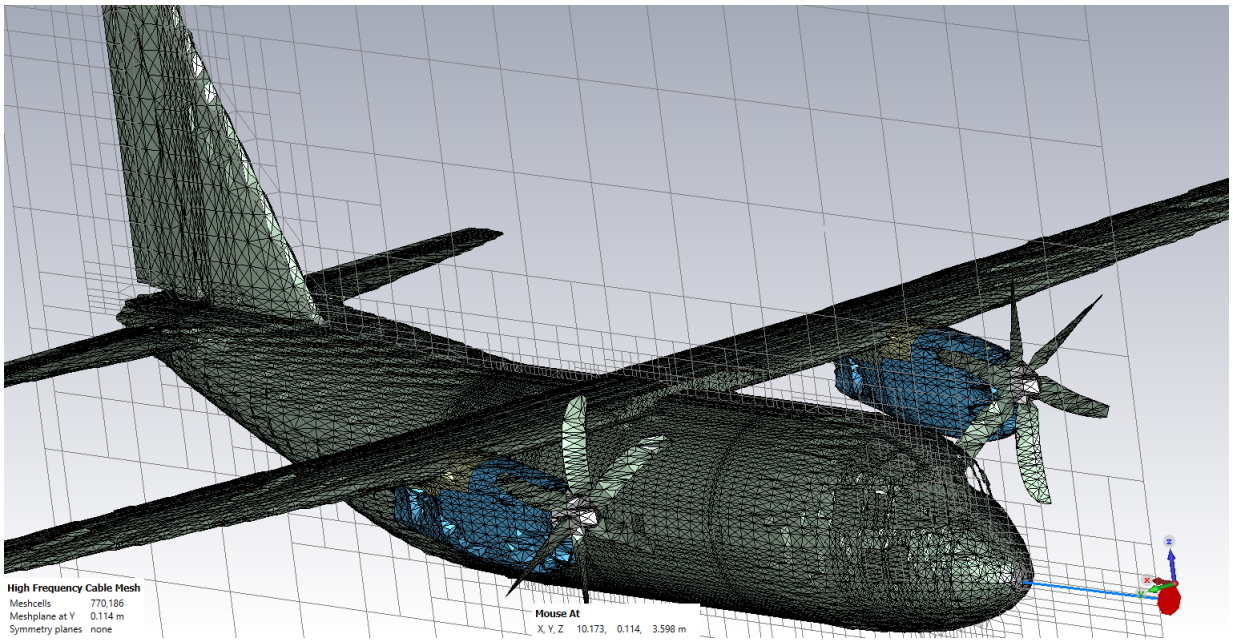

Figure 7.40: Mesh view of 3D Digital Mock-up Model of a Transport-Aircraft.

7.7 Simulation process and Results

The simulation process (virtual testing) must provide induced transient responses that can be used to determine the **ATLs** that can be compared to the **TCLs** and the **ETDLs**. Therefore, the aircraft lightning simulation should be setup to match the method by which the aircraft **TCLs** and the equipment **ETDLs** are defined. In the present thesis two types of **TCLs** are considered and analyzed:

1. Individual wire *Voltage* and *Current* flowing on a 50 Ohm impedance (representative of LRU impedance),

2. overall wire bundle current.

The data obtained by the present simulation campaign have as a final purpose the comparison with the **ETDLs** and corresponding equipment qualification tests, described in [23]. Consequentially, for each specific configuration simulated, according to procedures described in [8], the parameters monitored at the wiring network termination nodes were:

- **Screen current**,
- **Core Current**,
- **Core Voltage**.

In order to guarantee a conservative approach, for each LRU connection point and for each material configurations, the worst case among the **nine Entry/Exit attachment points configurations**, have to be considered as input for equipment qualification tests.

For each of the 27 Simulations runs (3 material configurations, 9 entry/exit points configurations), was possible to associated a maximum current- voltage peak occurred at each LRU connection points. It is possible to see from the Figure 7.41

an example of how the maximum point was taken of the current that flow on the screen of the cable bundle of the Left Empennage.

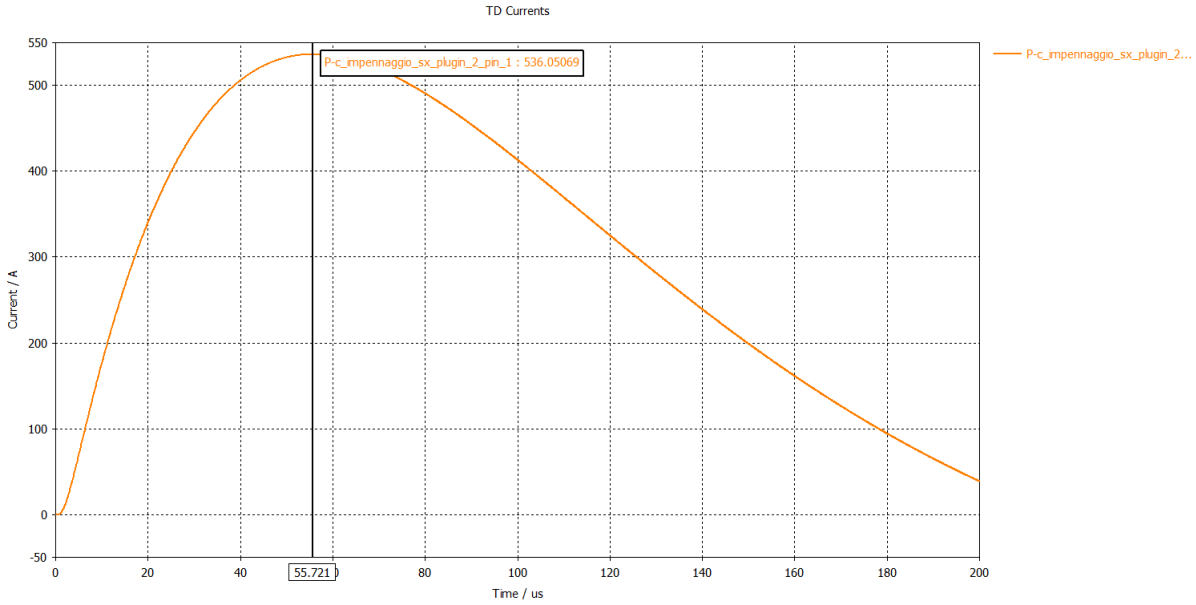

Figure 7.41: Marker in correspondence of the Max Current that flowed through the screen of the cable

The following Tables represented by the Figures 7.42, 7.43, 7.44, summarized all the peak values, as well as the **Worst case** in **A/V** and **dA/dV**:

PEC		A1	A2	A3	A4	A5	A6	A7	A8	A9	Worst Case (A,V)	Worst Case(dBA,dBV)
RIGHT EMPENNAGE	SCREEN (A)	0,078323693	0,053990508	0,053708462	0,039248591	0,039304432	0,019872384	0,018802226	0,010766637	0,012052068	0,078323693	-22,12213687
	CORE (A)	0,078312294	0,0533293125	0,0536660460	0,0397706860	0,039273577	0,01985589	0,018793744	0,01075808	0,0120506100	0,078312294	-22,12340108
	CORE (V)	3,9156147	2,6646562	2,6833023	1,9885343	1,9636788	0,9927945	0,93968719	0,537904	0,60253049	3,9156147	11,85599901
LEFT EMPENNAGE	SCREEN (A)	0,058441909	0,051701084	0,048765211	0,041824102	0.041274254	0,011798185	0,011305927	0,01236613	0,013835047	0,058441909	-24,66551213
	CORE (A)	0,058429576	0,049509915	0,048811935	0,041882627	0,041330557	0,01782076	0,011311537	0,012351882	0,013803082	0,058429576	-24,6673453
	CORE (V)	2,9214788	2,4754958	2,4405968	2,0941314	2,0665279	0,58910382	0,56557683	0,61759412	0,69015411	2,9214788	9,312054783
RIGHT LIGHT	SCREEN (A)	0,16449746	0,1332969	0,20077139	0.10887604	0,15924702	0,088368739	0,08723551	0,11962036	0,069044119	0,20077139	-13,94596348
	CORE (A)	0.030126404	0,029325018	0,029376481	0,031601386	0,030699771	0,001961359	0,001533309	0,004838421	0,00458715	0,031601386	-30,00587739
	CORE (V)	1,5063202	1,4662509	1,468824	1,5800693	1,5349886	0,098067923	0,076665431	0,24192103	0,22935749	1,5800693	3,9735227
LEFT LIGHT	SCREEN (A)	0,20321615	0,13901759	0,17154418	0,14227628	0,14704362	0,098233833	0,11019879	0,071683931	0,085062411	0,20321615	-13,84083562
	CORE (A)	0,030228266	0,028954496	0,029318788	0,030648725	0,031458389	0,001365598	0,002165095	0,003840205	0,004993383	0,031458389	-30,04527043
	CORE (V)	1,5114133	1,4477248	1,4659394	1,5324363	1,5729194	0,068279917	0,10825474	0,19291026	0,24966912	1,5729194	3,934129379
RIGHT PROPELLER	SCREEN (A)	2,6192436	2,7005767	2,1207199	4,9171959	1,7634624	1,2194155	0,49448846	4,2141804	2,3316801	4,9171959	13,83435022
	CORE (A)	0,043167191	0,031722772	0,031775473	0,032722236	0,030686913	0,002414525	0,001919988	0,005284158	0,005300367	0,043167191	-27,29692422
	CORE (V)	2,1583596	1,5861386	1,5887736	1,6361118	1,5343456	0,12072626	0,095999409	0,2642079	0,26501836	2,1583596	6,682476066
LEFT PROPELLER	SCREEN (A)	2,3206372	2,2417703	2,2994751	1,3799584	3,8759827	0,43857263	0,75906092	1,8768216	5,4416071	5,4416071	14,71454362
	CORE (A)	0,043607195	0,034226571	0,033886202	0,030932048	0,031529393	0,001648886	0,002200817	0,005010468	0,007118208	0,043607195	-27,20883696
	CORE (V)	2,1803597	1,7113286	1,6943101	1,5466024	1,5764696	0,082444299	0,11004085	0,25052339	0,35591041	2,1803597	6,770562926
FIN TIP	SCREEN (A)	0,018891026	0,016695125	0,016651317	0,0159727	0,015652168	0,002126239	0,002126349	0,003007014	0,003143391	0,018891026	-34,47488909
	CORE (A)	0,019057956	0,016813961	0,016772067	0,016043498	0,015723612	0,002121067	0,00211967	0,003001935	0,00313867	0,019057956	-34,3984736
	CORE (V)	0,95289778	0,84069807	0,83860333	0,80217492	0,78618059	0,10605336	0,10598351	0,15009675	0,1569335	0,95289778	-0,419073697

Figure 7.42: PEC results

CFC		A1	A2	A3	A4	A5	A6	A7	A8	A9	Worst Case (A,V)	Worst Case(dBA,dBV)
RIGHT EMPENNAGE	SCREEN (A)	1546,936	14635,232	942,77727	254,93076	220,10278	1908,622	1335,5194	1326,7848	1220,0601	14635,232	83,30799223
	CORE (A)	5,41234	14,503726	5,5224427	1,6320529	1,687733	4,1591219	3,9560369	4,4660989	4,4551421	14,503726	23,22959173
	CORE (V)	270,6117	725,1863	276,12214	81,602643	84,386652	207,95609	197,80185	223,30494	222,7571	725,1863	57,20899182
LEFT EMPENNAGE	SCREEN (A)	1563,9424	960,66069	14736,174	221,91158	258,62181	1349,2826	1928,2026	1225,8443	1332,5618	14736,174	83,36769482
	CORE (A)	5,2506207	5,3400015	14,100103	1,6188887	1,6419066	3,8259768	3,9406089	4,2147982	4,2323208	14,100103	22,9844457
	CORE (V)	262,53104	267,0008	705,00515	80,944434	82,095328	191,29884	197,03044	210,73991	211,61604	705,00515	56,96384579
RIGHT LIGHT	SCREEN (A)	229,32896	236,99053	169,13982	8421,2122	102,40968	8029,0387	115,06362	262,19852	169,87085	8421,2122	78,50749222
	CORE (A)	1,8892112	2,0210562	1,8877488	16,28901	2,2212348	14,003577	0,38822985	3,5459818	0,5766202	16,28901	24,2378938
	CORE (V)	94,460561	101,05281	94,387438	814,45052	111,06174	700,17887	19,411493	177,29909	28,83101	814,45052	58,2172941
LEFT LIGHT	SCREEN (A)	227,72725	168,58091	236,33047	101,11775	8426,3229	114,54373	7919,1958	168,97761	260,65515	8426,3229	78,51276195
	CORE (A)	1,9080833	1,9079287	2,0404937	2,2142489	16,29475	0,36188198	14,003175	0,51250926	3,5682598	16,29475	24,24095403
	CORE (V)	95,404165	95,396435	102,02468	110,71244	814,7375	18,094099	700,15876	25,625463	178,41299	814,7375	58,22035412
RIGHT PROPELLER	SCREEN (A)	384,25783	302,96695	280,85241	1061,7757	218,75914	682,62406	151,78032	2817,5586	271,55985	2817,5586	68,99745915
	CORE (A)	1,7893975	1,8521787	1,8515212	5,1958814	2,1783525	3,4677157	0,36175362	4,8664419	0,33202309	5,1958814	14,31318459
	CORE (V)	89,469876	92,608937	92,57606	259,79407	108,91762	173,38578	18,087681	243,3221	16,601155	259,79407	48,29258467
LEFT PROPELLER	SCREEN (A)	66,607938	68,086778	130,17073	43,711293	365,26568	31,745747	302,97769	84,430023	3168,9827	3168,9827	70,01839737
	CORE (A)	1,7651219	1,8244596	1,8502744	2,1629322	5,3908708	0,37354451	3,6033417	0,35330136	4,936562	5,3908708	14,63317847
	CORE (V)	88,256093	91,222979	92,513719	108,14661	269,54354	18,677226	180,16709	17,665068	246,8281	269,54354	48,61257856
FIN TIP	SCREEN (A)	6342,07665	237,10824	318,55874	51,684769	55,691515	6580,7708	6566,687	6628,283	6626,0317	6628,283	76,42802085
	CORE (A)	11,100999	5,9559892	5,9960314	1,7578006	1,7286033	9,859481	9,8156962	10,282961	10,234958	11,100999	20,90724127
	CORE (V)	555,04993	297,79946	299,80157	87,89003	86,430164	492,97405	490,78481	514,14804	511,7479	555,04993	54,88664104

Figure 7.43: CFC results

CFC+MESH		A1	A2	A3	A4	A5	A6	A7	A8	A9	Worst Case (A,V)	Worst Case(dBA,dBV)
RIGHT EMPENNAGE	SCREEN (A)	620,9478	4580,2993	340,00455	94,879999	79,593942	768,79708	536,8649	483,21932	444,74737	4580,2993	73,21787716
	CORE (A)	1,6607691	4,4157878	1,6436757	0,44525505	0,49021879	1,3434301	1,2061822	1,3902728	1,3759411	4,4157878	12,90016391
	CORE (V)	83,038456	220,78939	82,183784	22,262753	24,510939	67,171505	60,309111	69,51364	68,268897	220,78939	46,87956399
LEFT EMPENNAGE	SCREEN (A)	621,49278	342,3842	4602,5199	79,676724	95,557166	536,05069	769,84973	445,86377	484,32619	4602,5199	73,2599135
	CORE (A)	1,6230912	1,6241232	4,2941729	0,46882121	0,45248773	1,1861973	1,2914957	1,3243297	1,3367598	4,2941729	12,65759054
	CORE (V)	81,154558	81,206159	214,70865	23,441061	22,624386	59,309865	64,574783	66,216487	66,837988	214,70865	46,63699083
RIGHT LIGHT	SCREEN (A)	64,61073	62,722241	40,576998	2237,7259	23,138077	1986,0196	27,697669	67,087819	47,954507	2237,7259	66,99613777
	CORE (A)	0,59315145	0,65321806	0,59152479	4,4340225	0,57060087	3,5503968	0,0632551	0,99332222	0,20965799	4,4340225	12,93595785
	CORE (V)	29,657573	32,660903	29,576238	221,70113	28,530043	177,51984	3,162755	49,666111	10,4829	221,70113	46,91535813
LEFT LIGHT	SCREEN (A)	63,960256	41,262922	63,052961	23,619584	2239,2205	28,217304	1982,9877	48,193036	67,680564	2239,2205	67,00193723
	CORE (A)	0,5977131	0,60184126	0,65681203	0,56866715	4,4313017	0,054101145	3,5509204	0,20270354	0,99771951	4,4313017	12,93062639
	CORE (V)	29,885655	30,092063	32,840602	28,433358	221,56509	2,705057	177,54602	10,135177	49,885976	221,56509	46,91002667
RIGHT PROPELLER	SCREEN (A)	154,601100	127,529940	114,834020	421,371100	87,725171	266,826850	61,713664	941,28061	112,06276	941,28061	59,47438225
	CORE (A)	0,522621	0,573736	0,543058	1,472747	0,529865	0,930966	0,023790	1,3958504	0,078794453	1,4727471	3,362563525
	CORE (V)	26,131007	28,686793	27,152925	73,637355	26,493266	46,5483050	1,189497	69,792522	3,9397227	73,637355	37,34196361
LEFT PROPELLER	SCREEN (A)	27,7109280	35,8518020	62,8401180	13,0481630	173,6199000	16,9506560	137,0659800	41,191365	1064,6467	1064,6467	60,54411025
	CORE (A)	0,5213015	0,5447419	0,5768774	0,5285457	1,5979155	0,0200074	1,0212343	0,13684567	1,4202027	1,5979155	4,07107619
	CORE (V)	26,0650730	27,2370960	28,8438680	26,4272870	79,8957730	1,000372	51,0617140	6,8422834	71,010136	79,895773	38,05047606
FIN TIP	SCREEN (A)	1538,2581	53,597597	90,733867	13,869381	17,593927	1600,2237	1561,5708	1605,8914	1600,6404	1605,8914	64,11432345
	CORE (A)	2,8610577	1,6846244	1,8686156	0,49315152	0,50616164	2,4694005	2,4549244	2,6455051	2,6304248	2,8610577	9,130532329
	CORE (V)	143,05289	84,231222	93,430782	24,657576	25,308082	123,47003	122,74622	132,27526	131,52124	143,05289	43,10993272

Figure 7.44: CFC+MESH results

It was presented from the Table in Figure 7.45 , the difference between the **Worst case** in **dA/dV** of the configurations **CFC+MESH** vs **CFC**. The result shows a globally decrease of 10 dB of currents on the connectors, due to the fact that the Conductivity of the structure was increased.

CFC+MESH vs CFC
-10,09011507
-10,32942783
-10,32942783
-10,10778132
-10,32685517
-10,32685496
-11,51135445
-11,30193595
-11,30193596
-11,51082472
-11,31032765
-11,31032745
-9,523076897
-10,95062106
-10,95062106
-9,474287121
-10,56210228
-10,5621025
-12,31369741
-11,77670894
-11,77670832

Figure 7.45: Comparison between **CFC+MESH** vs **CFC**

The **Final Table**, represented by the Figure7.46, it is possible to appreciate the effects of material configurations on the worst case **TCLs**.

In the first column was presented the difference between **TCLs** in dB for the configurations with **PEC** Material and **CFC** basic configuration, while in the second column the difference between **TCLs** in dB for the configurations with **PEC** Material and **CFC+MESH**.

Final results		CFC vs PEC	CFC + MESH vs PEC
RIGHT EMPENNAGE	SCREEN (A)	-105,4301291	-95,34001403
	CORE (A)	-45,35299281	-35,02356499
	CORE (V)	-45,35299281	-35,02356499
LEFT EMPENNAGE	SCREEN (A)	-108,0332069	-97,92542563
	CORE (A)	-47,65179101	-37,32493584
	CORE (V)	-47,65179101	-37,32493604
RIGHT LIGHT	SCREEN (A)	-92,4534557	-80,94210126
	CORE (A)	-54,24377118	-42,94183524
	CORE (V)	-54,2437714	-42,94183543
LEFT LIGHT	SCREEN (A)	-92,35359756	-80,84277284
	CORE (A)	-54,28622447	-42,97589682
	CORE (V)	-54,28622474	-42,97589729
RIGHT PROPELLER	SCREEN (A)	-55,16310893	-45,64003203
	CORE (A)	-41,61010881	-30,65948775
	CORE (V)	-41,61010861	-30,65948755
LEFT PROPELLER	SCREEN (A)	-55,30385374	-45,82956662
	CORE (A)	-41,84201543	-31,27991315
	CORE (V)	-41,84201563	-31,27991313
FIN TIP	SCREEN (A)	-110,9029099	-98,58921253
	CORE (A)	-55,30571487	-43,52900593
	CORE (V)	-55,30571474	-43,52900642

Figure 7.46: Final results

Chapter 8

Further results

8.1 2D/3D Results: H-field and Surface Current

From the 3D CST MICROWAVE STUDIO, it is possible to obtain the resulting of H-field that affect the aircraft and the Surface Current as in Figure In this Section for the Figures below was considered the **A1 Configuration CFC**. In particular the Figure 8.1 was obtained the **H-field** using the function *"Contour"*.

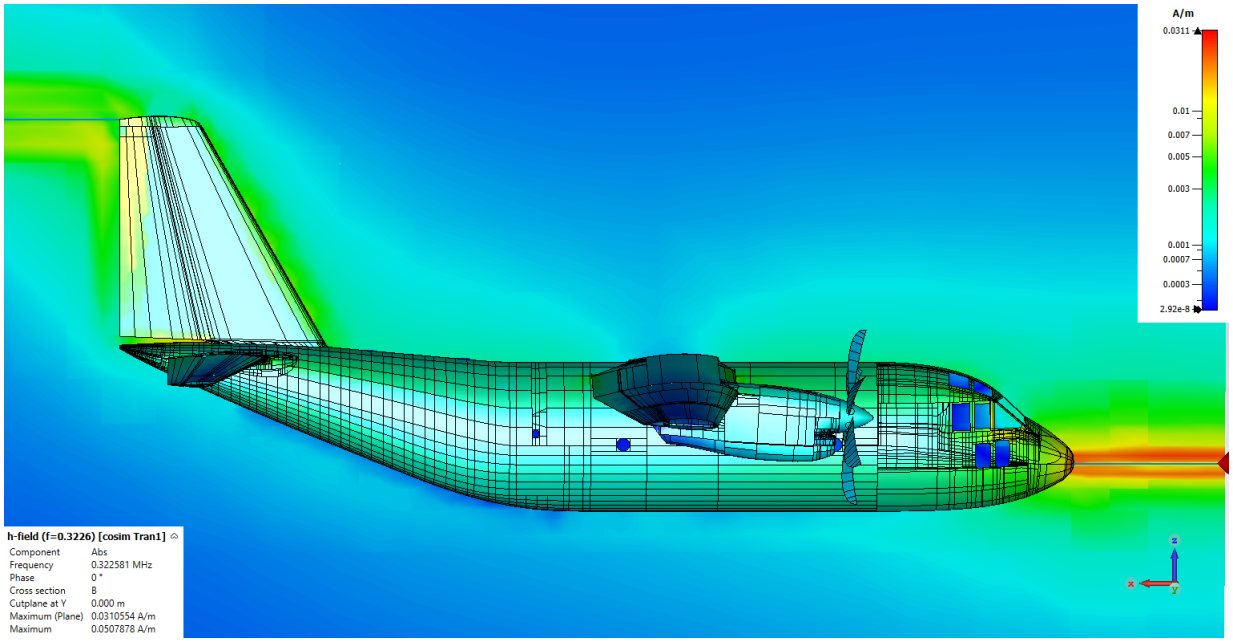

Figure 8.1: H-field for **A1 Configuration CFC**.

But, it is also possible to understand how the Inducted effect due to the Field affected the zones where are present the aperture, using the function of the *"Isolines"* and cut-plane at Y as in Figure 8.2.

For what concern instead the Surface Current, always using the function Contour, are highlighted the attachment points as the one with a major Surface current as in Figure

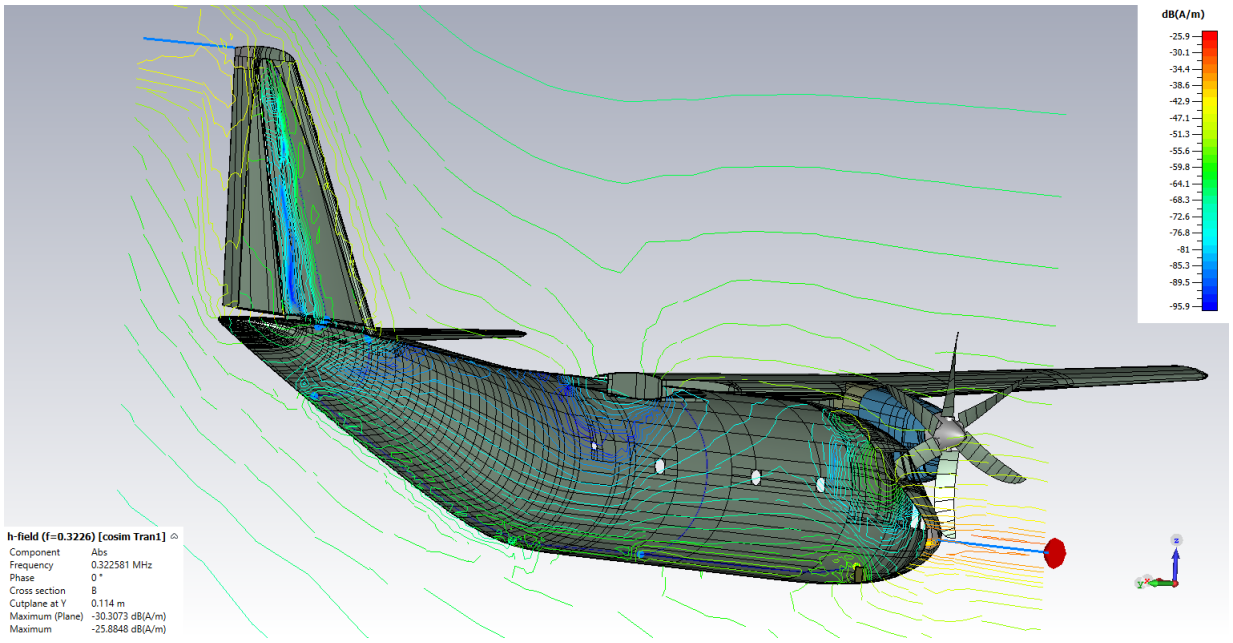

Figure 8.2: H-field for **A1 Configuration CFC**.

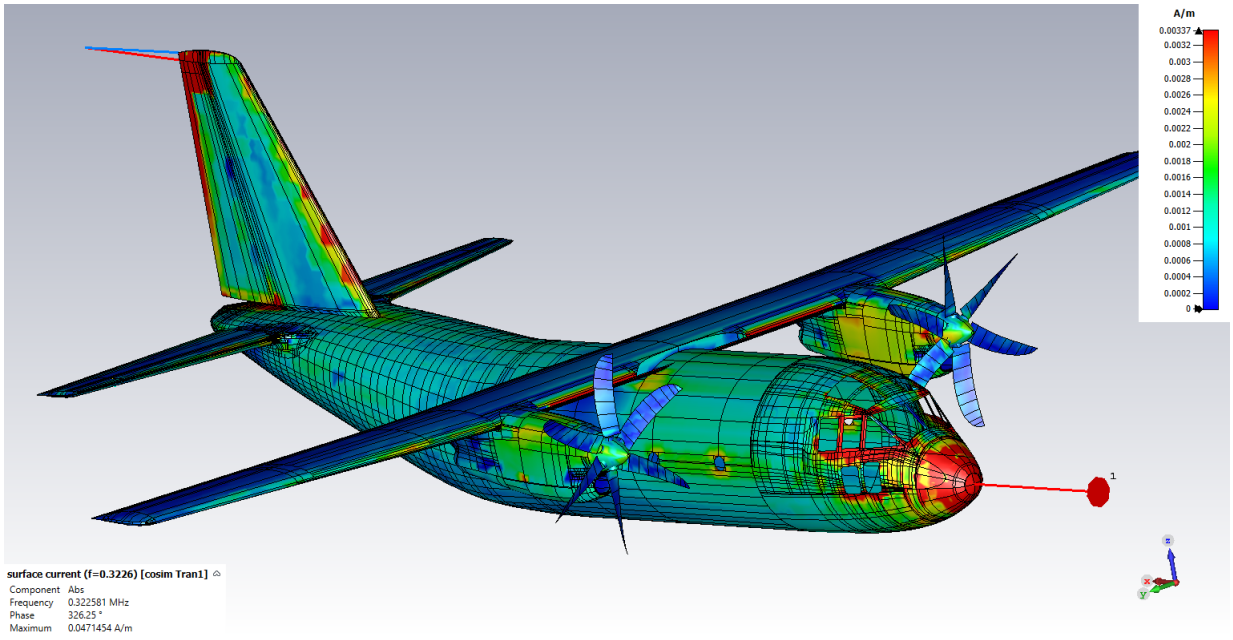

Figure 8.3: Surface Current **A1 Configuration CFC**.

Frequency spectrum result

Through the numerous functions provided by the tool CST, from the Figures 8.4, 8.5, 8.6, it is possible to observe the frequency spectrum of the induced transient (in the cable network) of the three different material configurations analyzed (**PEC**, **CFC**, **CFC+MESH**). It is interesting to highlight that some spikes occurs in the frequency range of 5-30 MHz; those spikes are due to the resonances of the cables network and the whole aircraft structure around 3 MHz

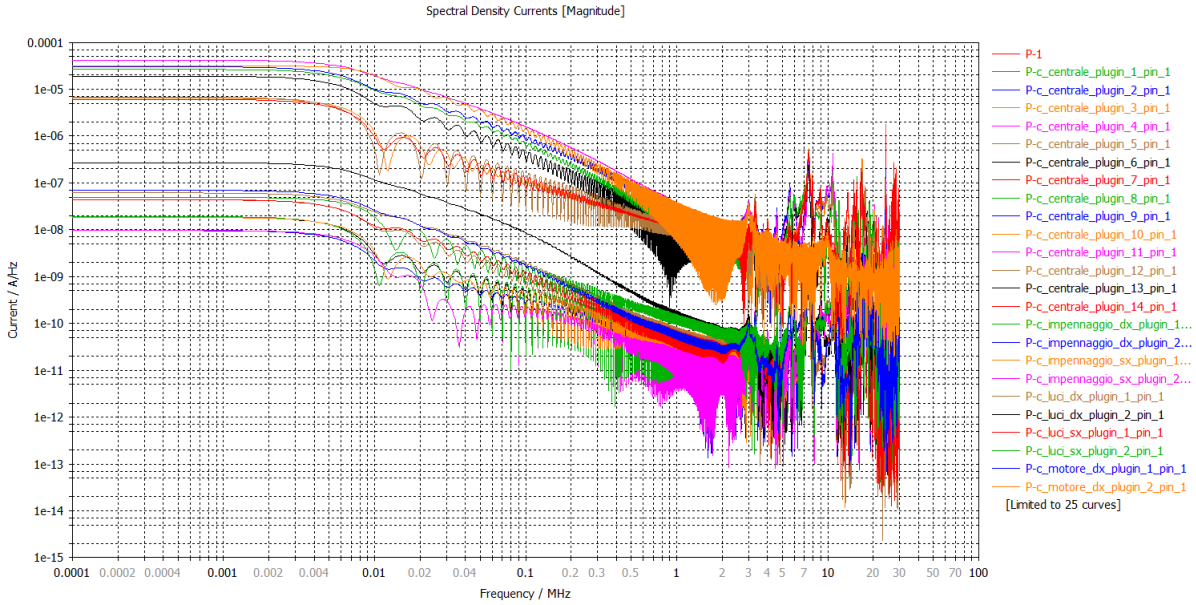

Figure 8.4: Final results PEC

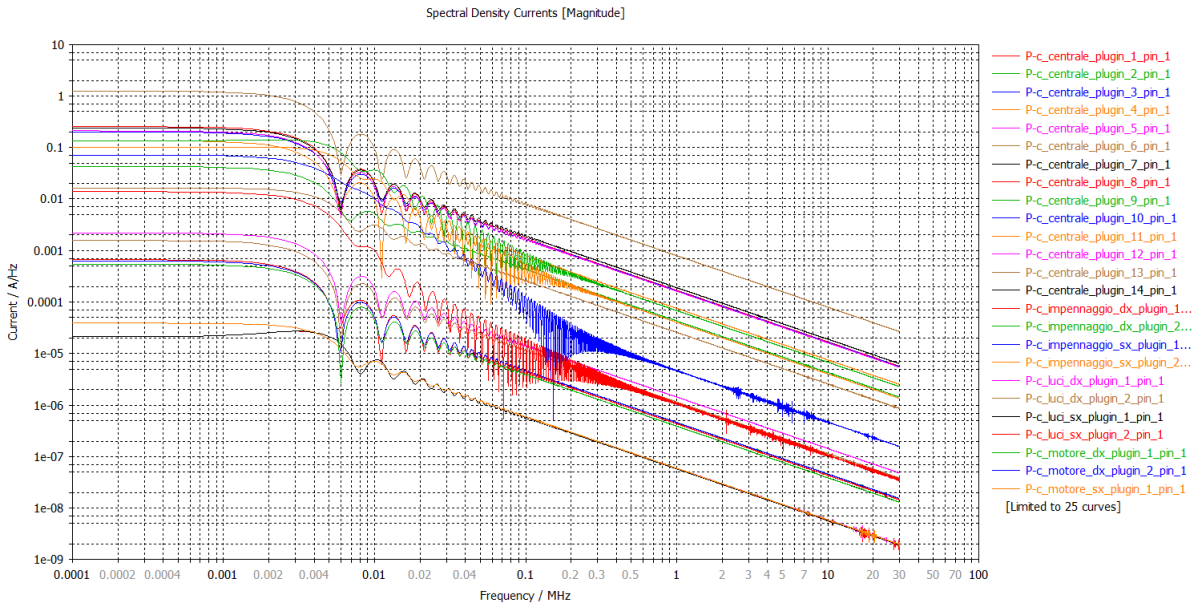

Figure 8.5: Final results CFC

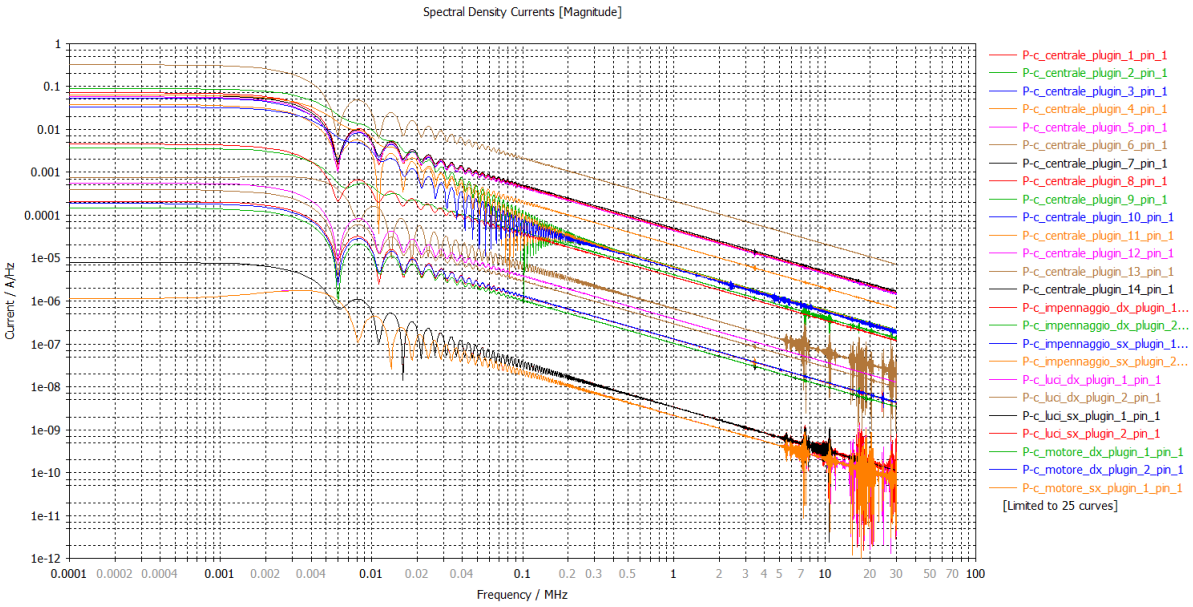

Figure 8.6: Final results CFC+MESH

Chapter 9

Conclusion and future work

The lightning is one of the most spectacular of natural phenomena and behind of this there are numerous theories, as it has always been a matter of disputes. During the Thesis work, carried out over a 10-month period at the Leonardo S.p.A, it was possible to deepen the knowledge starting from the physics behind it up to the definition of a certification-oriented numerical methodology for the evaluation of Lightning Indirect Effect (LIE) on a Mock-up Model of a Transport-Aircraft. Once the phenomenon of lightning has been studied as a whole with specific focus on the interaction of the lightning with the aircraft and on the certification process, finally important results have been achieved by means of the simulation campaign, basically implementing a virtualization of the real testing process. The simulation campaign was based on the use of the CST Studio Suite integrated in 3D Experience. According to the zones of major probability of lightning attachment and in order to detect the "worst case effect" on the cables network, nine different entry/exit points configurations were analyzed. The main purpose of the Thesis Work was to estimate by simulation the induced transient responses at the terminal points of the cable network, in order to determine the ATLs (Actual Transient Levels) to compared with the TCLs (Transient Control Levels) and with the EDTLs (Equipment Design Transient Levels). Moreover, the simulation campaign was repeated on the whole aircraft for three different configurations of materials (Perfect Electric Conductor, standard Carbon Fiber Composite, advanced Carbon Fiber Composite with Copper Mesh), giving the possibility to compare the Worst Cases, associated to the maximum current-voltage peak on the core and screen of each Cable, for the three materials configurations. An important result achieved by the present thesis work, is the evaluation of the impact of composite materials on the ATL Worst cases. Particularly, an interesting outcome is highlighted by comparing the configurations "Standard CFC versus Advanced CFC", in which it is shown a global decrease of 10 dB of coupled lightning current on all connectors, due to the fact that the conductivity of the aircraft structure has been increased approximately by a factor four. This Thesis Work aims to be a starting point for a future study, that will be characterized by the inclusion of the internal structure of the aircraft as well as by the inclusion of more representative Cable Bundle Network. The ultimate goal will be the application of the present methodology during the certification phase on a real aircraft in order to support or be an alternative to the testing campaign, cutting down testing time and time-to-market.

Bibliography

[1] Lawrence A.Kennedy Alexander Fridman. *Plasma Physics and Engineering*. Taylor & Francis, 1996.

[2] *ARP-5412 Aircraft Lightning Environment and Related Test Waveform*. SAE Aereospace, Revision,2005.

[3] *ARP-5413 Certification of Aircraft Electrical/Electronic Systems for the Indirect Effects of Lightning*. SAE Aereospace, 1999-11.

[4] *ARP-5414 Aircraft Lightning Zoning*. SAE Aereospace, 2005.

[5] M. Roshdi Hassan B. Alemour O. Badran. "A Review of Using Conductive Composite Materials in Solving Lightening Strike and Ice Accumulation Problems in Aviation". In: *J. Aerosp. Technol. Manag. vol.11* (2019). URL: http://dx.doi.org/10.5028/jatm.v11.1022..

[6] *Bonding, Electrical and Lightning protection Systems*. US Military Specification MIL-B5087B, 1964.

[7] S.J. Haigh D. Morgan and J.Meakins. "The interaction of Lightning with aircraft and the challenges of lightning testing". In: *Jounal Aerospace* (Dec. 2012).

[8] *ED-105 "Aircraft Lightning Test Methods"*. EUROCAE, 2005.

[9] W.S Zaengl E.Kuffel and J.Kuffel. *High Voltage Engineering Fundamentals*. Butterworth-Heinemann, 2000.

[10] *Environmental Conditions and Test Procedures for Aircraft Systems*. Version D, Chapters 22 and 23, 2006.

[11] F.A Fisher, J.A Plumer, and R.A Perala. *Aircraft Lighting Protection Handbook*. FAA,Federal Aviation Administration, 1989.

[12] J. Anderson Plumer Franklin A.Fisher. *Lightning protection of Aircraft*. NASA, 1977.

[13] John Gokcen G.Sweers Bruce Birch. "Lightning strikes: Protection, Inspection and Repair". In: *Boeing Aero_Magazine* (2012). URL: https://www.boeing.com/BOEINGEDGE/aeromagazine..

[14] C.J Hardwick. *Introduction to Induced Effects*. Cobham, 2018.

[15] C.J Hardwick. *The Lightning aircraft interaction*. Cobham, 2018.

[16] L.B Loeb. *Electrical Coronas*. University of California Press, 1965.

[17] L.B Loeb and J.M Meek. *The Mechanism of Electric Spark*. Stanford University Press, 1940.

[18] Houston Lyndon B. Johnson Space Center. *Analysis of Lightning Current Waveforms through the Space Shuttle*. National Aeronautics and Space Administration, January 17, 1975.

[19] Skouby McBrayer and Weinstock. *"Lightning Attachment Characteristics for metal/composite materials"*. IEE, EMC Conference, 1977.

[20] V.Kamaraju M.S Naidu. *High Voltage Engineering, second edition*. McGraw-Hill, 1996.

[21] A. Delannoy P. Lalande. "Numerical Methods for Zoning Computation". In: *Jounal Aerospace* (Dec. 2012). hal-: `01184414`.

[22] *Plane & Helicopter Lightning Strike Zone Diagrams*. URL: `http://www.astrosealproducts.com/diagrams.html`.

[23] *RTCA / DO-160 E - Environment conditions and test procedures for airborne equipment – section 22: lightning induced transient susceptibility*. RTCA Inc, December 2004.

[24] Ed Rupke. *Lightning Direct Effects Handbook*. Lightning Technologies Inc., 2002.

[25] Sir Basil Schonland. *Lightning and the Long Electric Spark*. Advancement of science,pp 306-313, 1962.

[26] *Short Course on Lightning Protection of Aircraft*. Cobham Technical Services Lightning and Testing consultancy.

[27] Leonardo S.p.A. *Leonardo-Aerospace, Defence and Security*. URL: `https://www.leonardocompany.com/en/about-us/our-company/profile`.

[28] C.L. Wadhwa. *High Voltage Engineering*. New Age International Publishers, Third edition.